

7.3 HABC-run2e - Corner

HABC-run2e is a package CG over corner impact with a 30-foot impact (time = 0 to 0.015 seconds) followed by a crush impact (0.015 to 0.05 seconds).

The configuration after the 30-foot impact is shown in Figure 7.3.1. The maximum effective plastic strain in the CV body is 0.0371 in/in as shown in Figure 7.3.2.

Figure 7.3.3 shows that the maximum effective plastic strain in the CV lid is 0.0051 in/in near the outer radius of the center boss.

The maximum effective plastic strain in the lid studs is in the stud at the impact with the rigid plane (0° position) and is 0.5233 in/in. It can be seen from the insert in Figure 7.3.4, that strains near the maximum exist across the thickness of the stud. Therefore, it should be noted that slight differences between the modeled length and actual length of the stud could be significant relative to possible failure of the stud. Other differences such as friction and local flexibility in the test pad armored plate could also significantly effect this stud and cause failure. The maximum effective plastic strains of other components for this impact are listed in Table 7.3.1.

Component	Effective Plastic Strain, in/in
CV Nut Ring	0.0002
Angle	0.0394
Drum	0.3247
Drum Bottom Head	0.0000
Liner	0.3983
Lid	0.2791
Lid Stiffener	0.0272
Lid Stud Nuts	0.2260
Lid Stud Washers	0.1528
Plug Liner	0.1152

Figure 7.3.5 shows the final configuration for the crush impact. Figure 7.3.6 shows that the maximum effective plastic strain in the CV body due to the crush impact is 0.0371 in/in.

Figure 7.3.7 shows the effective plastic strain in the CV lid maximum to be 0.0051 in/in. The maximum occurs near the outer radius of the center boss, nearest the impact.

The maximum effective plastic strain in the drum studs is shown to be 0.5598 in/in in Figure 7.3.8. The elevated values of plastic strain occur through out the cross section of the stud. As explained in the 30-foot impact results, slight variances in the length/configuration in this vicinity could prove detrimental for the stud in the test due to the relatively high level of strain through the thickness of the stud.

The maximum effective plastic strain in the liner is 0.5254 in/in as shown in Figure 7.3.9. The maximum is a surface strain and occurs in the folding at about the 80° position at the attachment of the liner to the angle. Investigation shows that the membrane maximum strain is 0.2205 in/in and occurs at the same location.

Component	Effective Plastic Strain, in/in
CV Nut Ring	0.0002
Angle	0.0462
Drum	0.3830
Drum Bottom Head	0.0761
Liner	0.5254
Lid	0.3622
Lid Stiffener	0.0272
Lid Stud Nuts	0.2266
Lid Stud Washers	0.1528
Plug Liner	0.1166

The CV lid separation time histories for the nodes shown in Figure 3.1.30 are given in Figure 7.3.10 for the HABC-run2e. Spike separation occurs (about 0.013 in) during the 30-foot impact with the general separation of about 0.008 in. The general separation lasts about 0.01 seconds, then settles to 0.003 in or less. The general separation due to the crush impact is 0.005 in or less, with some spiking to about 0.010 in noted. Nominal separation of 0.003 in or less would be expected.

Figure 7.3.11 shows the location of the nodes used to obtain the minimum kaolite thickness in the plug. Figure 7.3.12 shows the minimum plug thickness time history. A minimum

thickness of about 3.5 inches is reached in the 30-foot impact, and about 3.0 inches is reached in the successive crush impact.

Figure 7.3.13 shows the location of the nodes used to obtain the minimum kaolite thickness in the package bottom. The time history thickness is shown in Figure 7.3.14 for the bottom kaolite. A minimum thickness of about 1.75 inches is shown.

Figure 7.3.15 shows the nodes used to obtain overall drum heights for the impacts. The final lengths from the bottom head to the lid are used to describe the deformations. Curve A in Figure 7.3.16 gives the length response of the 30-foot impacted lid corner to the drum bottom. The length after the 30-foot lid impact is about 40.5 in and goes to about 39 in after the crush impact. The Curve B in Figure 7.3.16 shows that the length from the crushed corner of the bottom to the lid reaches about 38 in in length.

3100 HABC-RUN2E CORNER DEC04 KOH
Time = 0.015

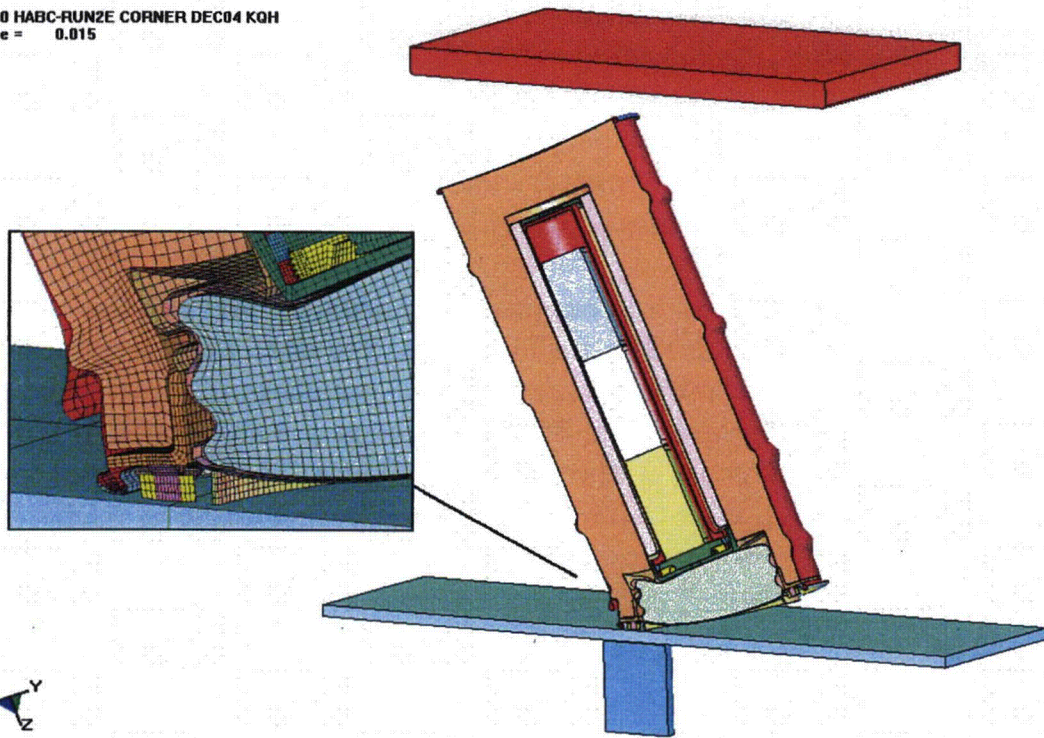


Figure 7.3.1 - HABC-run2e, Configuration of the ES-3100 After the 30-Foot Impact

3100 HABC-RUN2E CORNER DEC04 KOH
Time = 0.015
Contours of Effective Plastic Strain
max ipt. value
min=0, at elem# 53
max=0.0370912, at elem# 75531

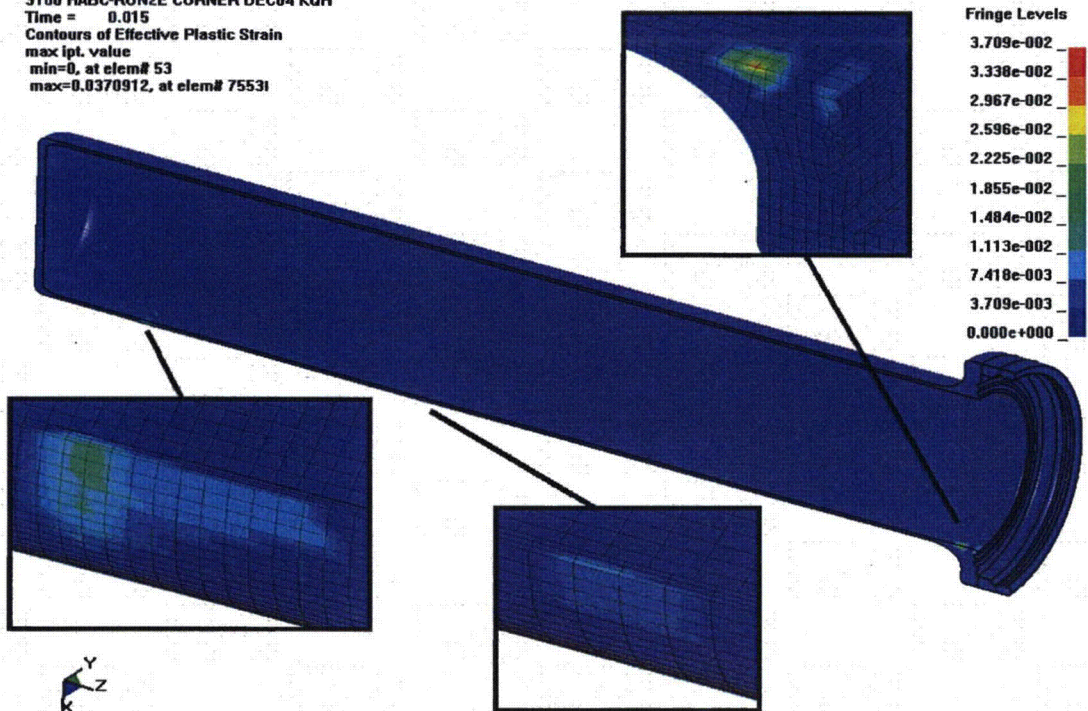


Figure 7.3.2 - HABC-run2e, 30-Foot Impact, Effective Plastic Strains in the CV Body

3100 HABC-RUN2E CORNER DEC04 KQH
 Time = 0.015
 Contours of Effective Plastic Strain
 max ipt. value
 min=0, at elem# 51849
 max=0.00505700, at elem# 54305i

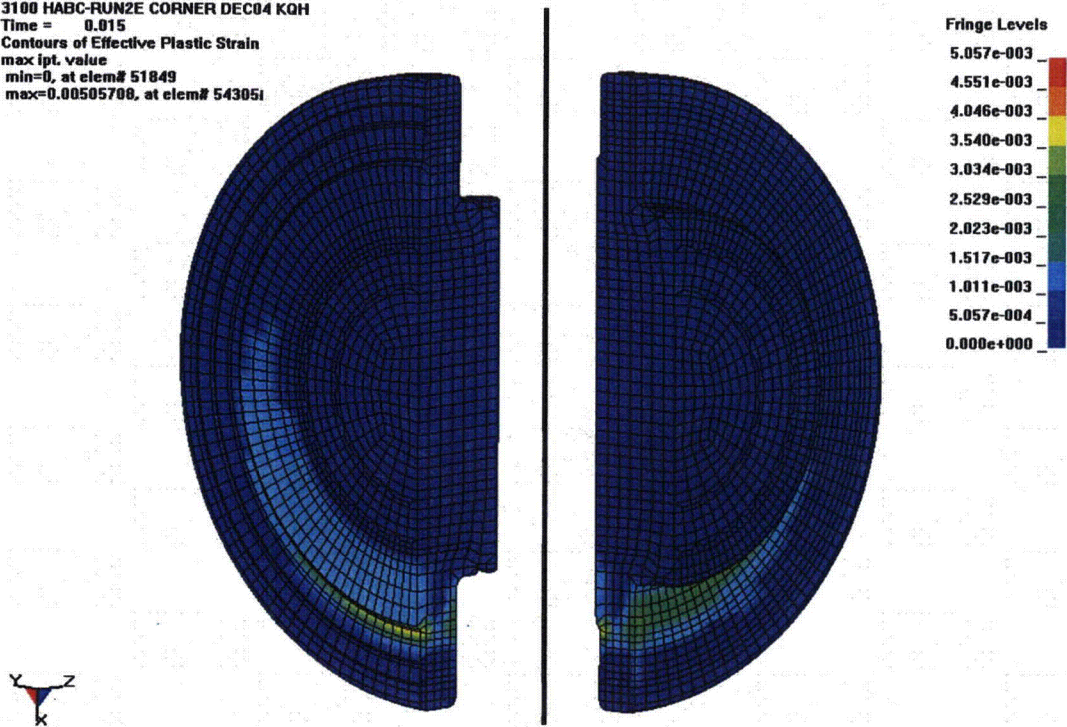


Figure 7.3.3 - HABC-run2e, 30-Foot Impact, Effective Plastic Strain in the CV Body

3100 HABC-RUN2E CORNER DEC04 KQH
 Time = 0.015
 Contours of Effective Plastic Strain
 max ipt. value
 min=0, at elem# 72025
 max=0.523269, at elem# 71992i

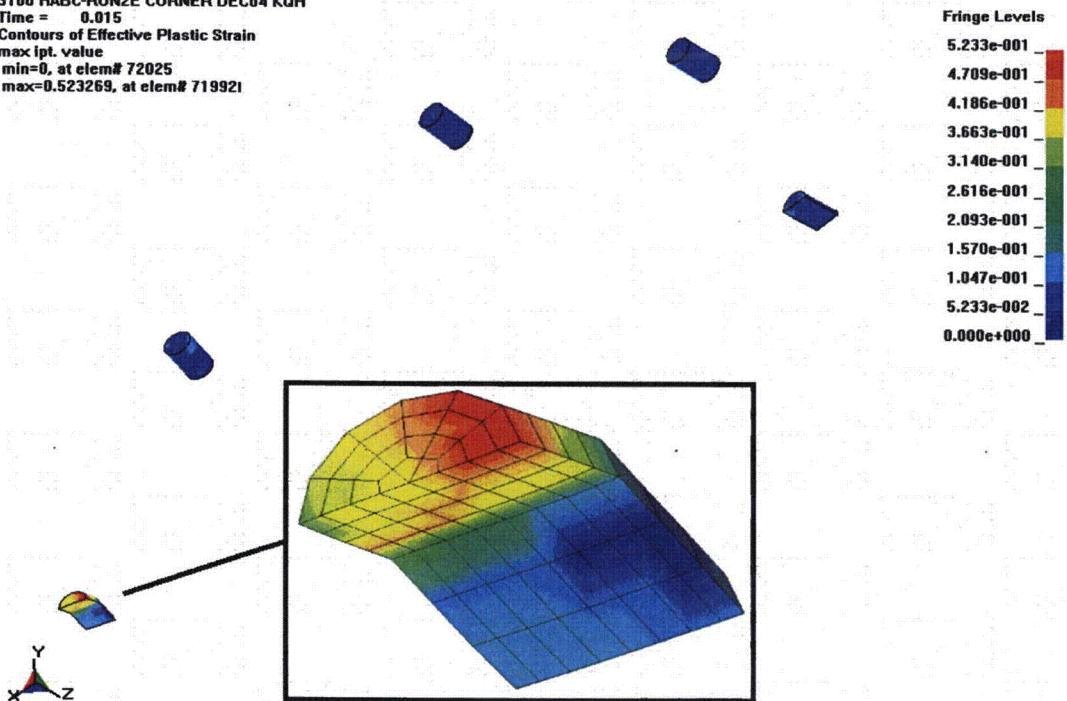
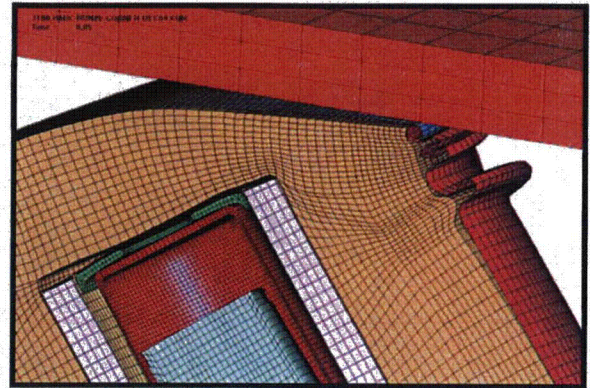


Figure 7.3.4 - HABC-run2e, 30-Foot Impact, Effective Plastic Strain in the Studs



3100 HABC-RUN2E CORNER DEC04 KQH
Time = 0.05

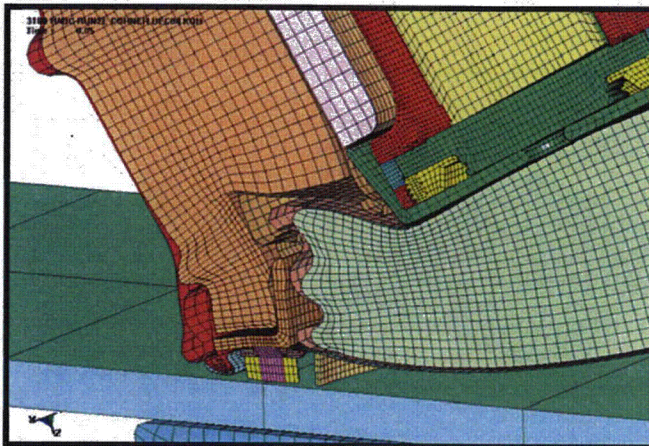
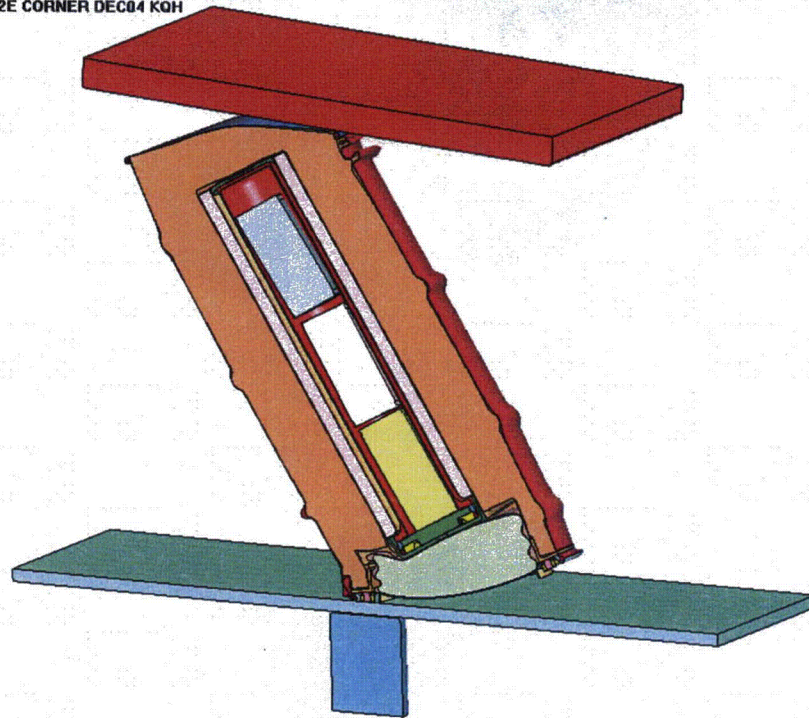


Figure 7.3.5 - HABC-run2e, Configuration After the Crush Impact

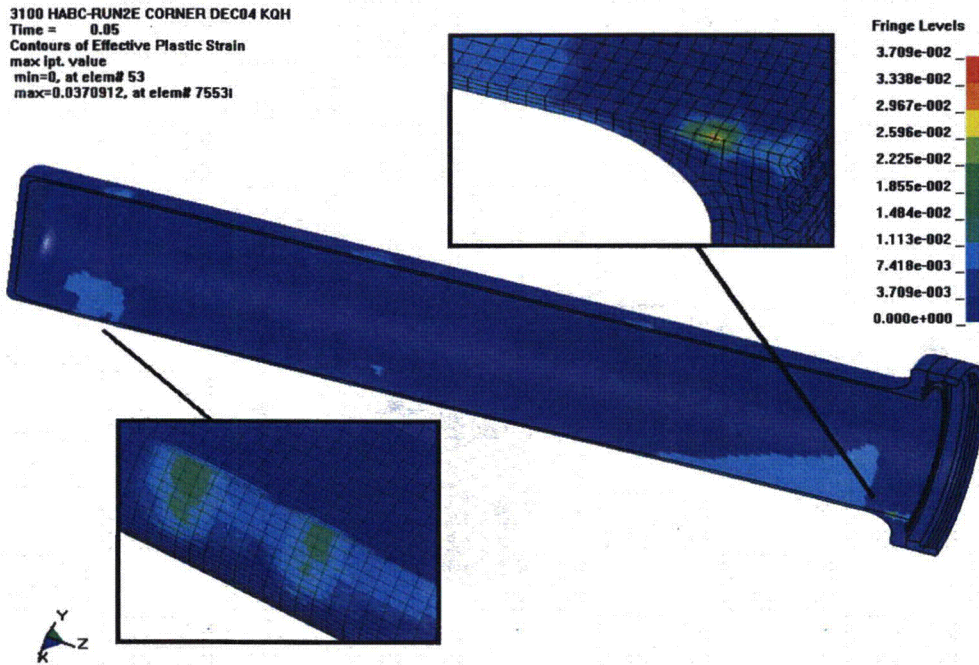


Figure 7.3.6 - HABC-run2e, Crush Impact, Effective Plastic Strain in the CV Body

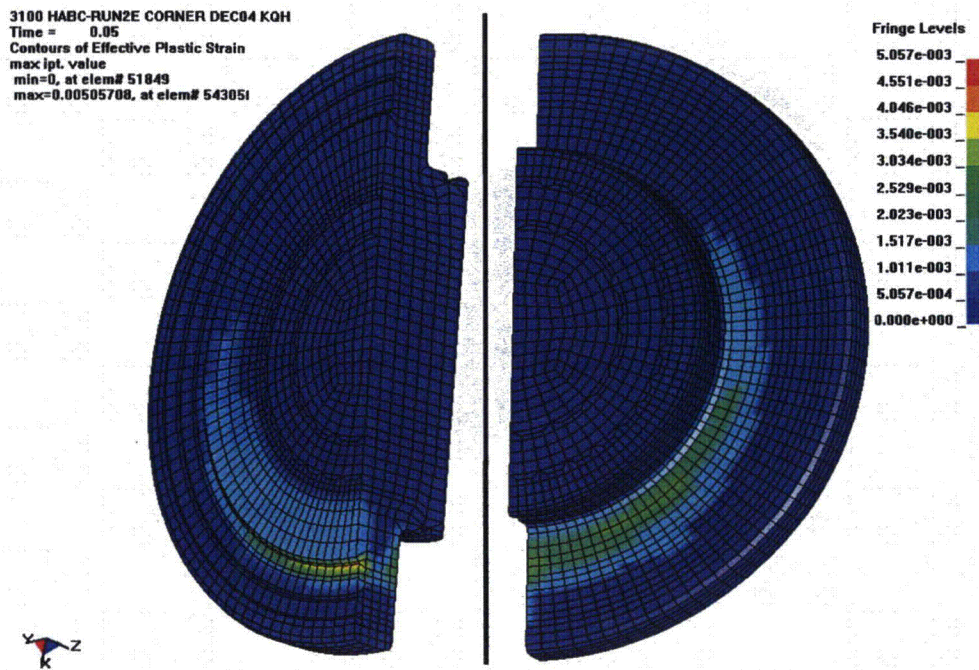


Figure 7.3.7 - HABC-run2e, Crush Impact, Effective Plastic Strain in the CV Lid

3100 HABC-RUN2E CORNER DEC04 KOH
 Time = 0.05
 Contours of Effective Plastic Strain
 max ipt. value
 min=0, at elem# 72169
 max=0.559845, at elem# 719921

Fringe Levels

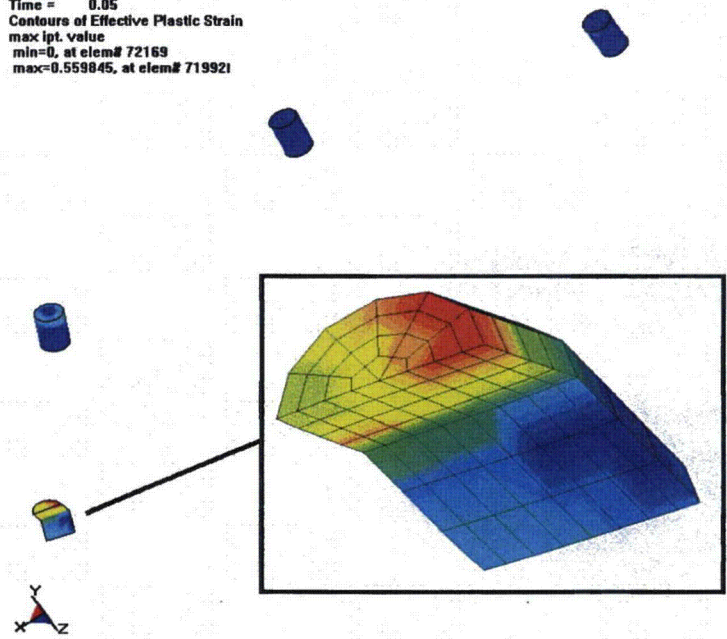
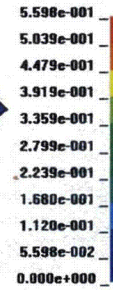


Figure 7.3.8 - HABC-run2e, Crush Impact, Effective Plastic Strain in the Studs

3100 HABC-RUN2E CORNER DEC04 KOH
 Time = 0.05
 Contours of Effective Plastic Strain
 max ipt. value
 min=0, at elem# 18909
 max=0.525399, at elem# 188271

Fringe Levels

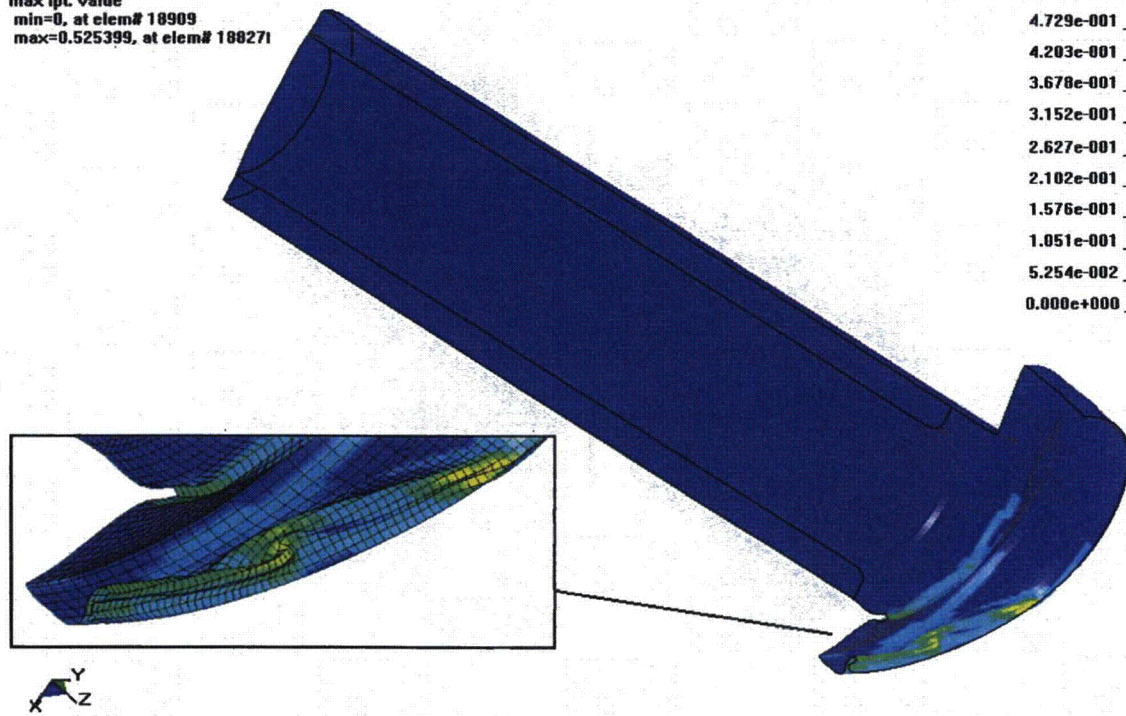
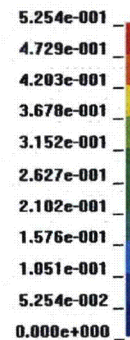


Figure 7.3.9 - HABC-run2e, Crush Impact, Effective Plastic Strain in the Liner

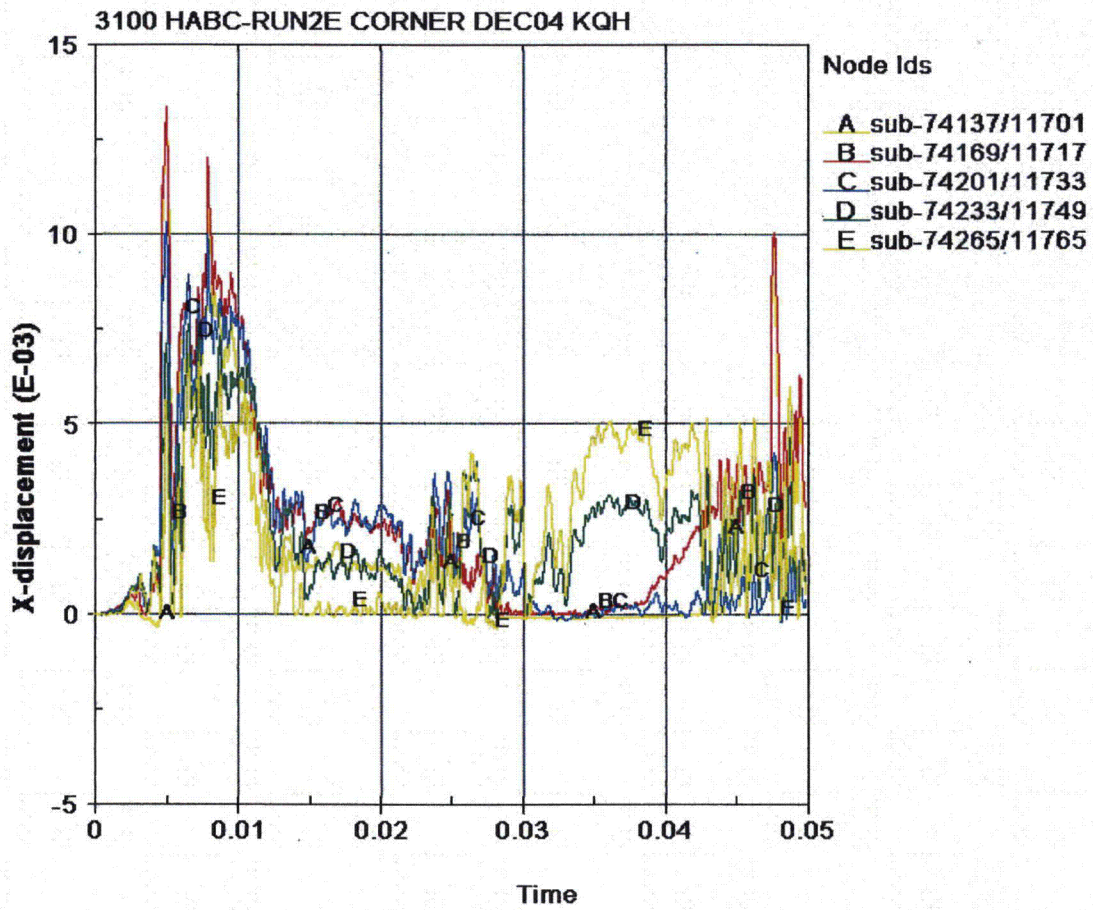


Figure 7.3.10 - HABC-run2e, Crush Impact, CV Lid/Body Separation Time History

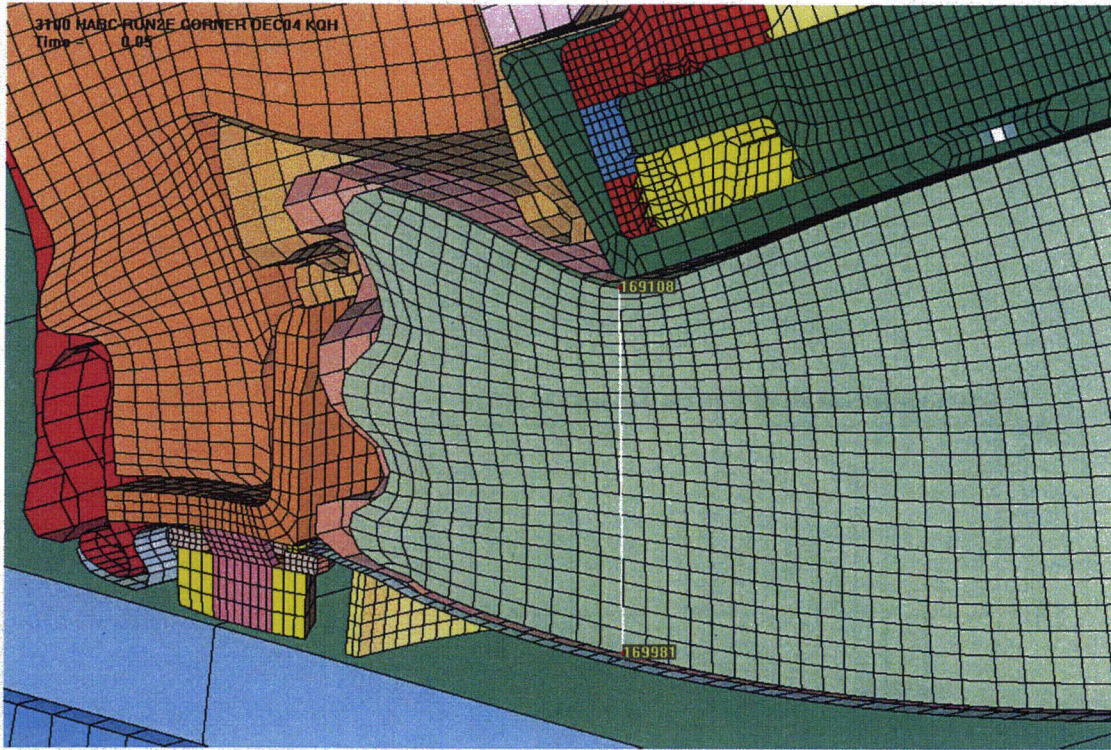


Figure 7.3.11 - HABC-run2e, Plug Thickness After the Crush Impact

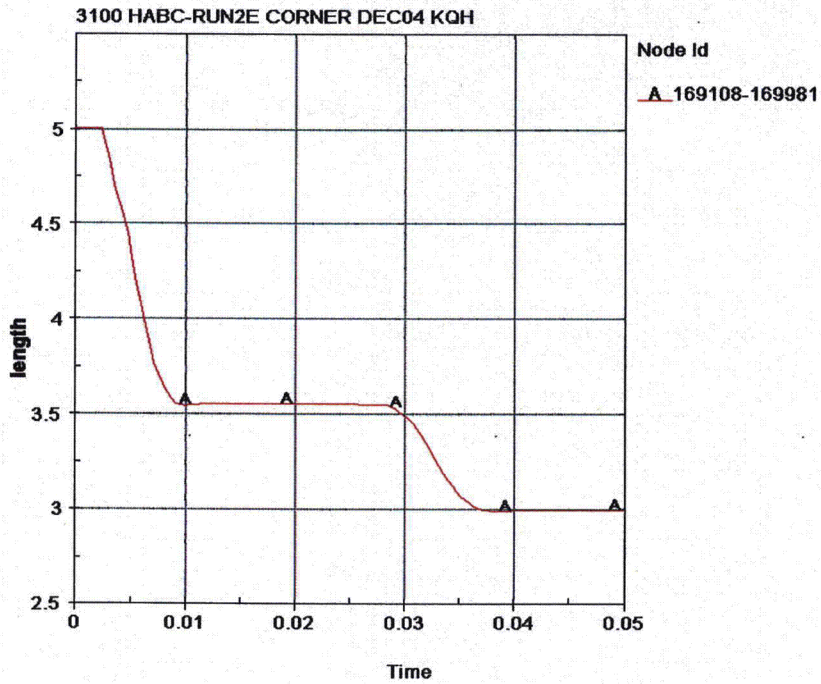


Figure 7.3.12 - HABC-run2e, Plug Thickness Time History

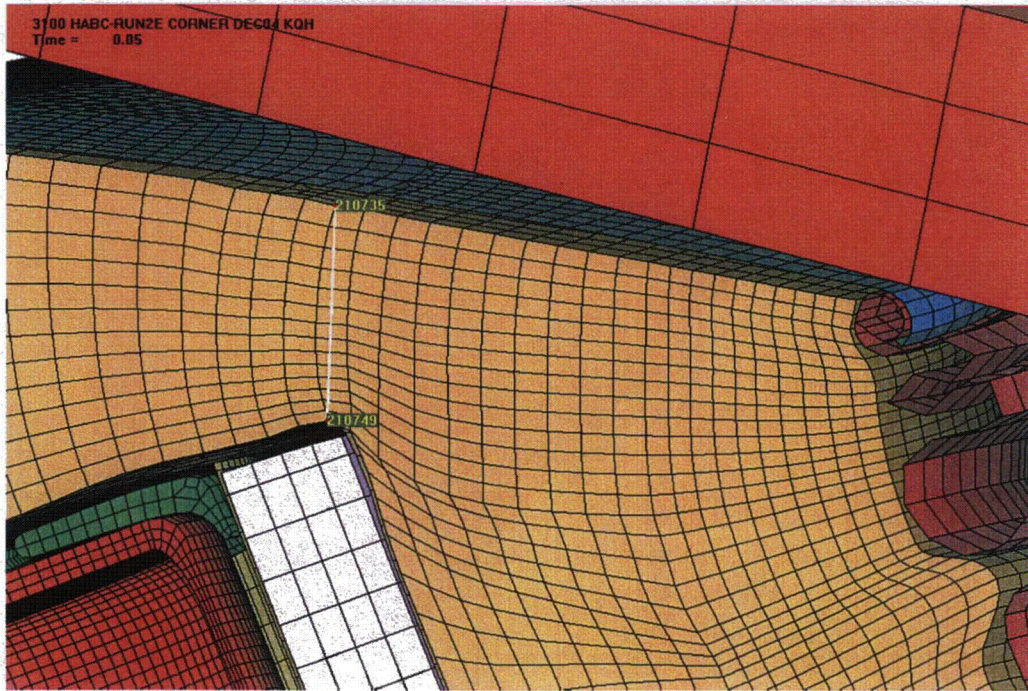


Figure 7.3.13 - HABC-run2e, Bottom Kaolite Thickness After the Crush Impact

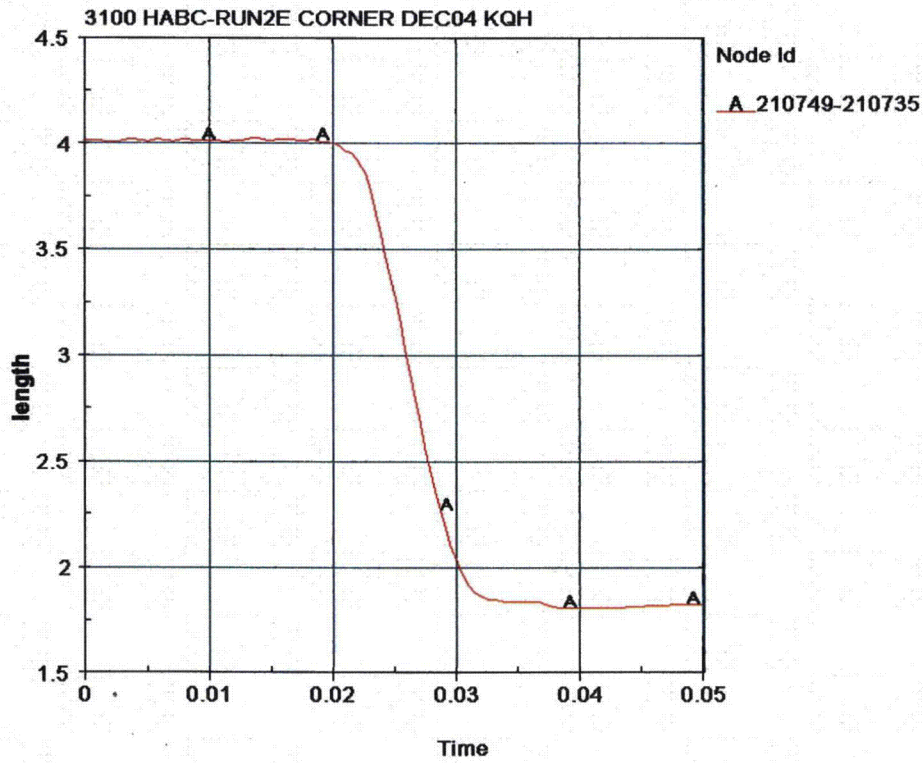


Figure 7.3.14 - HABC-run2e, Bottom Kaolite Thickness Time History

3100 HABC-RUN2E CORNER DEC04 KQH
Time = 0.05



Figure 7.3.15 - HABC-run2e, Length Dimensions in the Drum

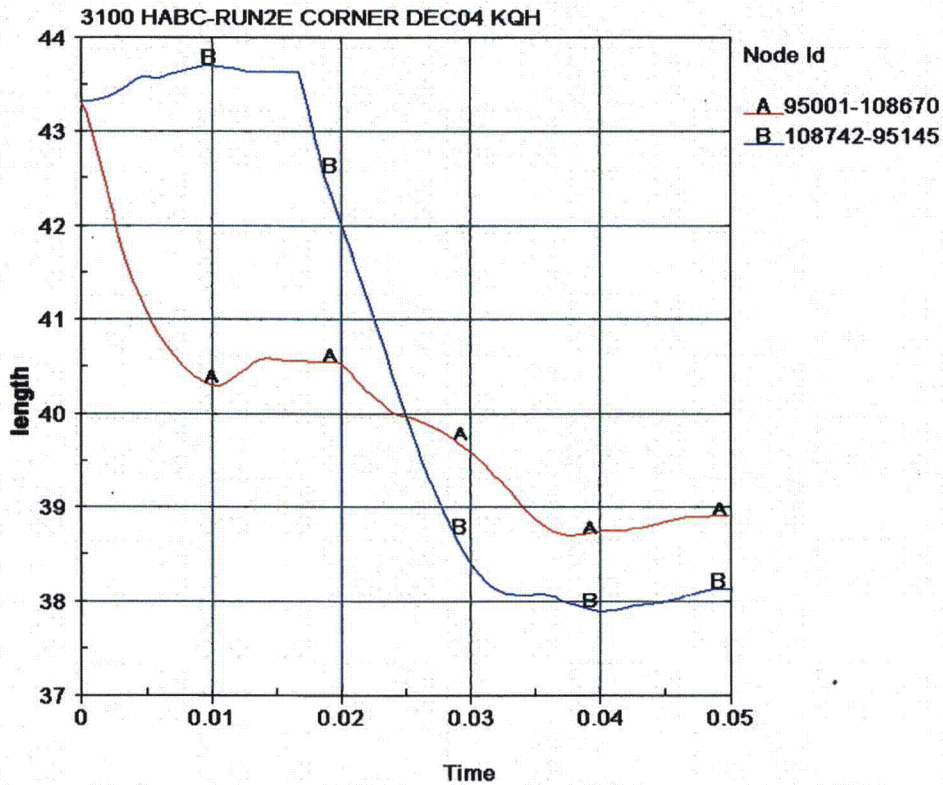


Figure 7.3.16 - HABC-run2e, Drum Length Time History

7.4 HABC-run3b - End

HABC-run3b is a 30-foot lid end impact (time = 0 to 0.010 seconds) followed by a crush impact onto the package bottom (0.010 to 0.028 seconds). Figure 7.4.1 shows the configuration of the container at the end of the 30-foot impact. Figure 7.4.2 shows that the maximum effective plastic strain in the CV body is 0.0028 in/in. The maximum plastic strain occurs in the bottom head. Figure 7.4.3 shows the CV lid. The maximum effective plastic strain is found to be 0.0072 in/in and occurs just outboard of the center boss on the outer surface.

The maximum effective plastic strain in the nut ring is shown to be 0.0011 in/in in Figure 7.4.4. It is believed this plastic strain is an anomaly with the contact surface because: 1) the fringes of plastic strain are not symmetrical, 2) the maximum value of plastic strain occurs at single nodes on an edge of the component and 3) the nut ring bares on the relatively soft silicone pad. Table 7.4.1 summarizes the maximum effective plastic strains in the other package components.

Component	Effective Plastic Strain, in/in
Angle	0.0287
Drum	0.0557
Drum Bottom Head	0.0031
Liner	0.0607
Lid	0.1082
Lid Stiffener	0.0069
Lid Studs	0.0962
Lid Stud Nuts	0.0166
Lid Stud Washers	0.0506
Plug Liner	0.0670

Figure 7.4.5 shows the final configuration for the successive crush impact. Figure 7.4.6 shows that the maximum effective plastic strain in the CV body is 0.0083 in/in. The ring of plastic deformation in the sidewall at the bottom head is due to the bending of the bottom head. The other components are summarized in Table 7.4.2.

Table 7.4.2 - HABCrun3b, Crush Impact, Effective Plastic Strain Levels in Some Components	
Component	Effective Plastic Strain, in/in
CV Lid	0.0072
CV Nut Ring	0.0011
Angle	0.0308
Drum	0.1237
Drum Bottom Head	0.0267
Liner	0.3812
Lid	0.1389
Lid Stiffener	0.0100
Lid Studs	0.1535
Lid Stud Nuts	0.0173
Lid Stud Washers	0.0506
Plug Liner	0.0960

The CV lid separation time history is shown in Figure 7.4.7. The response during the 30-foot impact are separation spikes up to about 0.018 in with a general separation of about 0.012 in. The spikes occur for about 0.001 sec, while the general separation occurs for about 0.005 sec. During the crush impact, the gap response oscillates about values of general separation. The general separation remains below a gap of about 0.005 in.

Figure 7.4.8 shows the nodes chosen to observe the plug and bottom kaolite thicknesses and the overall drum height. Figure 7.4.9 shows the time history of the drum height. After the 30-foot impact and the successive crush impact, the drum height is found to be about 39 inches. Figure 7.4.10 shows the minimum plug thickness time history with Curve B. The minimum plug thickness after the 30-foot impact is about 3.75 in. The minimum plug thickness after the successive crush impact is about 3.4 in. Curve A shows the bottom kaolite minimum thickness is about 2.2 in after the crush impact.

3100 HABC-RUN3B END DEC 2004 KQH
Time = 0.01

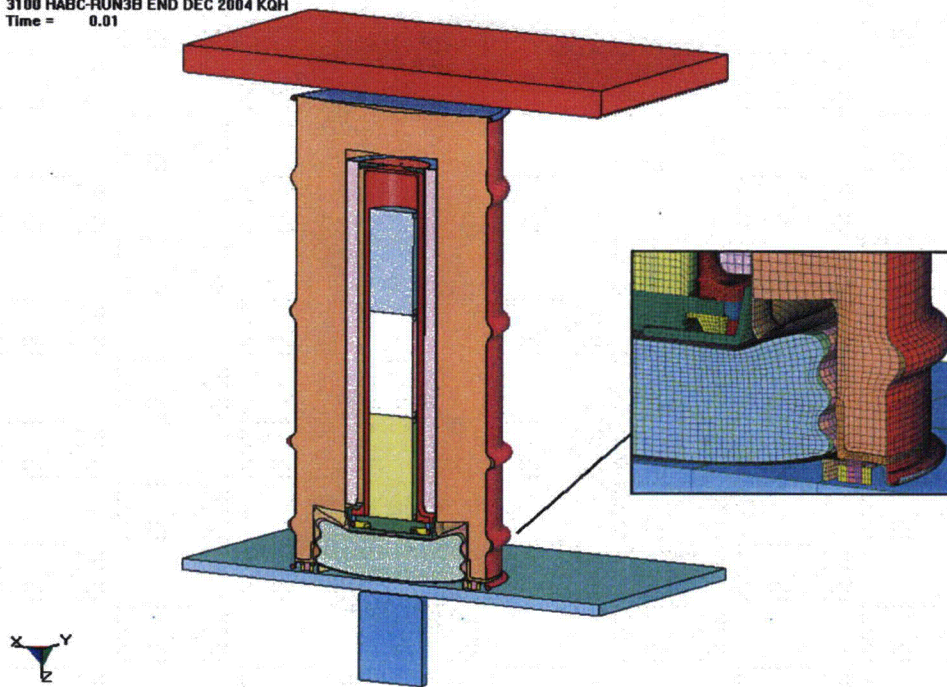


Figure 7.4.1 - HABC-run3b, Configuration After the 30-Foot Impact

3100 HABC-RUN3B END DEC 2004 KQH
Time = 0.01
Contours of Effective Plastic Strain
max ipt. value
min=0, at elem# 2
max=0.00277337, at elem# 468361

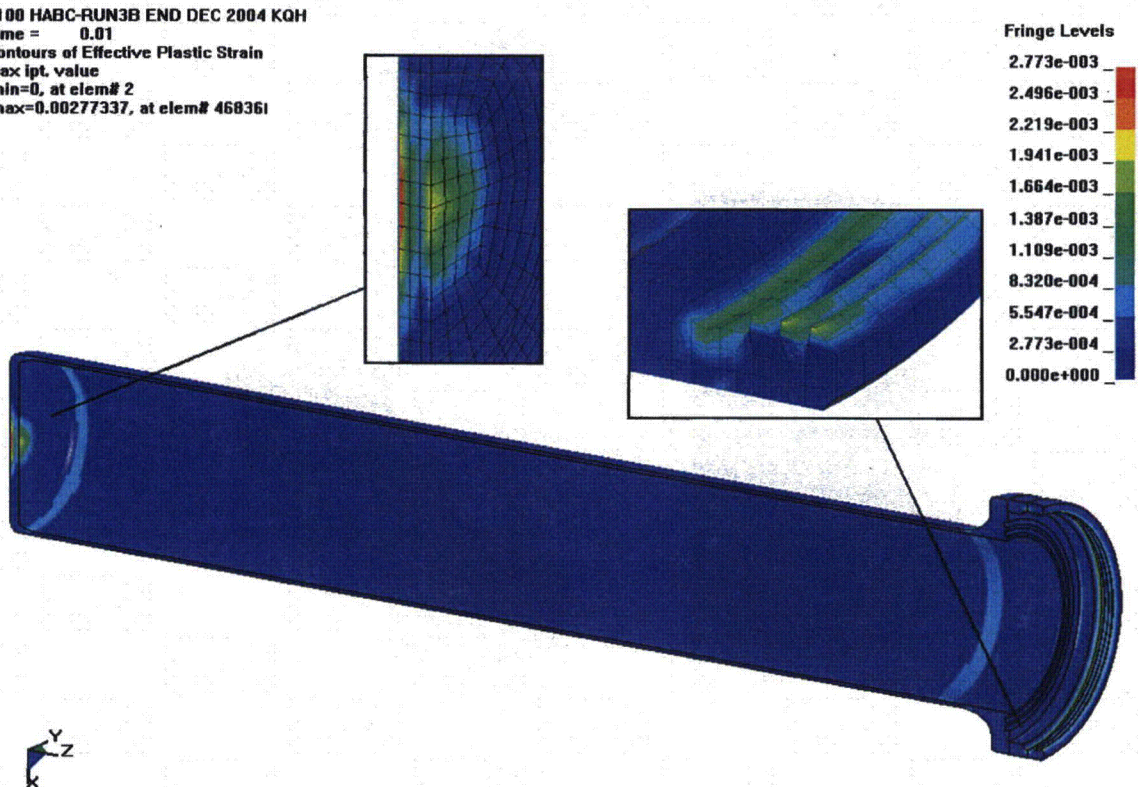


Figure 7.4.2 - HABC-run3b, 30-Foot Impact, Effective Plastic Strain in the CV Body

3100 HABC-RUN3B END DEC 2004 KQH
 Time = 0.01
 Contours of Effective Plastic Strain
 max ipt. value
 min=0, at elem# 52193
 max=0.00723051, at elem# 536011

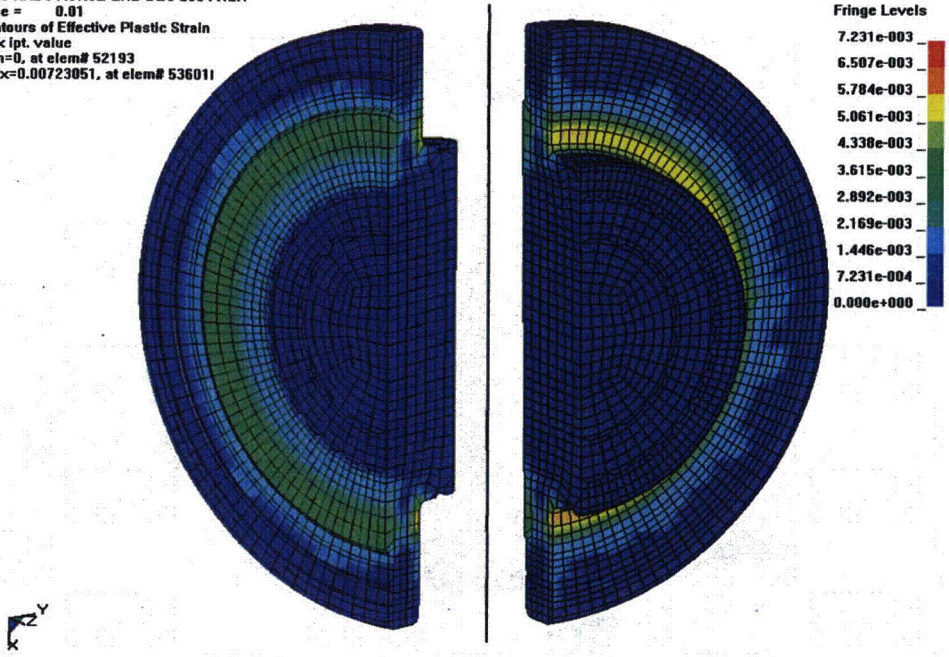


Figure 7.4.3 - HABC-run3b, 30-Foot Impact, Effective Plastic Strain in the CV Lid

3100 HABC-RUN3B END DEC 2004 KQH
 Time = 0.01
 Contours of Effective Plastic Strain
 max ipt. value
 min=0, at elem# 47073
 max=0.00111111, at elem# 499641

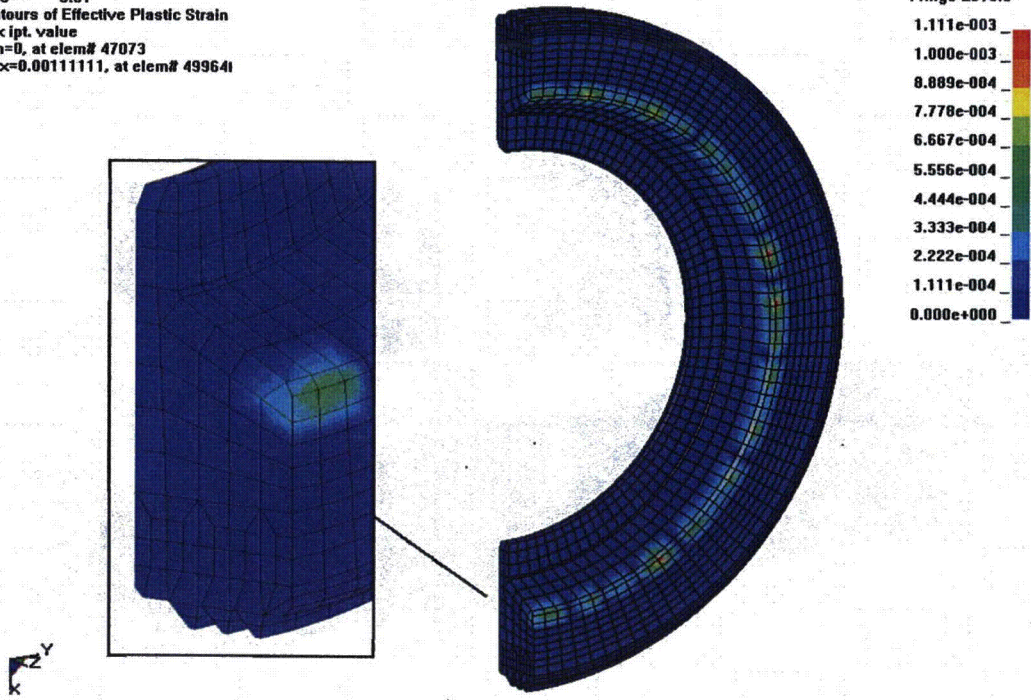


Figure 7.4.4 - HABC-run3b, 30-Foot Impact, Effective Plastic Strain in the CV Nut Ring

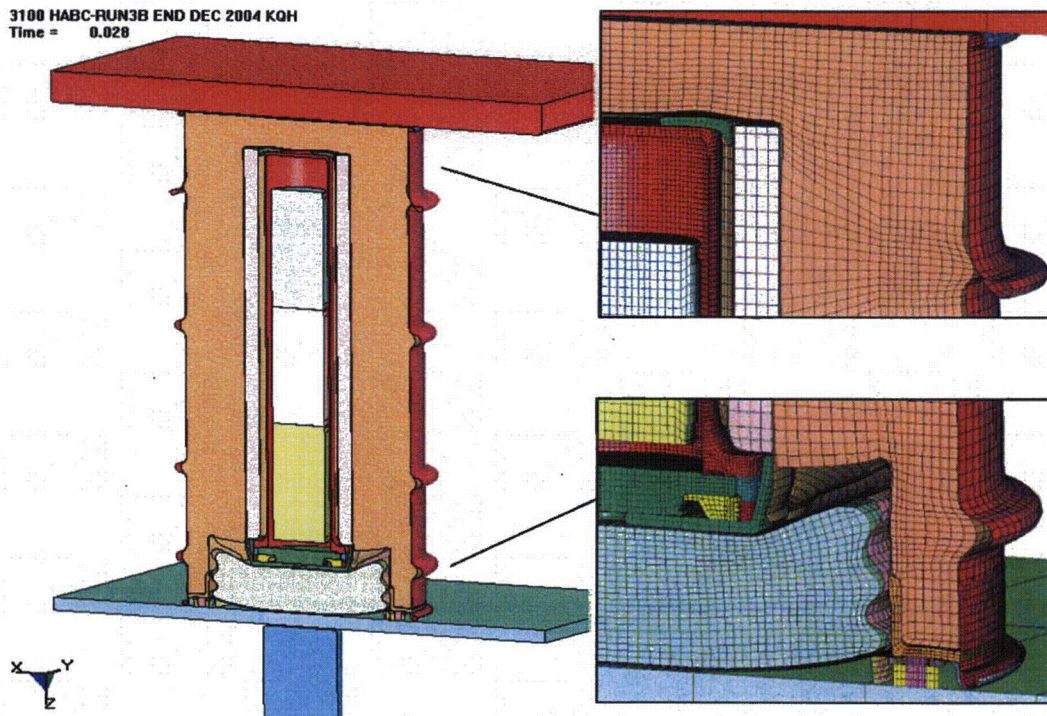


Figure 7.4.5 - HABC-run3b, Configuration After the Crush Impact

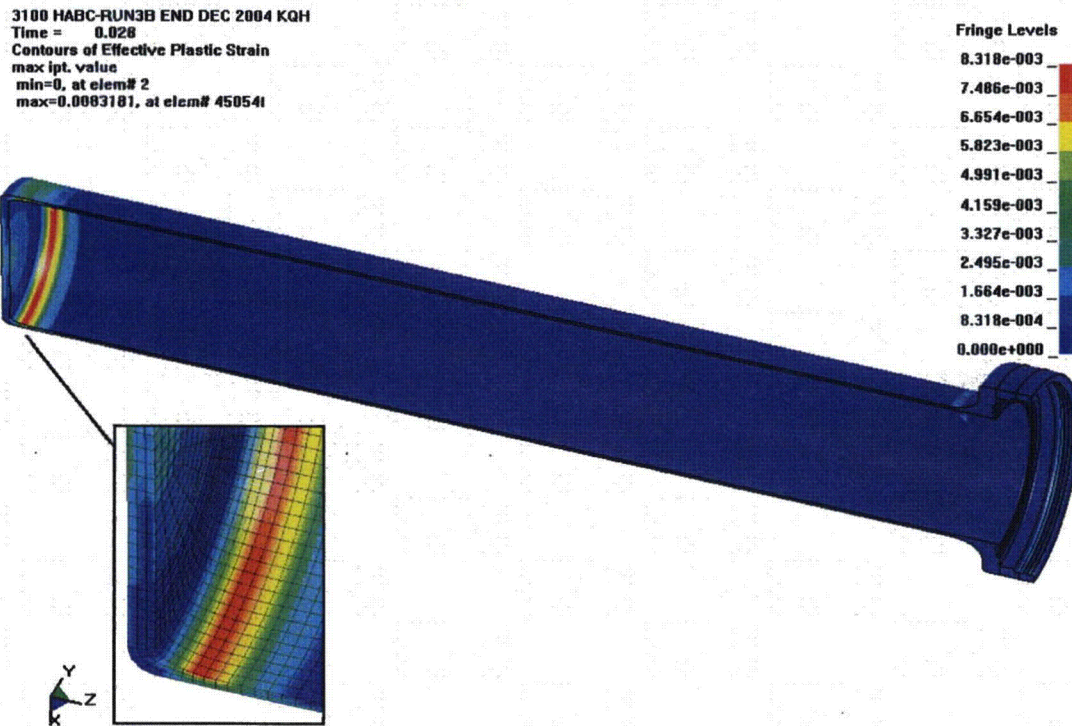


Figure 7.4.6 - HABC-run3b, Crush Impact, Effective Plastic Strain in the CV Body

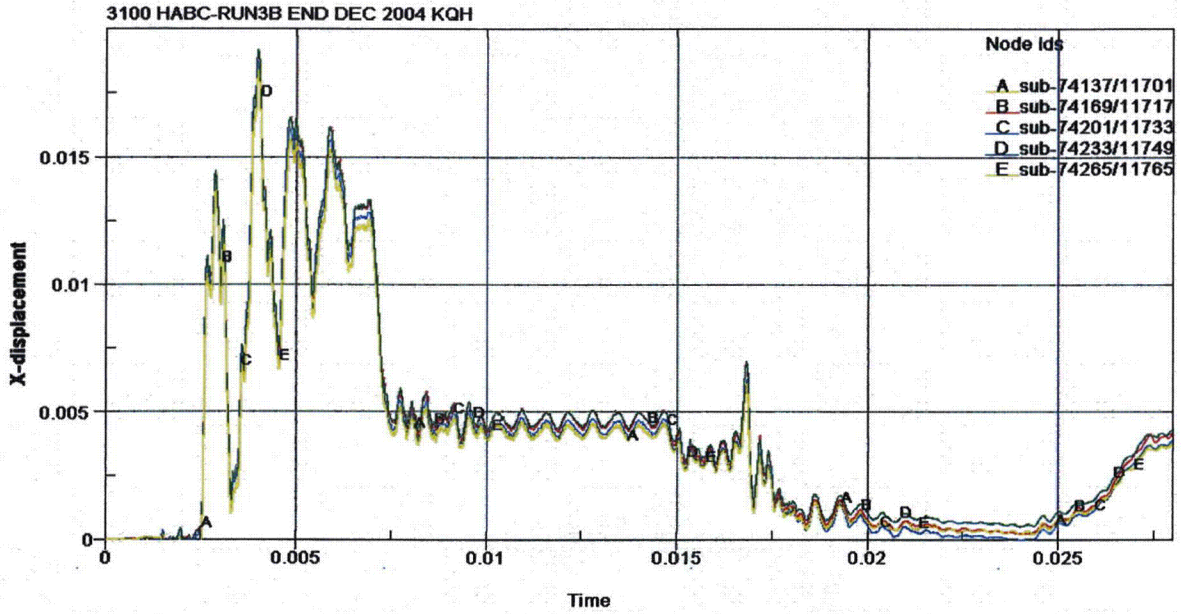


Figure 7.4.7 - HABC-run3b, CV Lid Separation Time History

3100 HABC-RUN3B END DEC 2004 KQH
Time = 0.028

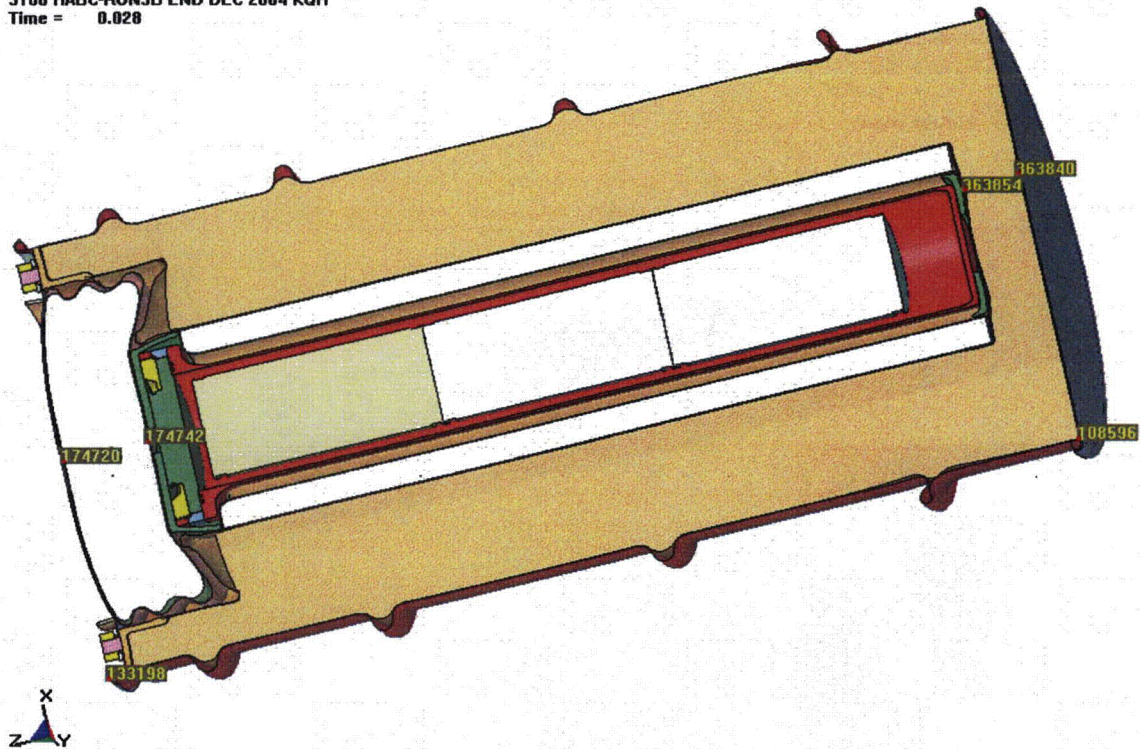


Figure 7.4.8 - HABC-run3b, Nodes to Determine Drum/Kaolite Heights

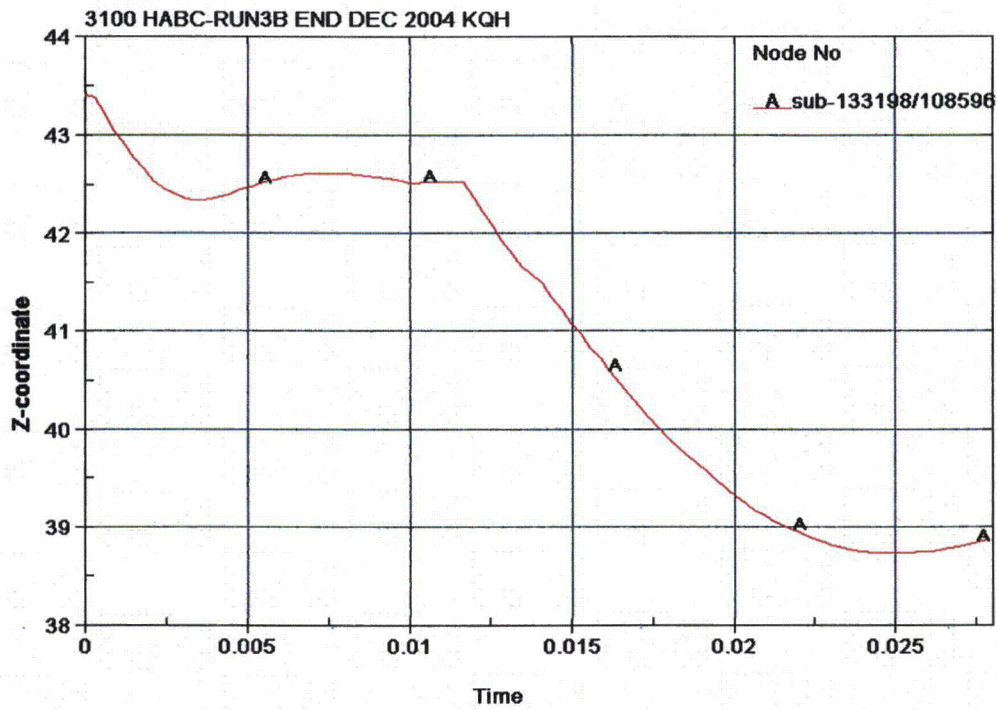


Figure 7.4.9 - HABC-run3b, Drum Height Time History

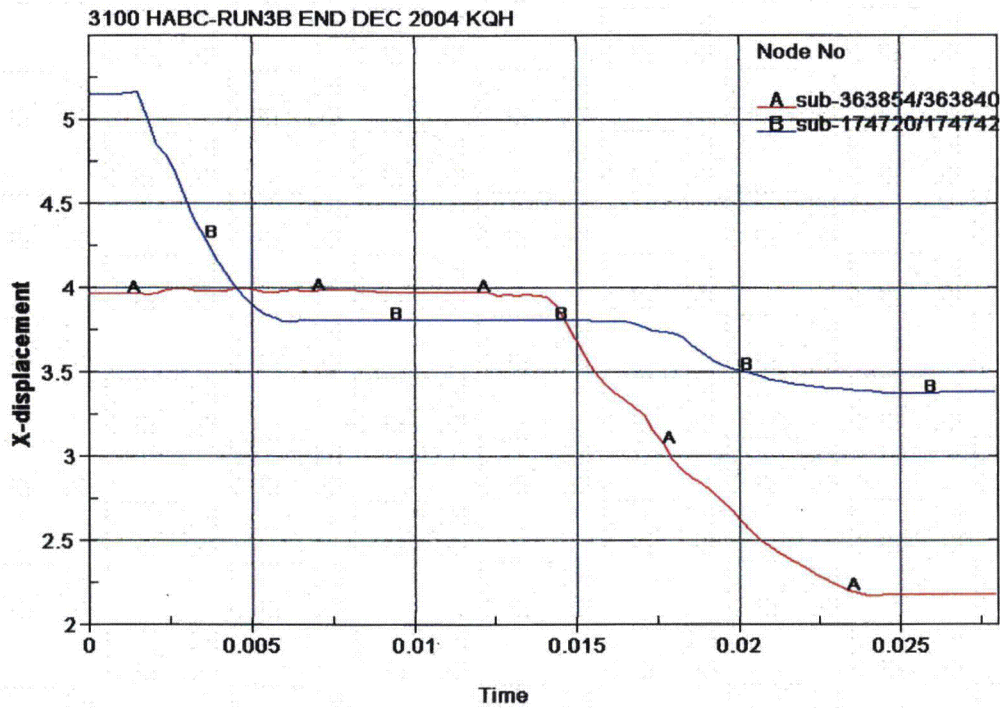


Figure 7.4.10 - HABC-run3b, Kaolite Thickness Time Histories

7.5 HABC-run4g - Slapdown

HABC-run4g is a 12° slapdown, 30-foot impact (time 0 to 0.02 seconds) followed by an offset crush with the crush plate CG over the CV flange (0.0202 to 0.04 seconds). From 0.0200 to 0.0202 sec, the crush plate is moved (via nodal velocities) such that its geometric center is approximately in line with the CV flange.

The initial configuration of the model is shown in Figure 7.5.1. The deflected shape of the package after the 30-foot impact is shown in Figure 7.5.2. Figure 7.5.3 shows enlargements of the corners of the package due to the 30-foot slapdown impact. The maximum effective plastic strain in the CV body for the 30-foot impact is 0.0376 in/in and occurs below the flange and nearest the impacted rigid surface as shown in Figure 7.5.4. Figure 7.5.5 shows that the maximum effective plastic strain in the drum is 0.3018 in/in. The maximum occurs at the bottom drum roll attachment to the drum, as is shown by the element number in the enlargement of the base region of the drum. Figure 7.5.5 does not show this by color fringes due to the nodal averaging of adjacent elements by the plot routine. The maximum strain is a highly localized bending strain in the bottom drum roll. The maximum effective plastic strain in the lid is 0.5278 in/in as shown in Figure 7.5.6. The maximum occurs due to the bearing of the lid onto the stud at the 0° position. The maximum effective plastic strains in other components for the 30-foot impact are listed in Table 7.5.1.

Component	Effective Plastic Strain, in/in
CV Lid	0.0004
CV Nut Ring	0.0000
Angle	0.0900
Drum Bottom Head	0.2879
Liner	0.1458
Lid Stiffener	0.0213
Lid Studs	0.1892
Lid Stud Nuts	0.0000
Lid Stud Washers	0.0724
Plug Liner	0.1258

Figure 7.5.7 shows the initial configuration for the offset impact. Figure 3.5.8 shows the final configuration for the crush impact for run4g. Figure 3.5.9 shows enlargements of the package corners after the crush.

The maximum effective plastic strain in the CV body is 0.0564 in/in as shown in Figure 7.5.10. Figure 7.5.11 shows the maximum effective plastic strain in the drum to be 0.3920 in/in, and it occurs on the crush plate side of the drum at the attachment of the angle. Figure 7.5.12 shows the lid after the offset crush impact. The maximum bending effective plastic strain is 0.9689 in/in and occurs at the 90° stud hole. The fringe range in Figure 7.5.12 has been defined to show all values near 0.57 in/in in the color red. The maximum membrane strain is 0.8935 in/in and also occurs at the 90° stud hole. This extremely high level of plastic strain is the lid response to the package trying to ovalize due to the crush impact. Due to the extreme level of effective plastic strain (>0.57 in/in), some localized tearing of the lid would be expected.

Figure 7.5.13 shows the effective plastic strain in the drum studs at the end of the crush impact, 0.4018 in/in. The stud at the 90° position has failed (evident by removed element row at the base of the stud). All of the elements on the cross section at the stud base attachment to the angle reached the prescribed failure strain of 0.57 in/in and were deleted by LS-Dyna. Therefore, the 0.4108 in/in is the plastic strain of the remaining elements. The stud elements reach failure and elements begin to be deleted at about time = 0.0311 seconds. By 0.0319 seconds, all the elements on the stud cross section have been deleted by LS-Dyna.

The lid uses a power law material model, which does not allow material failure in the model. Investigation shows that the lid reaches 0.57 in/in in membrane at about 0.0272 seconds, a time at which the stud strain is about 0.2451 in/in. This demonstrates that the lid reaches failure levels before the stud and at a time which the stud effective plastic strain is relatively low. Therefore, it would be expected that the lid would tear before the stud reaches failure. Due to the extent of the effective plastic strain fringe patterns in the lid plus the conservative modeling of the stud relative to lid shear (Section 2.1 discussion), it is believed that the tearing would be local and that the lid (and by default the plug) would be restrained by the large washers. Table 7.5.2 shows the maximum effective plastic strain in the remainder of the package components for the crush impact.

Table 7.5.2 - HABC-run4g, Crush Impact, Effective Plastic Strain Levels in Some Components	
Component	Effective Plastic Strain, in/in
CV Lid	0.0013
CV Nut Ring	0.0001
Angle	0.1070
Drum	0.3920
Drum Bottom Head	0.2879
Liner	0.2060
Lid Stiffener	0.0894
Lid Stud Nuts	0.0028
Lid Stud Washers	0.0790
Plug Liner	0.2665

Figure 7.5.14 shows the CV lid separation time history. During the 30-foot impact, the maximum spikes reach the 0.0065 in range with a general gap of about 0.005 in reached. During the crush impact, the spikes in gap reach about 0.009 in, while the general separation is about 0.007 in. At the end of the crush impact, the separations appear oscillatory from 0.0 in to about 0.006 in, therefore if a permanent gap were to exist, the maximum separation would be about 0.003 in.

Figure 7.5.15 gives the kaolite thickness time history for chosen kaolite nodes. The nodes are given in Figure 7.1.16.

The nodes on the drum chosen to investigate the diameter/radius changes during the impact are shown in Figure 3.1.34. Figure 7.5.16 shows the drum diameter time histories in the X direction. Figure 7.5.17 shows the drum radial changes in the Y direction.

Figure 7.5.18 shows the diameter time history for the inner liner. The position of the nodes is shown in Figure 3.1.37 and Table 3.1.3.

3100 HABCRUN4G 12SLAP DEC 04 KQH
Time = 0

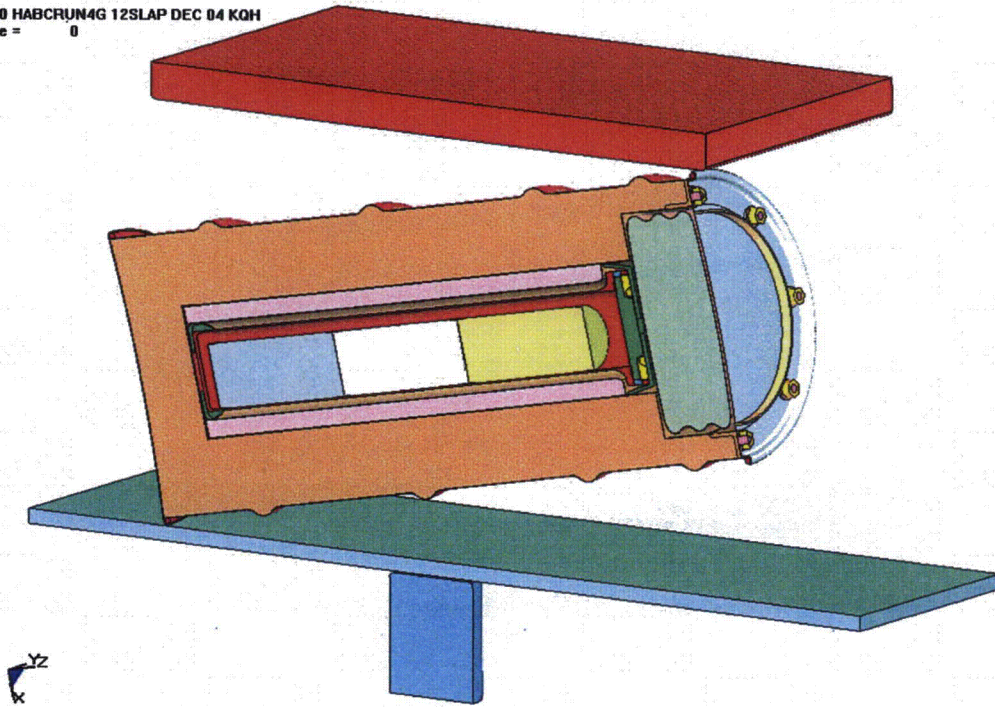
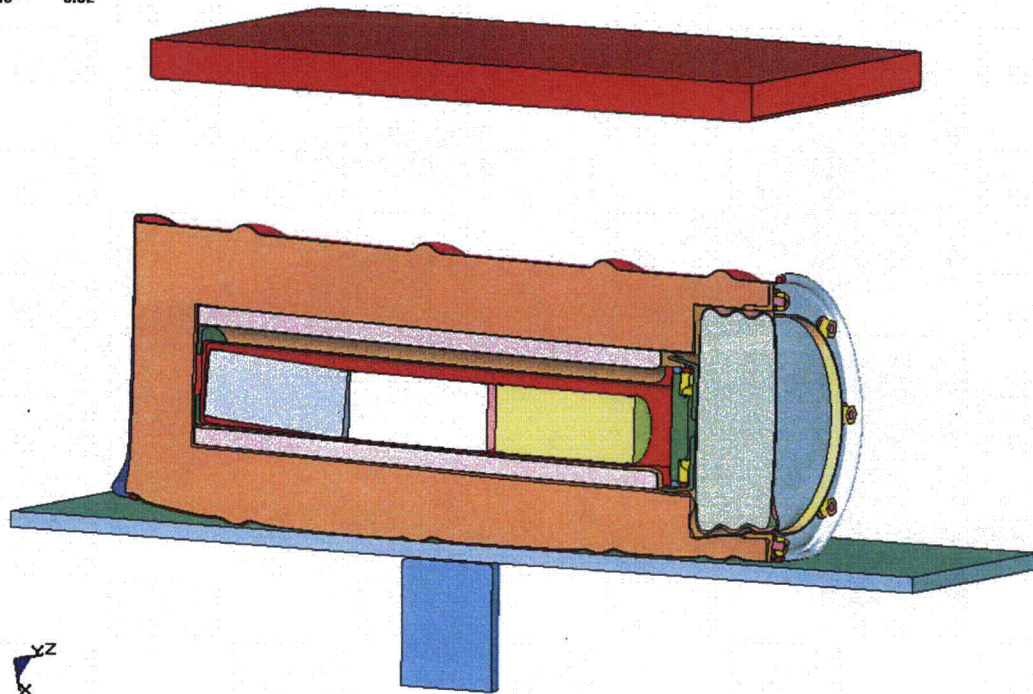


Figure 7.5.1 - HABC-run4g, 12 Degree Slapdown Initial Configuration

3100 HABCRUN4G 12SLAP DEC 04 KQH
Time = 0.02



7.5.2 - HABC-run4g, Configuration After the 30-Foot Impact

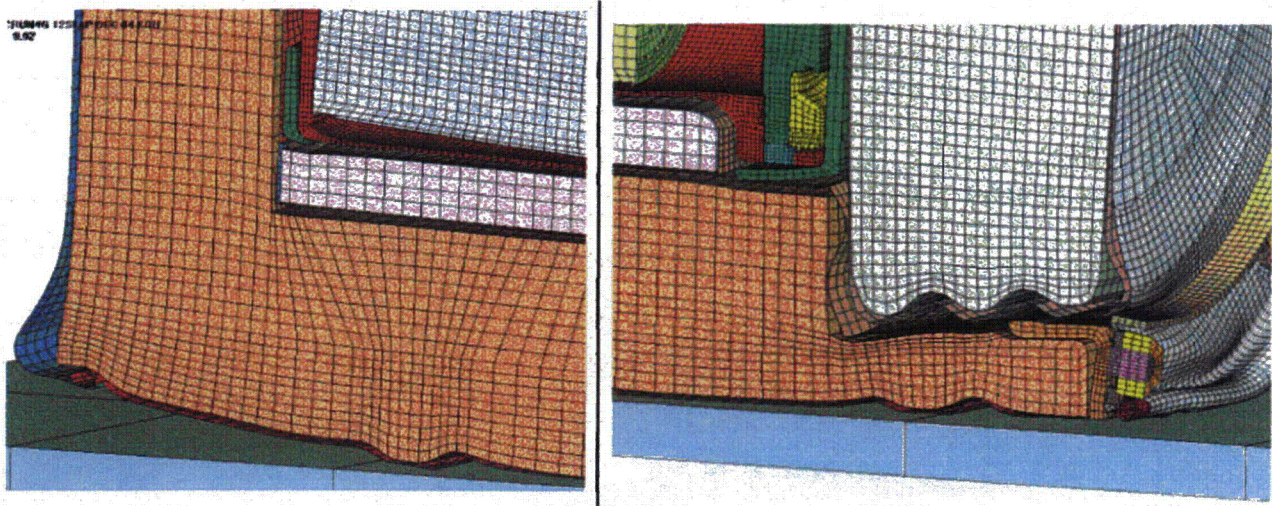


Figure 7.5.3 - HABC-run4g, 30-Foot Impact, Bottom and Lid Configurations

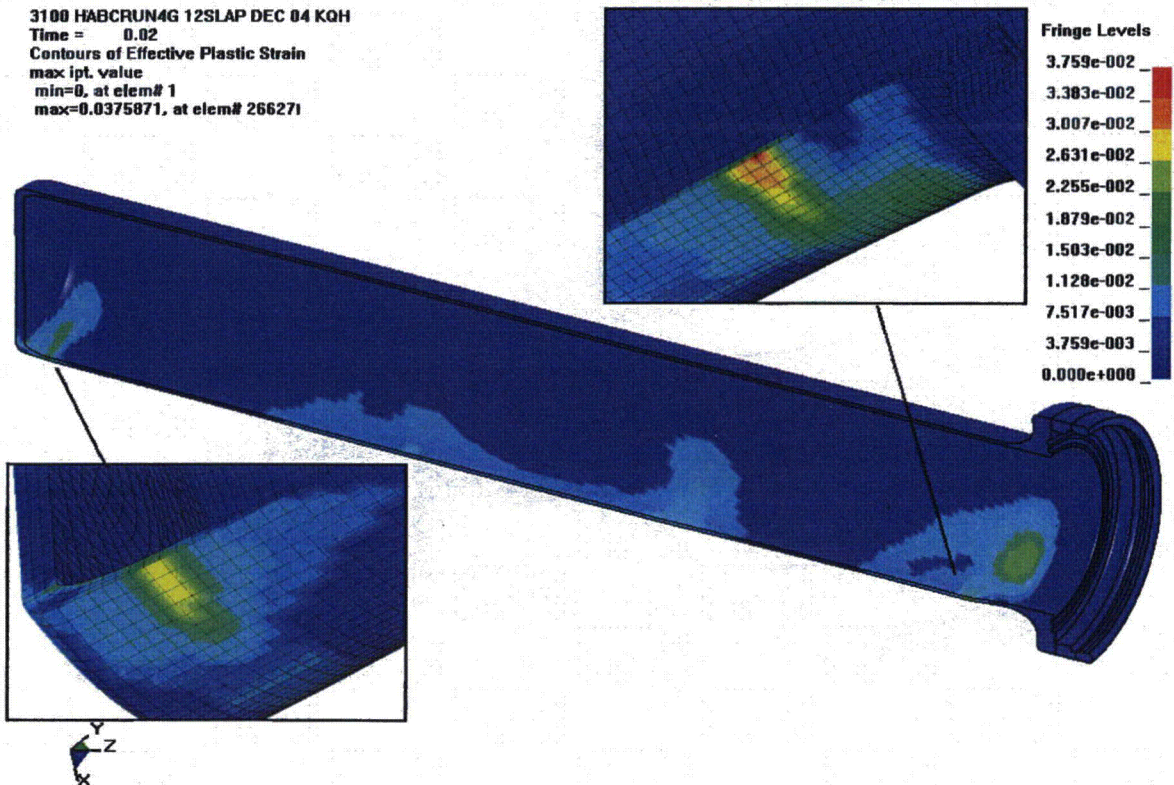


Figure 7.5.4 - HABC-run4g, 30-Foot Impact, Effective Plastic Strain in the CV Body

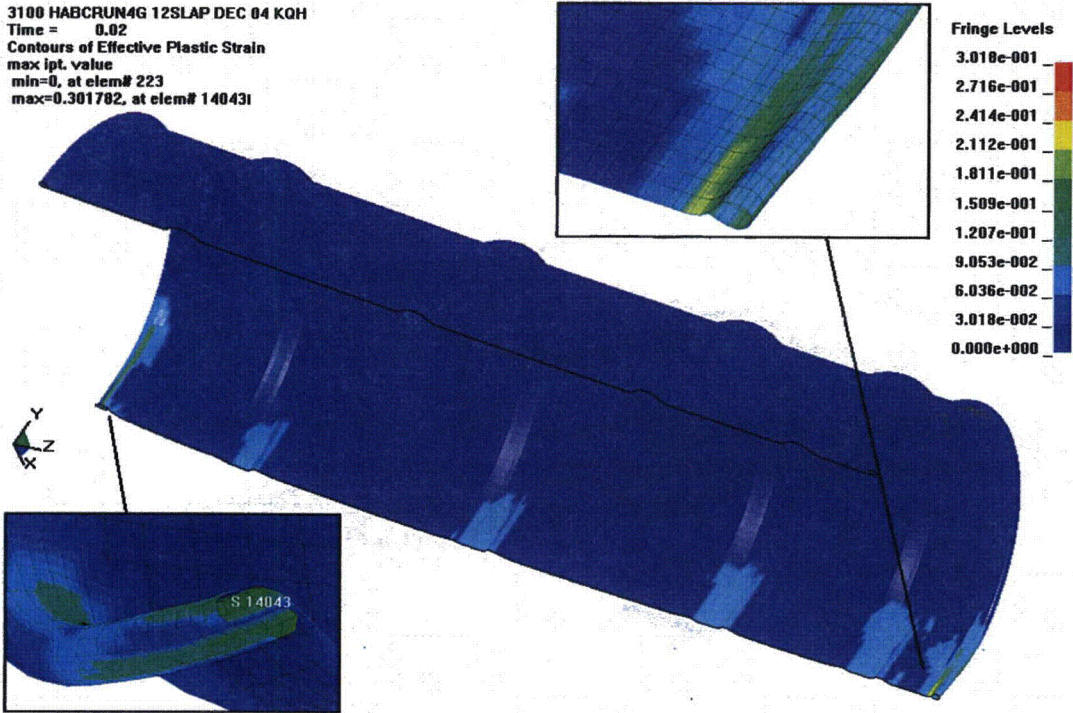


Figure 7.5.5 - HABC-run4g, 30-Foot Impact, Effective Plastic Strain in the Drum

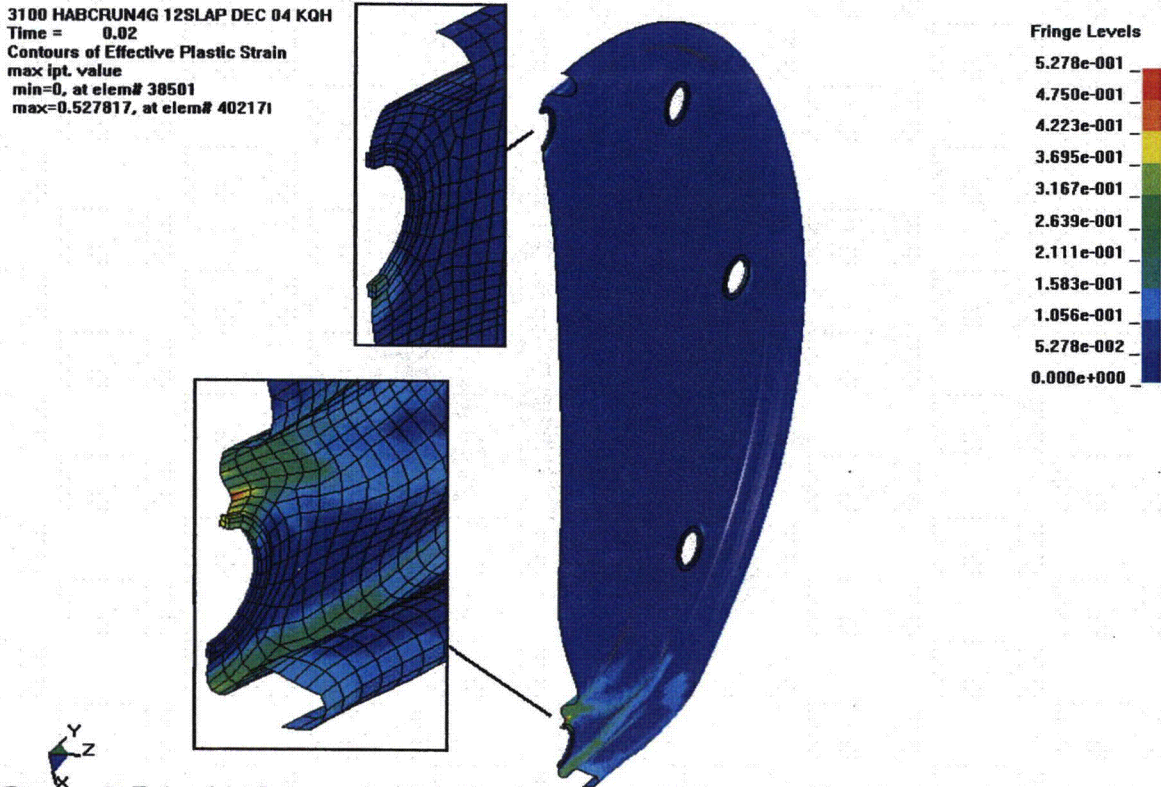


Figure 7.5.6 - HABC-run4g, 30-Foot Impact, Effective Plastic Strain in the Lid

3100 HABC RUN4G 12SLAP DEC 04 KQH
Time = 0.0204

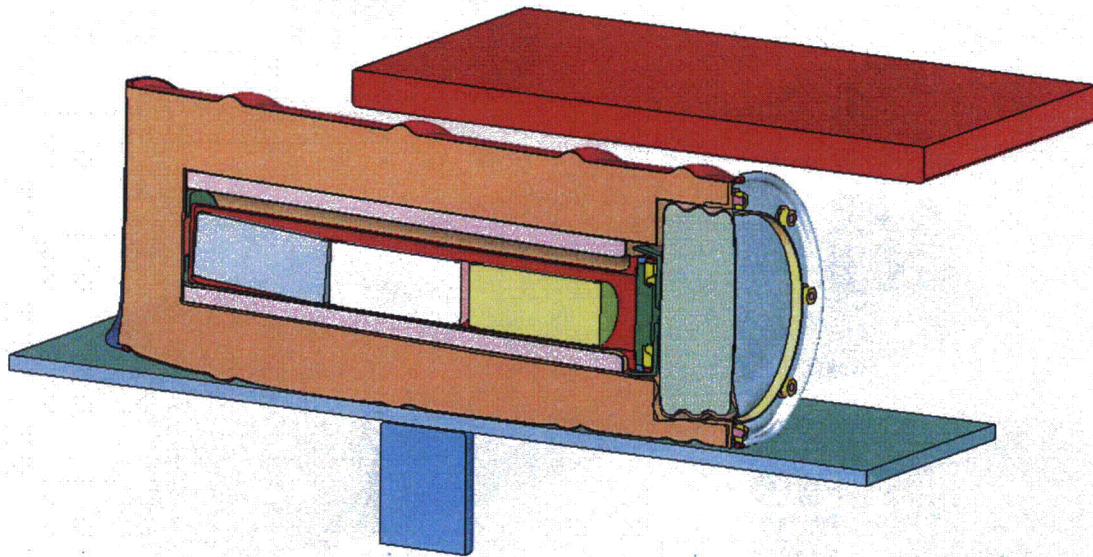


Figure 7.5.7 - HABC-run4g, Initial Configuration of the Offset Crush Impact

3100 HABC RUN4G 12SLAP DEC 04 KQH
Time = 0.04

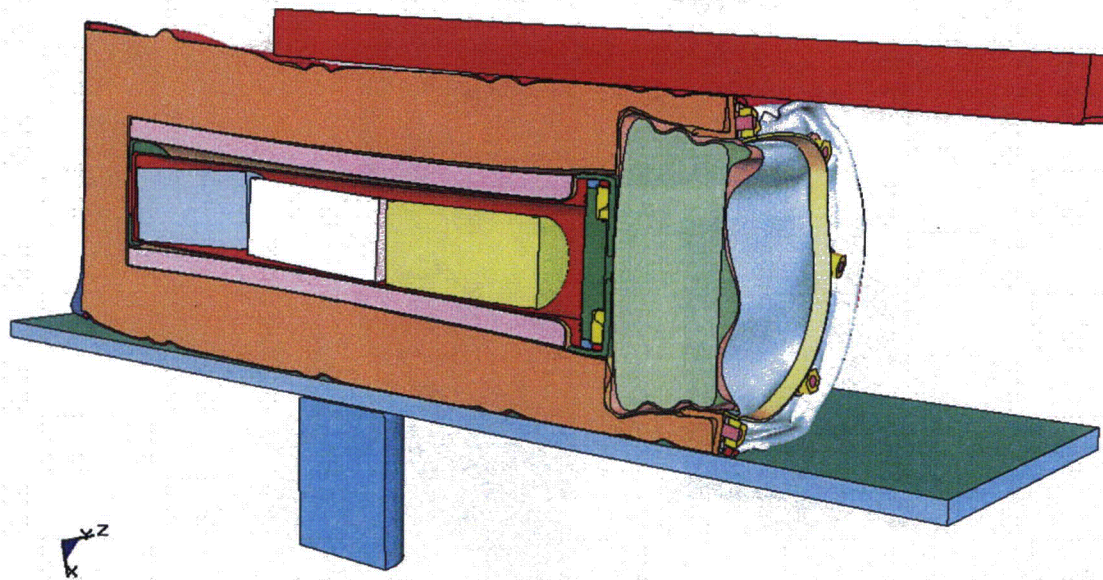


Figure 7.5.8 - HABC-run4g, Final Configuration After the Offset Crush Impact

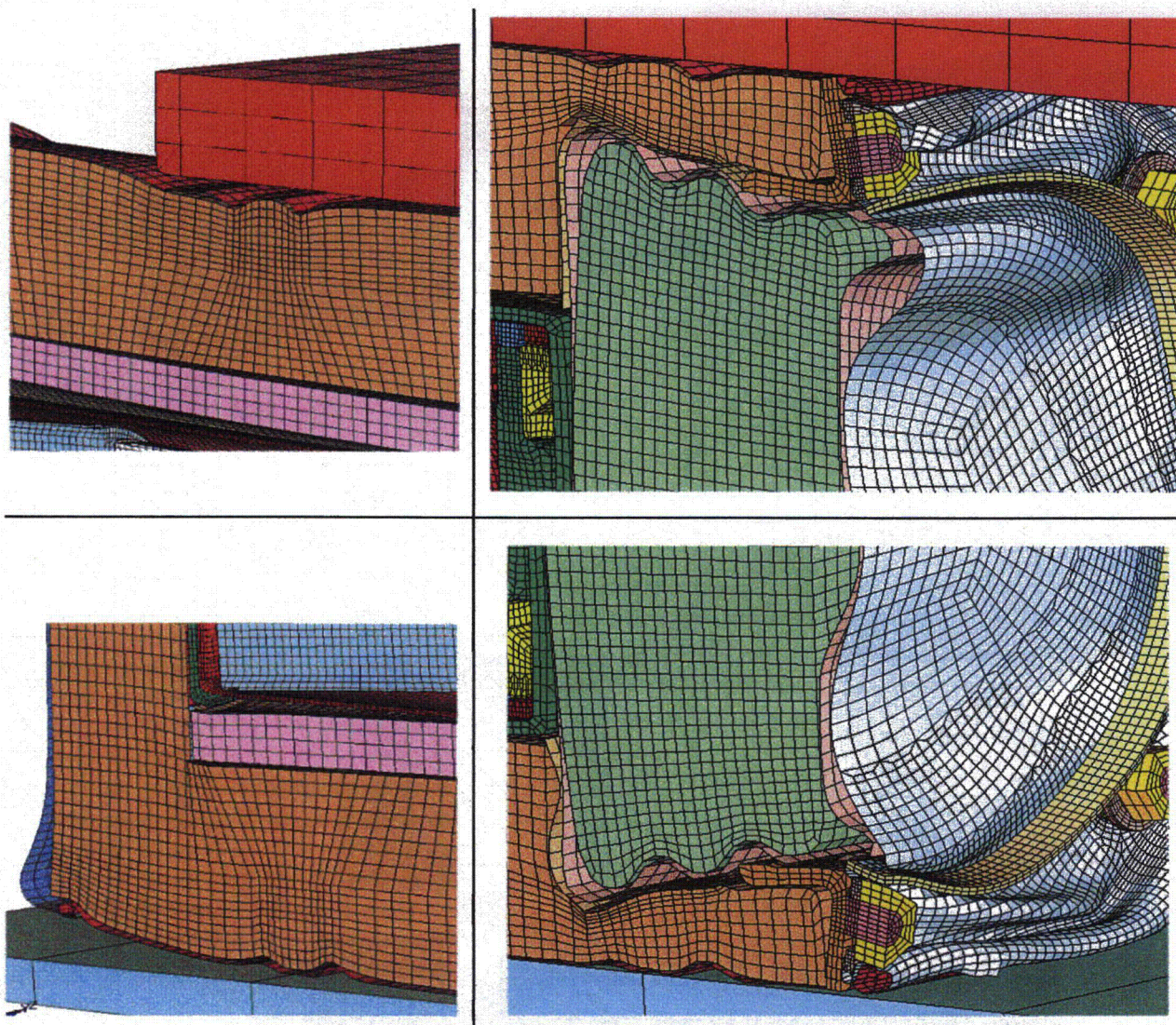


Figure 7.5.9 - HABC-run4g, Crush Impact, Enlarged Views of the Resulting Configuration

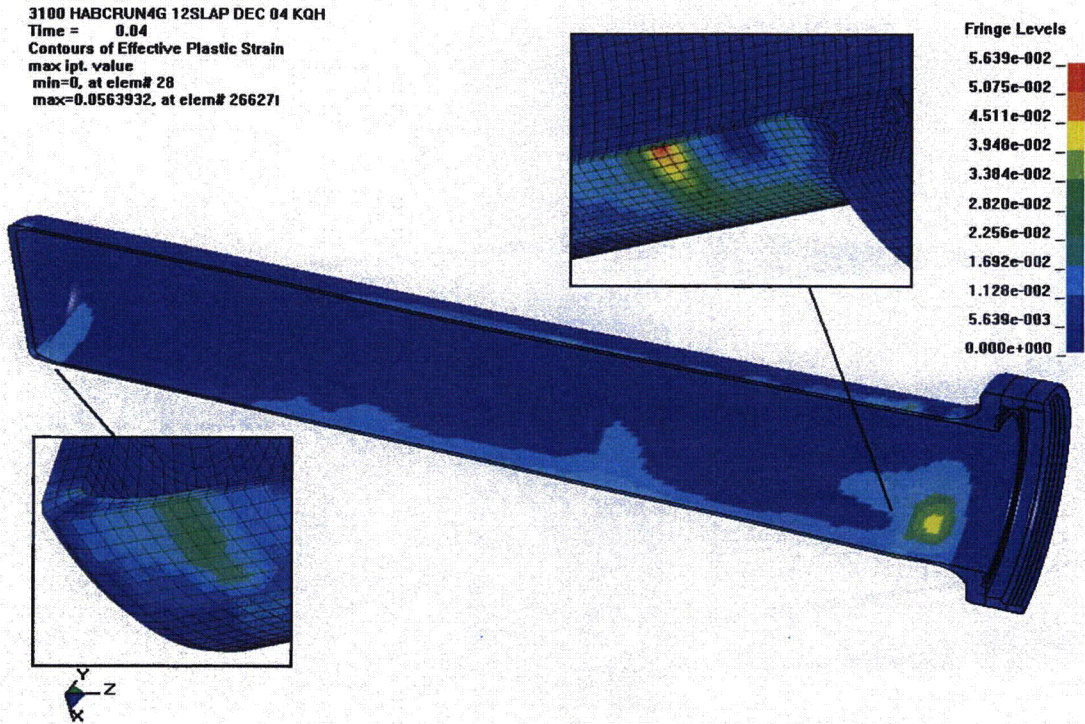


Figure 7.5.10 - HABC-run4g, Crush Impact, Effective Plastic Strain in the CV Body

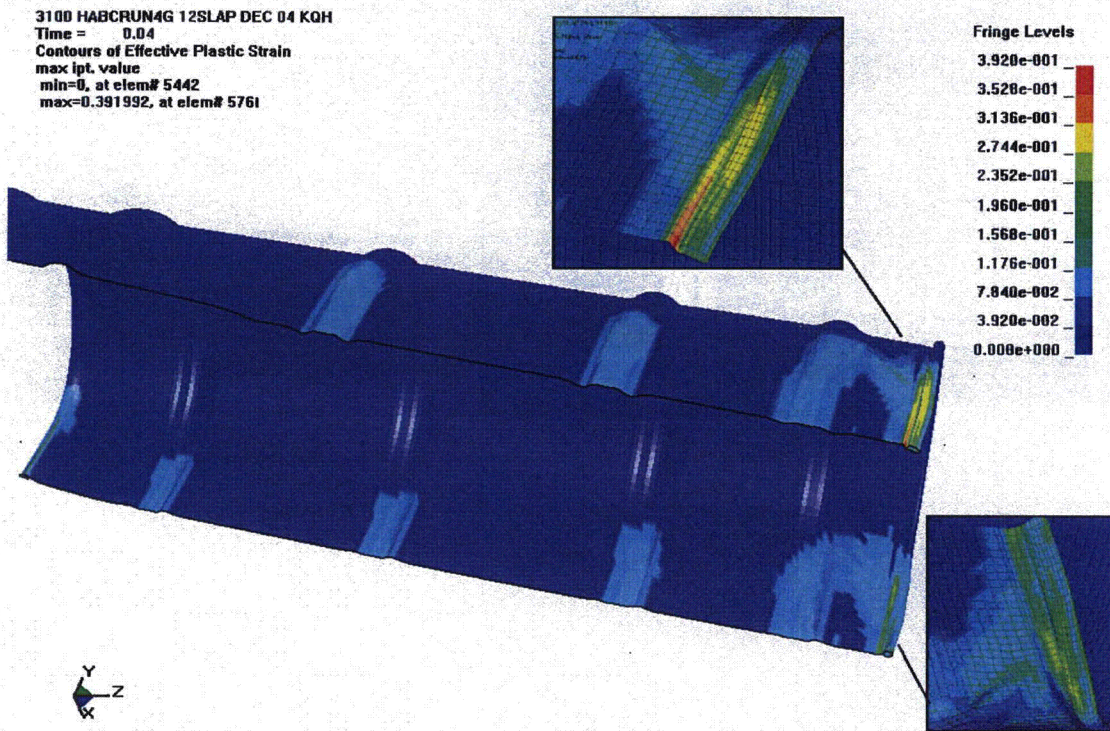


Figure 7.5.11 - HABC-run4g, Crush Impact, Effective Plastic Strain in the Drum

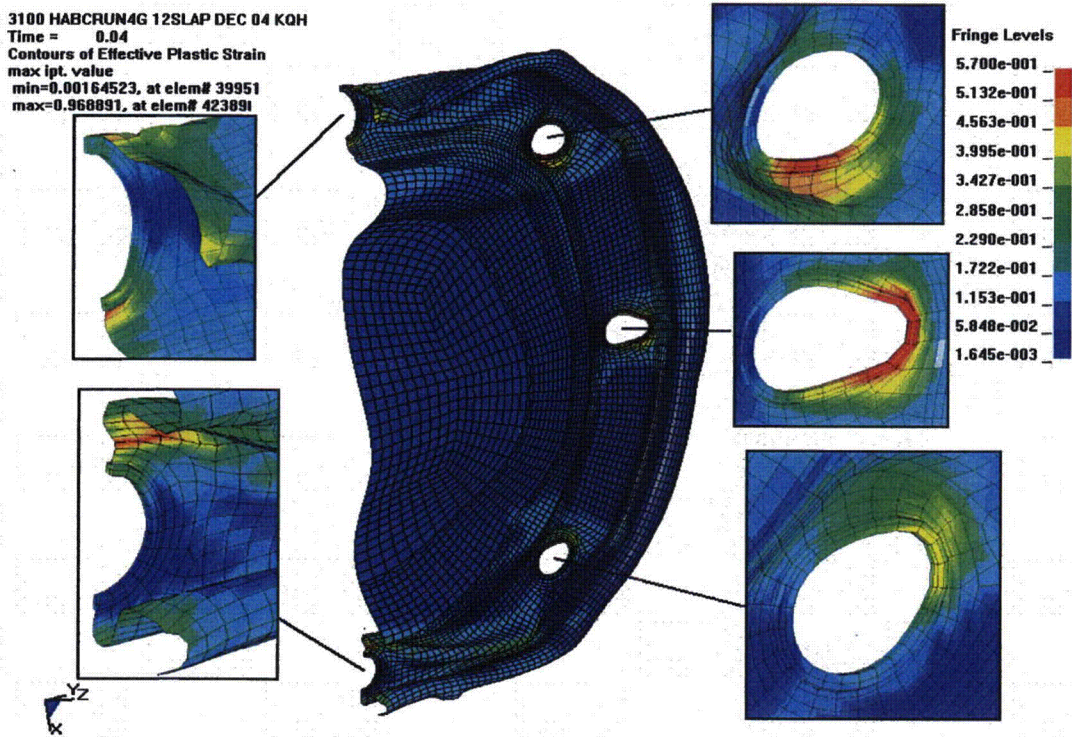


Figure 7.5.12 - HABC-run4g, Crush Impact, Effective Plastic Strain in the Lid

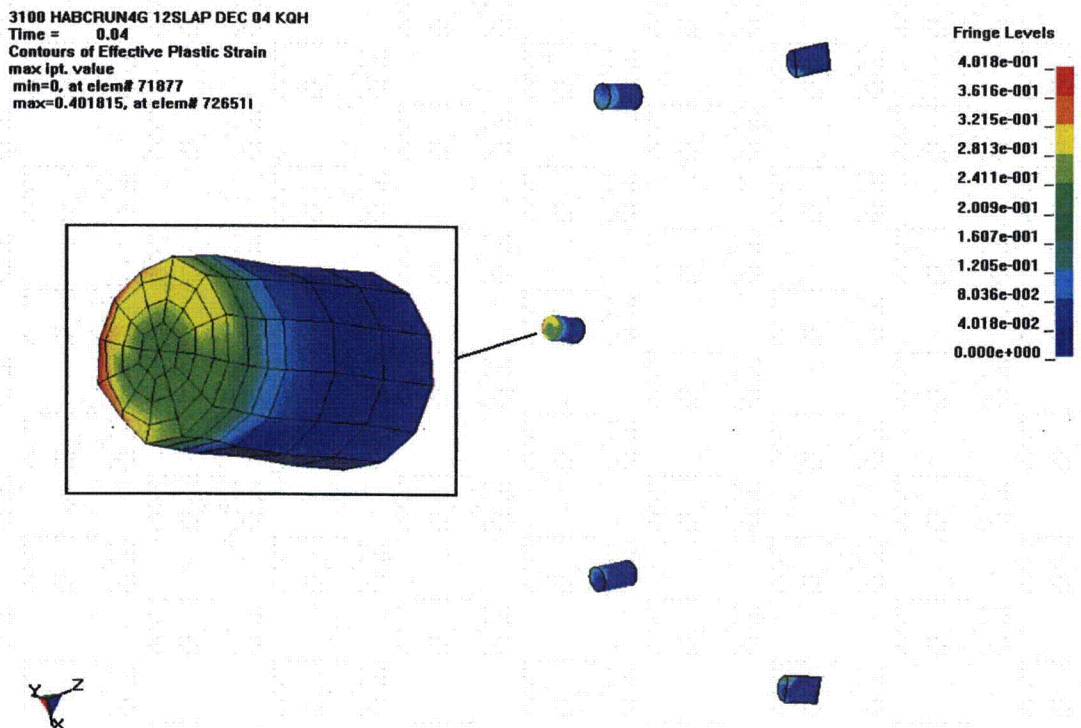


Figure 7.5.13 - HABC-run4g, Crush Impact, Effective Plastic Strain in the Studs

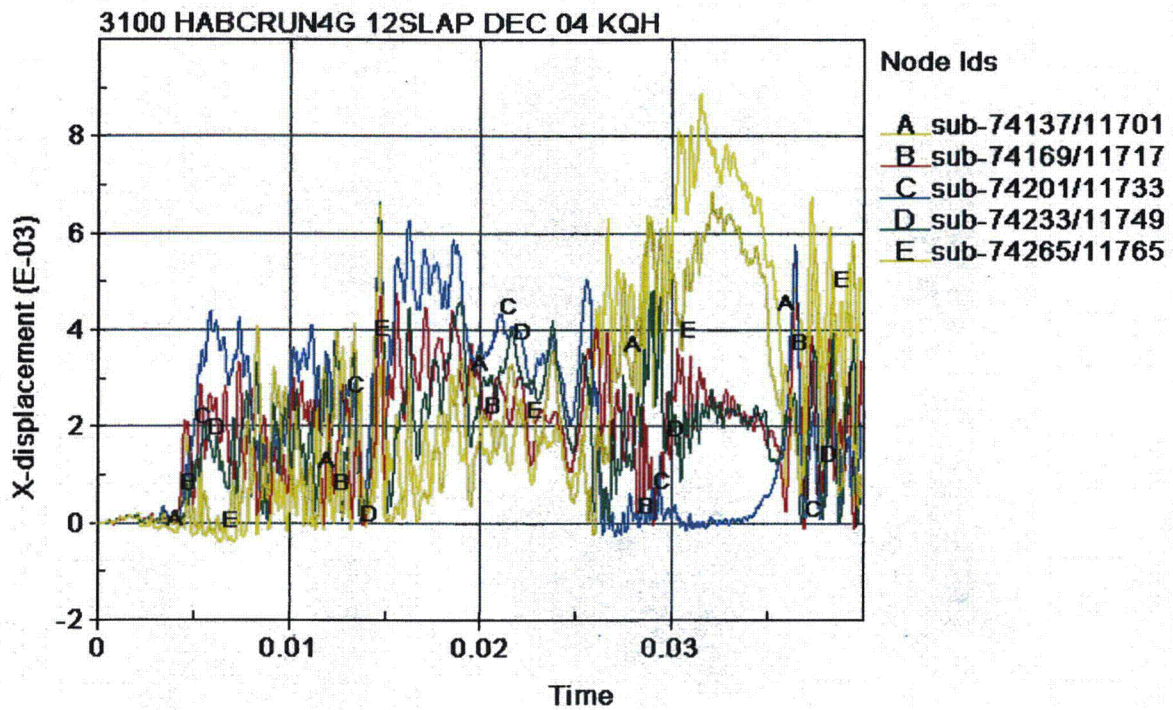


Figure 7.5.14 - HABC-run4g, CV Lid/Body Separation Time History

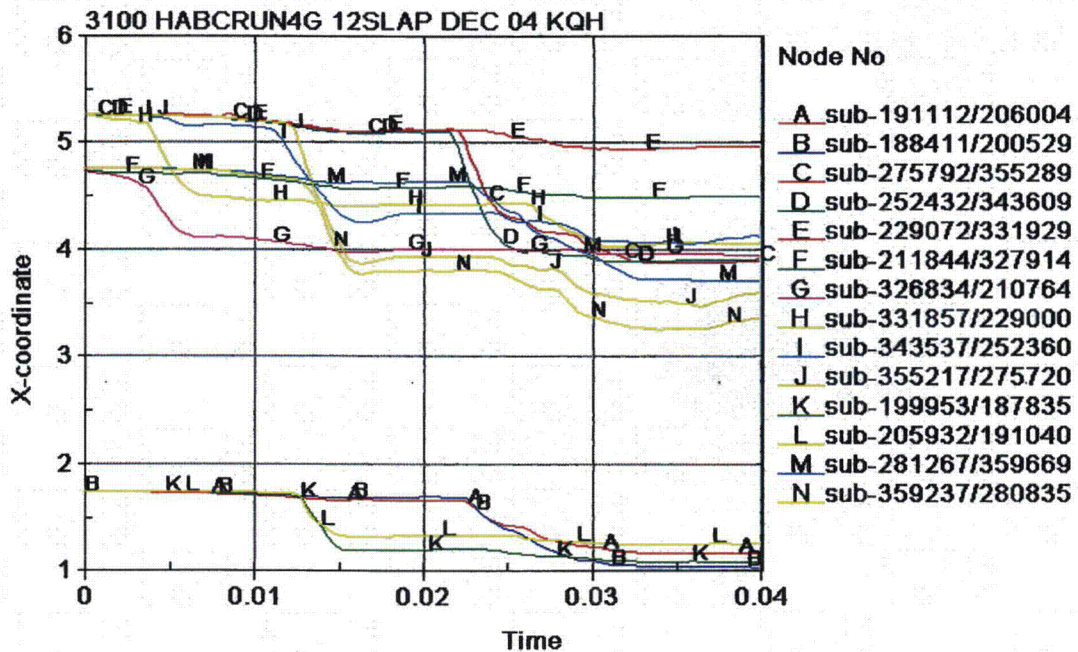


Figure 7.5.15 - HABC-run4g, Kaolite Thickness Time History

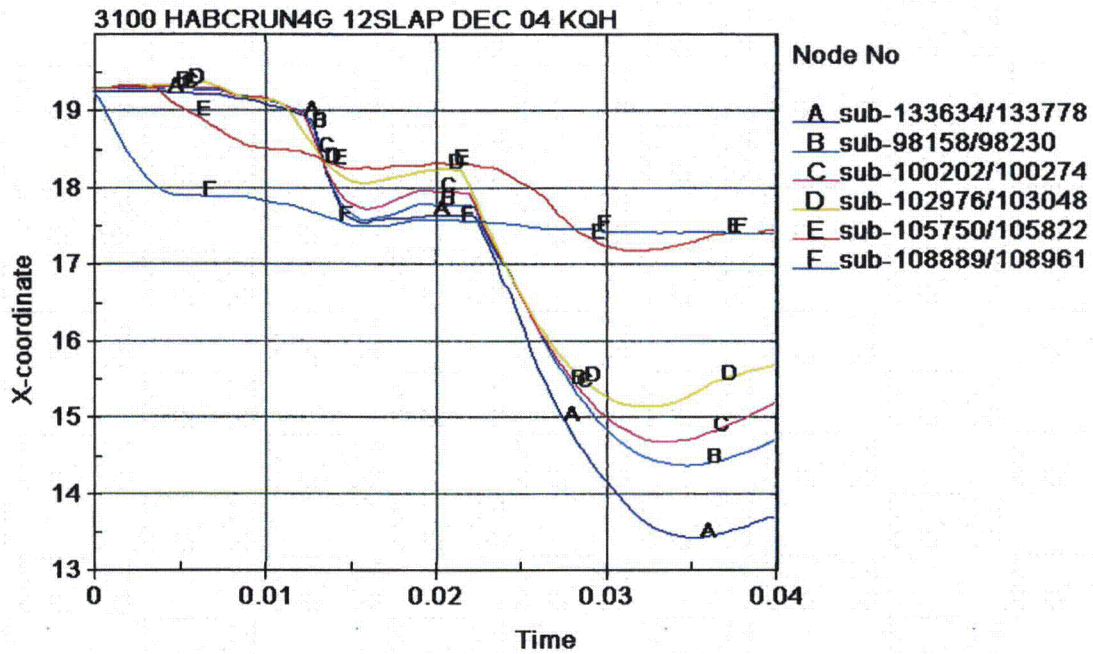


Figure 7.5.16 - HABC-run4g, Diameter Time History for the Drum in the X Direction

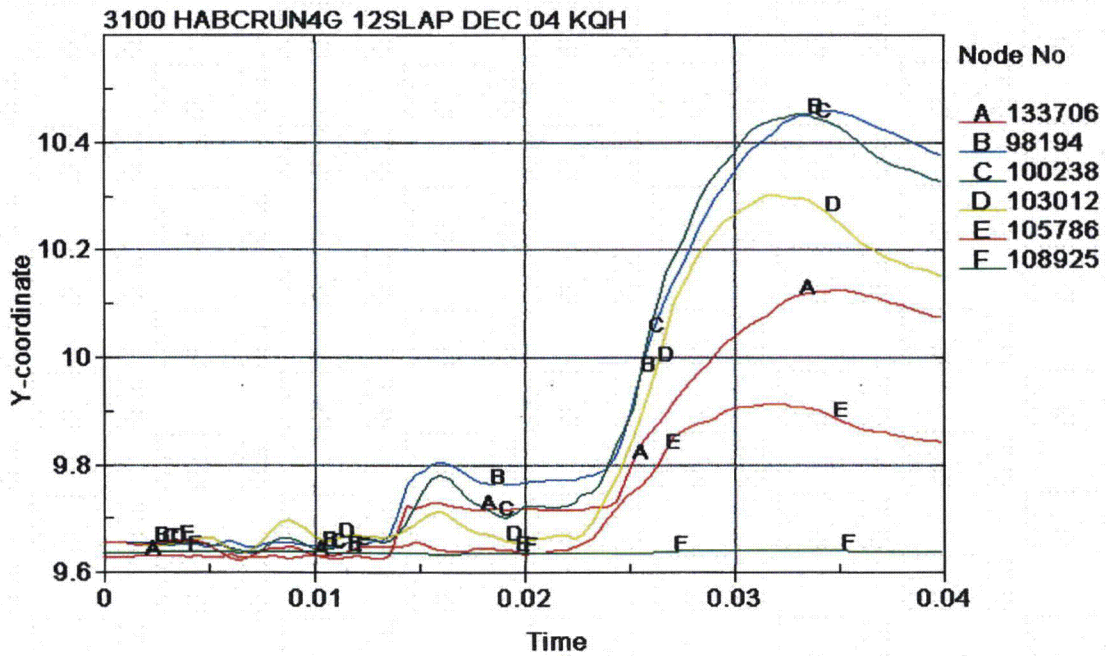


Figure 7.5.17 - HABC-run4g, Radius Time History for the Drum in the Y Direction

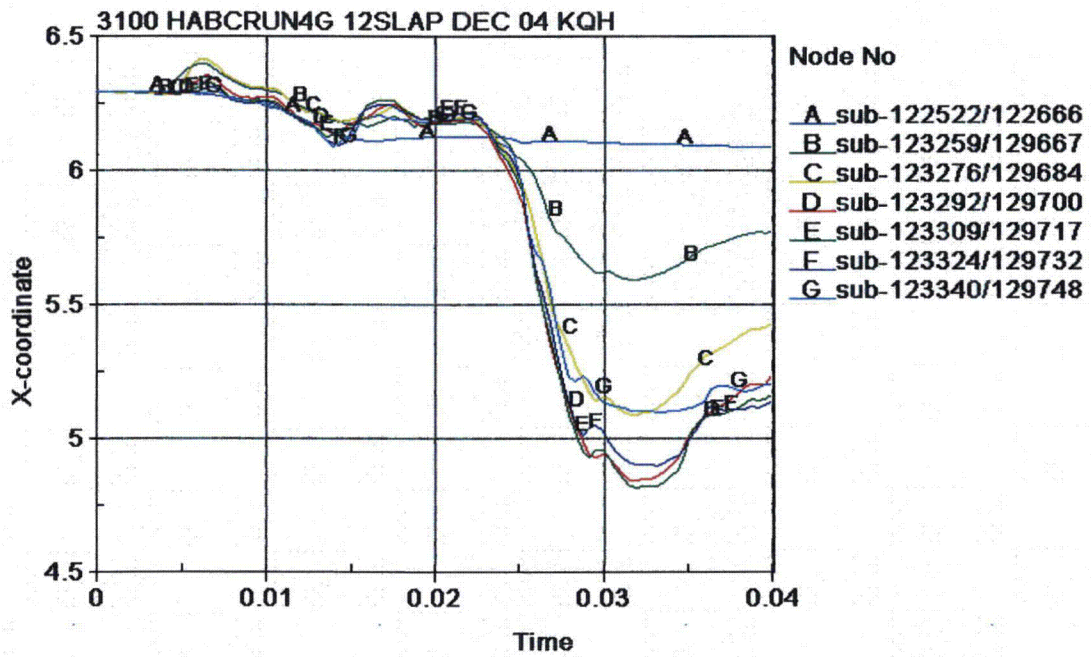


Figure 7.5.18 - HABC-run4g, Diameter Time History for the Inner Liner

7.6 HABC-run4ga - Slapdown

HABC-run4ga is a 30-foot, 12° slapdown impact (time - 0 to 0.02 sec) followed by a crush impact with the crush plate centered on the drum (0.0201 to 0.0400 sec). The HABC-run4g, 30-foot impact is the 30-foot impact for both the HABC-run4g offset crush and this HABC-run4ga centered crush. The difference between the 4g and 4ga impacts is the location to which the crush plate is moved by way of specifying velocities for specific times. In HABC-run4ga, the translation of the crush plate occurs from 0.02 to 0.0201 sec. Therefore, the 30-foot impact results are presented in Section 7.5 and the centered crush results are presented in this section (7.6).

The initial configuration for the start of the centered crush is shown in Figure 7.6.1. The final configuration for the HABC-run4ga crush impact is shown in Figure 7.6.2. Figure 7.6.3 shows the configuration at each end of the package following the centered crush impact.

The maximum effective plastic strain in the CV body is shown to be 0.0643 in/in in Figure 7.6.4. The maximum occurs in the body side wall, on the side nearest the crush plate. Figure 7.6.5 shows the fringes of effective plastic strain in the drum. The maximum strain in the drum is 0.3443 in/in and occurs near the lid in the crimped region shown in the enlarged view. Figure 7.6.6 shows that the maximum effective plastic strain in the lid is 0.5828 in/in. The maximum occurs at the 180° stud hole, and is localized. This value is a surface, or bending strain, the membrane strain is 0.4736 in/in. Therefore, the bending strain is above the failure limit of 0.57 in/in, however the membrane strain is below the limit. Some cracking may occur, but tearing of the lid is not expected. The large washers would provide restraint of the lid.

Table 7.6.1 presents the maximum effective plastic strain in other shipping package components for the run4ga crush impact.

Table 3.6.1 - Run4ga, Crush Impact, Effective Plastic Strain Levels in Some Components	
Component	Effective Plastic Strain, in/in
CV Lid	0.0018
CV Nut Ring	0.0000
Angle	0.0944
Drum Bottom Head	0.3000
Liner	0.2846
Lid Stiffener	0.0288
Lid Studs	0.2390
Lid Stud Nuts	0.0000
Lid Stud Washers	0.0775
Plug Liner	0.1644

The CV lid separation time history is shown in Figure 7.6.7. For the crush impact (0.0201 to 0.0400 sec) the spikes in the gap reach just over 0.01 in. The general gap during the impact reaches about 0.009 in. At the time the impact was halted, the maximum separation was on the order of 0.006 in.

Figure 7.6.8 shows the kaolite thickness time history. The nodes chosen are shown in Figure 7.1.16

Figure 7.6.9 shows the X direction diameter changes in the drum. Figure 7.6.10 shows the Y direction radial changes in the drum. Figure 3.1.34 shows the location of the nodes in the Figure 7.6.9 and 7.6.10 time histories.

Figure 7.6.11 shows the diameter time history for the inner liner. The position of the nodes are shown in Figure 3.1.37 and Table 3.1.3.

3100 HABCRUN4GA 12SLAP DEC 04 KQH
Time = 0.0201

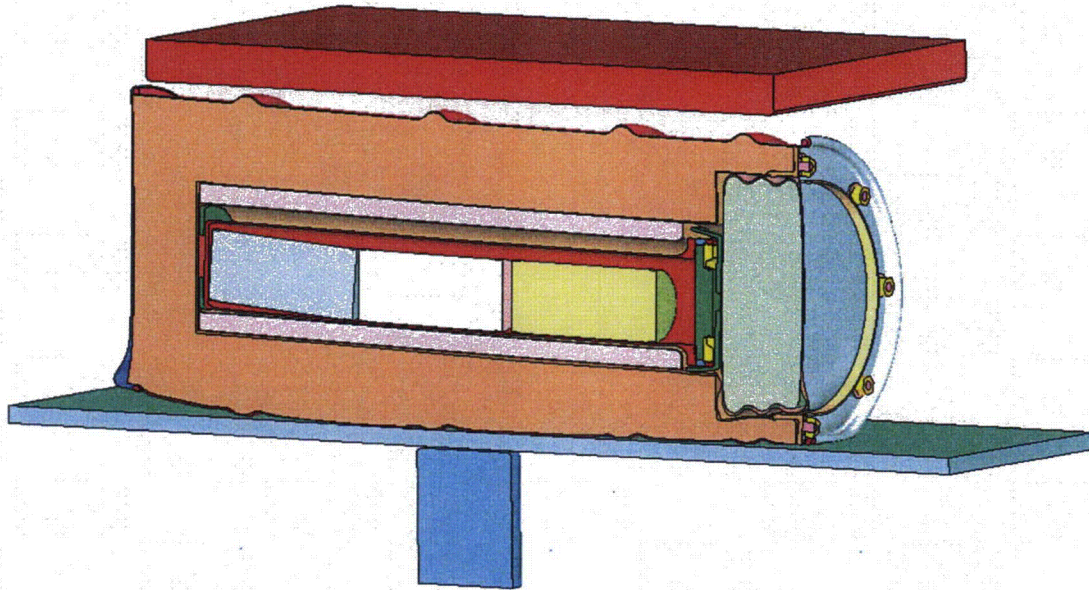


Figure 7.6.1 - HABC-run4ga, Initial Configuration for the Centered Crush Impact

3100 HABCRUN4GA 12SLAP DEC 04 KQH
Time = 0.04

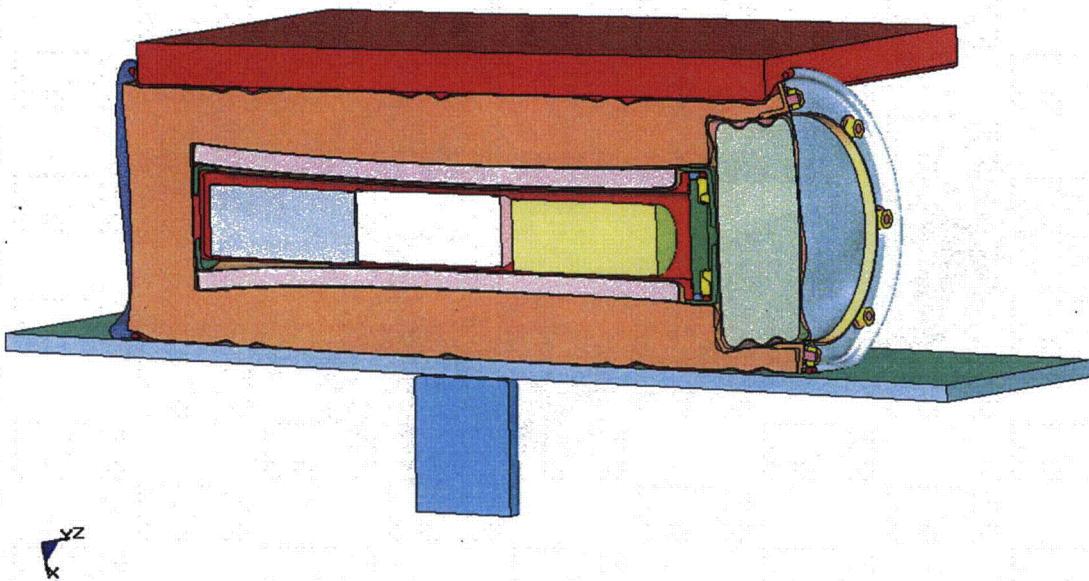


Figure 7.6.2 - HABC-run4ga, Final Configuration of the Centered Crush Impact

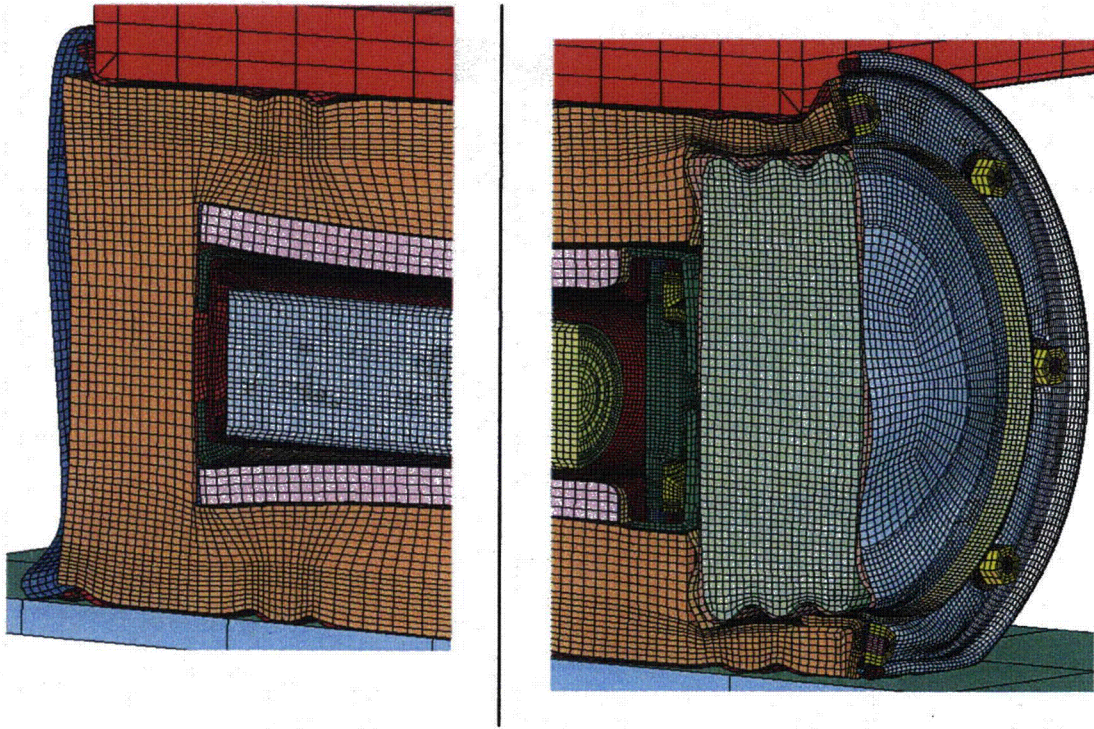


Figure 7.6.3 - HABC-run4ga, Crush Impact, Configurations at the Package Ends

3100 HABC RUN4GA 12SLAP DEC 04 KQH
Time = 0.04
Contours of Effective Plastic Strain
max ipt. value
min=0, at elem# 18
max=0.0643247, at elem# 448641

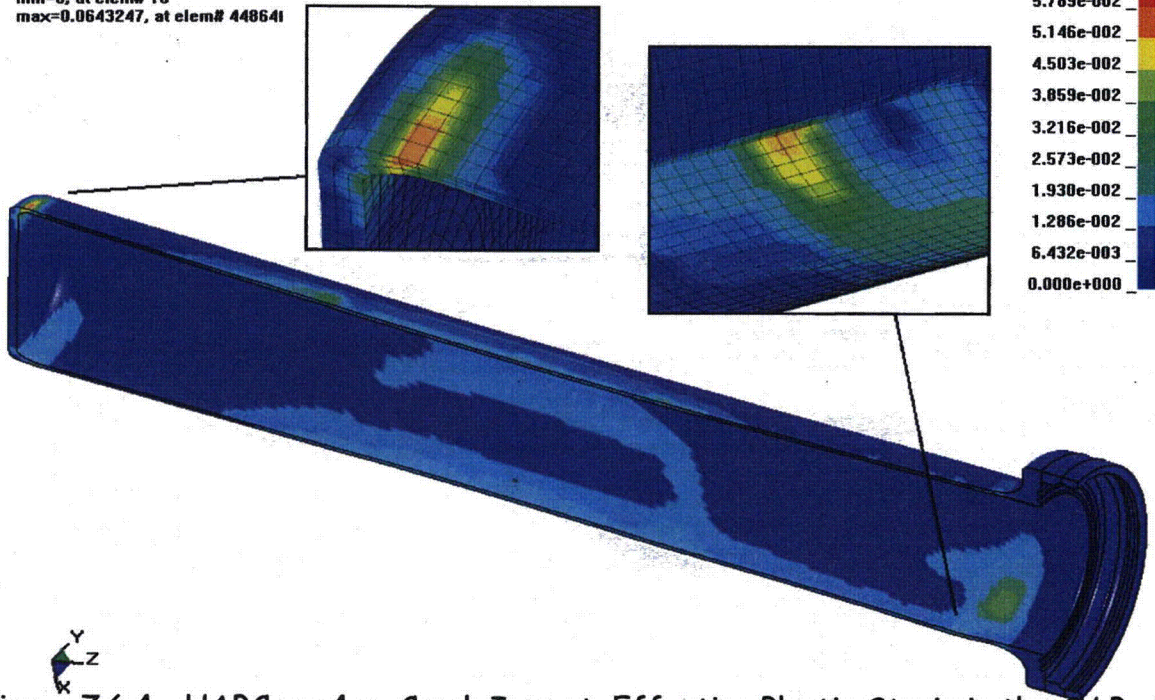


Figure 7.6.4 - HABC-run4ga, Crush Impact, Effective Plastic Strain in the CV Body

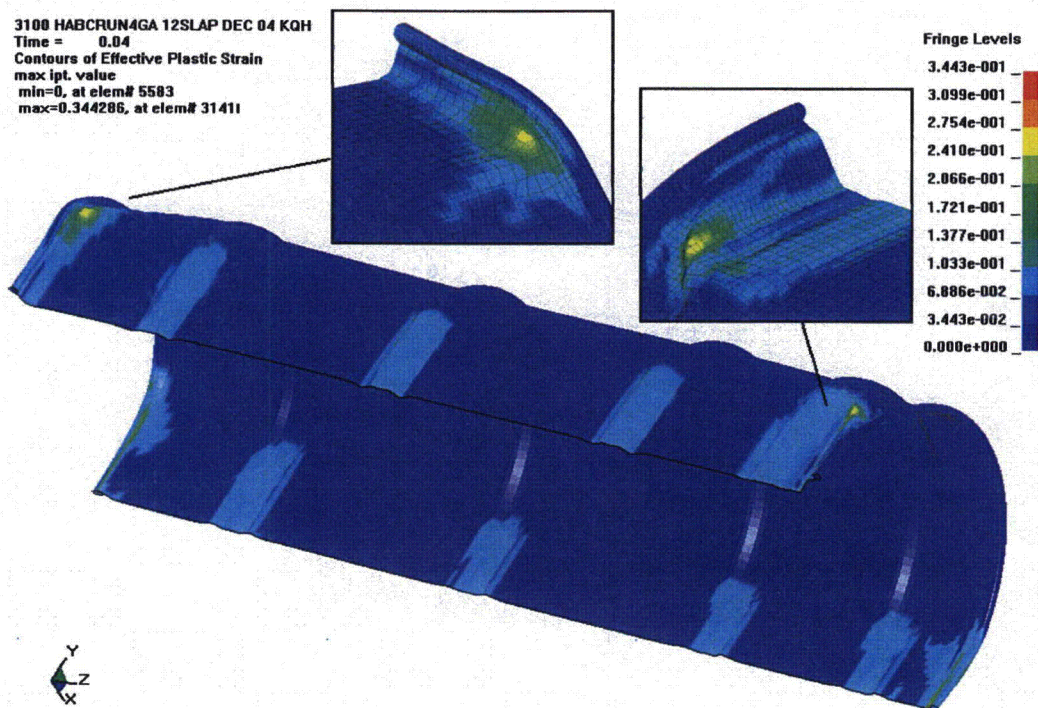


Figure 7.6.5 - HABC-run4ga, Crush Impact, Effective Plastic Strain in the Drum

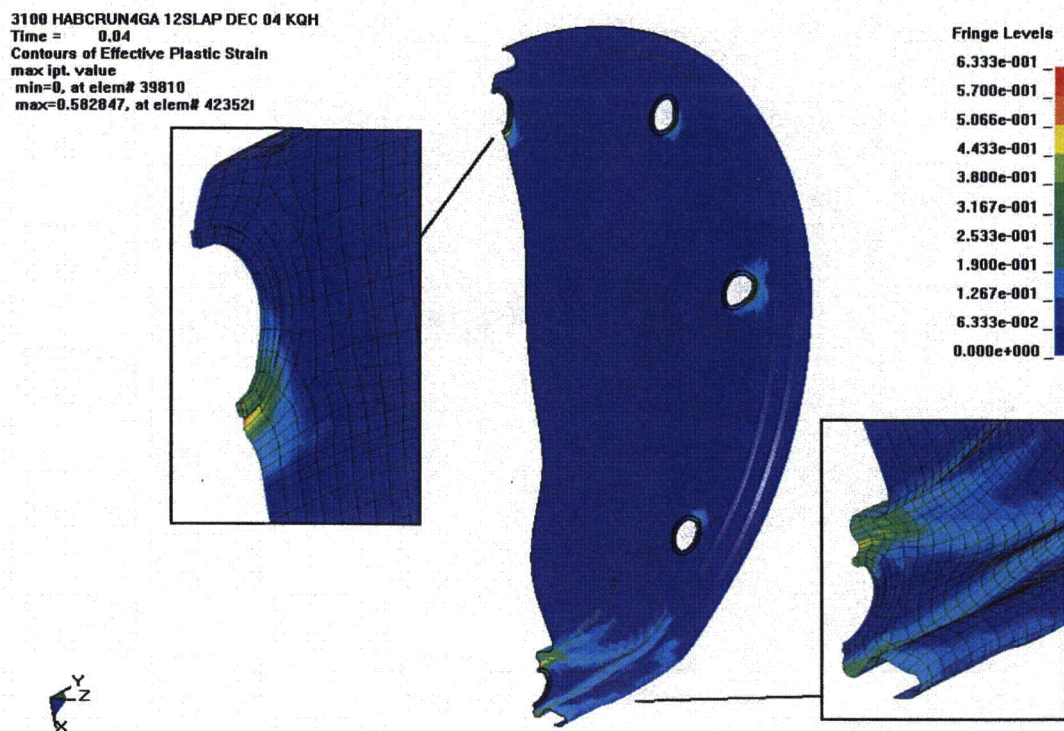


Figure 7.6.6 - HABC-run4ga, Crush Impact, Effective Plastic Strain in the Lid

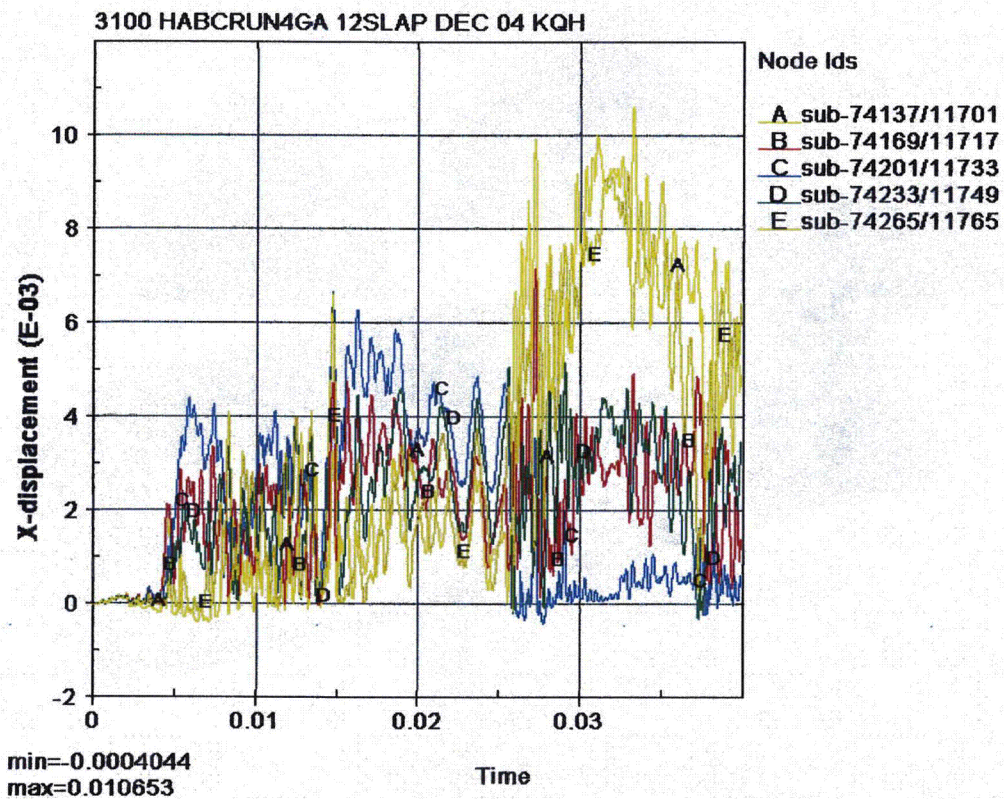


Figure 7.6.7 - HABC-run4ga, CV Lid Separation Time History

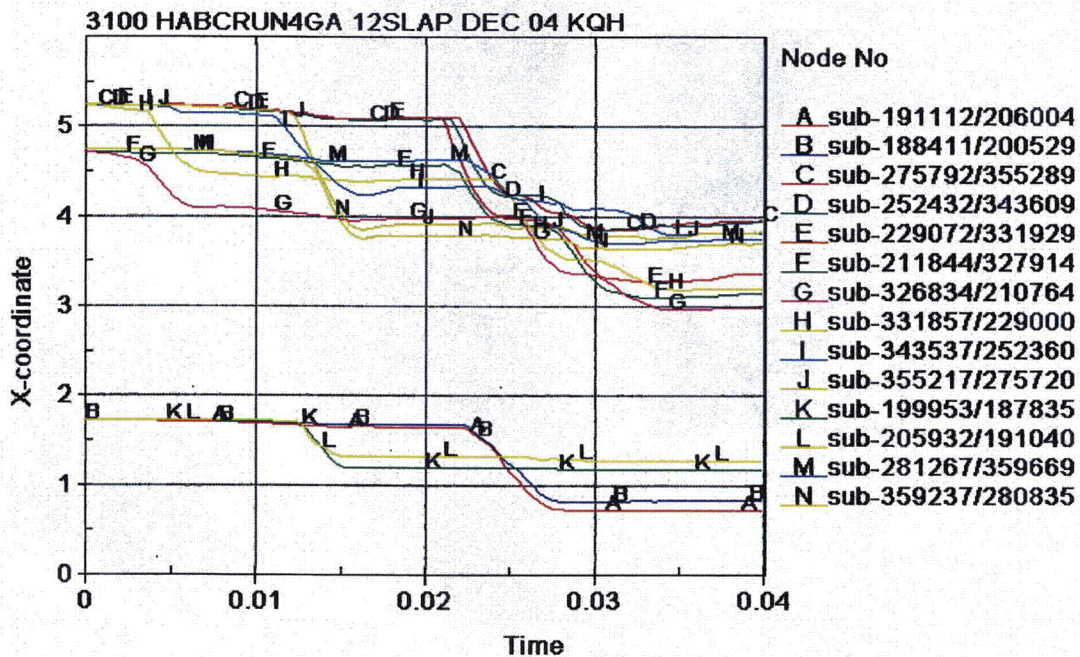


Figure 7.6.8 - HABC-run4ga, Kaolite Thickness Time History

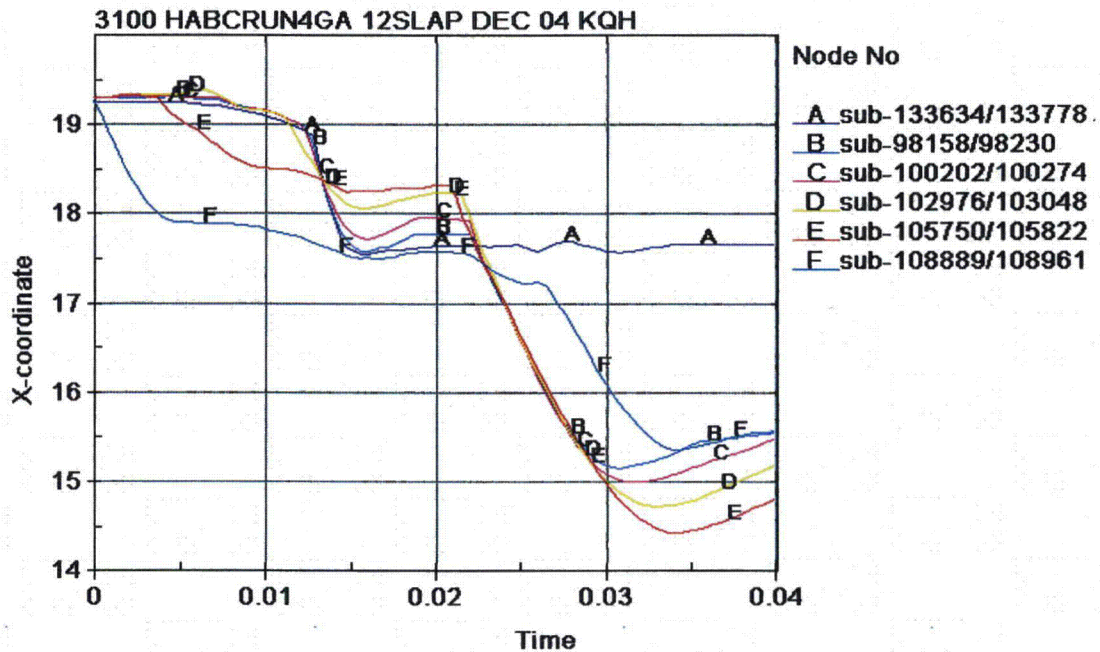


Figure 7.6.9 - HABC-run4ga, Diameter Time History for the Drum in the X Direction

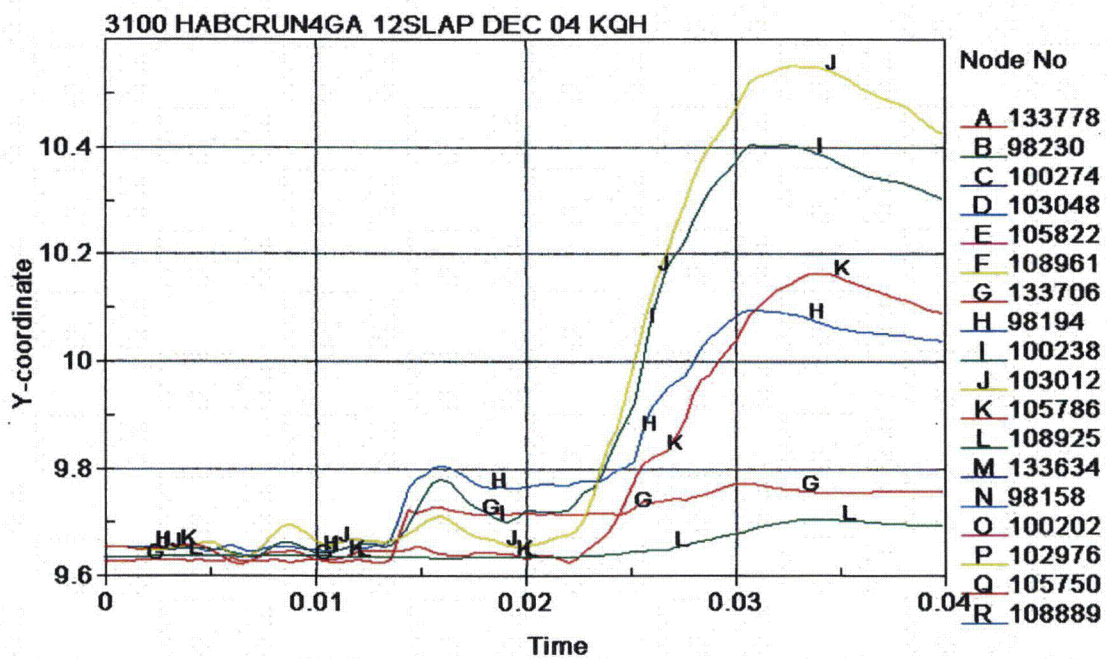


Figure 7.6.10 - HABC-run4ga, Radius Time History for the Drum in the Y Direction

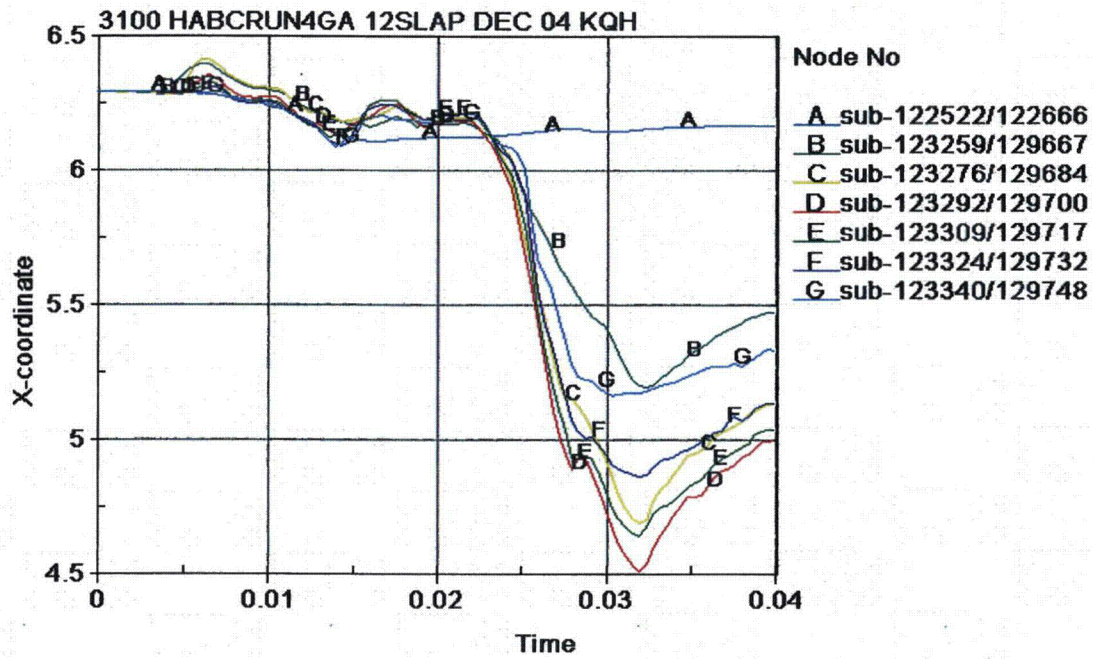


Figure 7.6.11 - HABC-run4ga, Diameter Time History for the Inner Liner

7.7 Comparison of Test vs Analysis

The HABC analysis runs are compared to the test results similar to that performed in Section 3.12 for the initial design using borobond. It should be noted that the testing was with specimen of the borobond neutron absorber design, whereas the analysis models in this section are of the HABC design.

7.7.1 Comparison of HABC Run4g to TU1

The HABC-run4g is a 30-foot, 12° slakedown impact followed by an offset crush (crush plate centered over the CV flange). TU1 is a 12° slakedown with a 4-foot impact, 30-foot impact, offset crush, and punch test specimen. The following Table 7.7.1.1 shows the initial diameter comparisons (pre-impact) using the test data compared to the analysis results.

Location	0° - 180°		90° - 270°	
	Test	Analysis	Test	Analysis
Top Chime	19.25	19.32	19.25	19.32
Top Hoop	19.25	19.37	19.25	19.37
Top CG Hoop	19.25	19.37	19.25	19.37
CG Hoop	19.25	19.37	19.25	19.37
Bottom Hoop	19.25	19.37	19.25	19.37
Bottom Chime	19.25	19.38	19.25	19.38

The Table 7.7.1.2 shows the results of the 30-foot test and analysis impacts. The test diameters are after the 4 and 30-foot impacts, while the analysis is after the 30-foot impact.

	0°-180°		90°-270°	
	Test	Analysis	Test	Analysis
Top Chime	18-1/2	18.1	19-3/8	19.5
Top Hoop	18-1/2	18.2	19-3/8	19.6
Top CG Hoop	18-1/2	18.4	19-3/8	19.5
CG Hoop	18-5/8	18.8	19-3/8	19.4
Bottom Hoop	18-5/8	18.9	19-1/4	19.3
Bottom Chime	17-13/16	18.1	19-3/8	19.4

Figure 7.7.1.1 shows the final configuration of the test specimen after the 4-foot and 30-foot impacts. Figure 7.7.1.2 shows the analytical model configuration after the 30-foot impact.



Figure 7.7.1.1 - TU1, Results of 30-Foot Impact

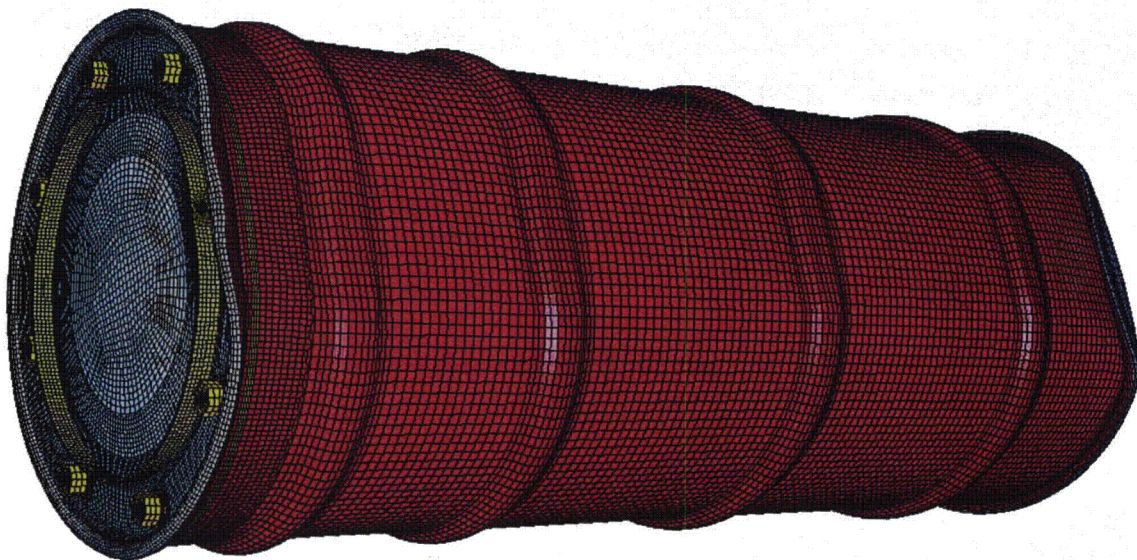


Figure 7.7.1.2 - HABC-run4g, Results of the 30-Foot Impact

Table 7.7.1.3 shows the comparison of the results of the crush impacts. The test data is for the cumulative effects of a 4-foot, 30-foot, and crush impact. The analysis data is for a cumulative 30-foot impact and crush impact.

	0°-180°		90°-270°	
	Test	Analysis	Test	Analysis
Top Chime	15-5/8	14.9	20-5/8	20.7
Top Hoop	16	15.1	20-7/16	20.8
Top CG Hoop	16-1/4	15.7	20-1/4	20.7
CG Hoop	16-1/2	16.2	19-7/8	20.4
Bottom Hoop	18-1/4	18.1	19-1/2	19.8
Bottom Chime	17-13/16	18.0	19-1/4	19.4

Figure 7.7.1.3 shows an isometric view of the test specimen with the crush side up. Figure 7.7.1.4 shows a similar view for the analysis results.



Figure 7.7.1.3 - TU1, View of Crush Damage with the Crush Side Up

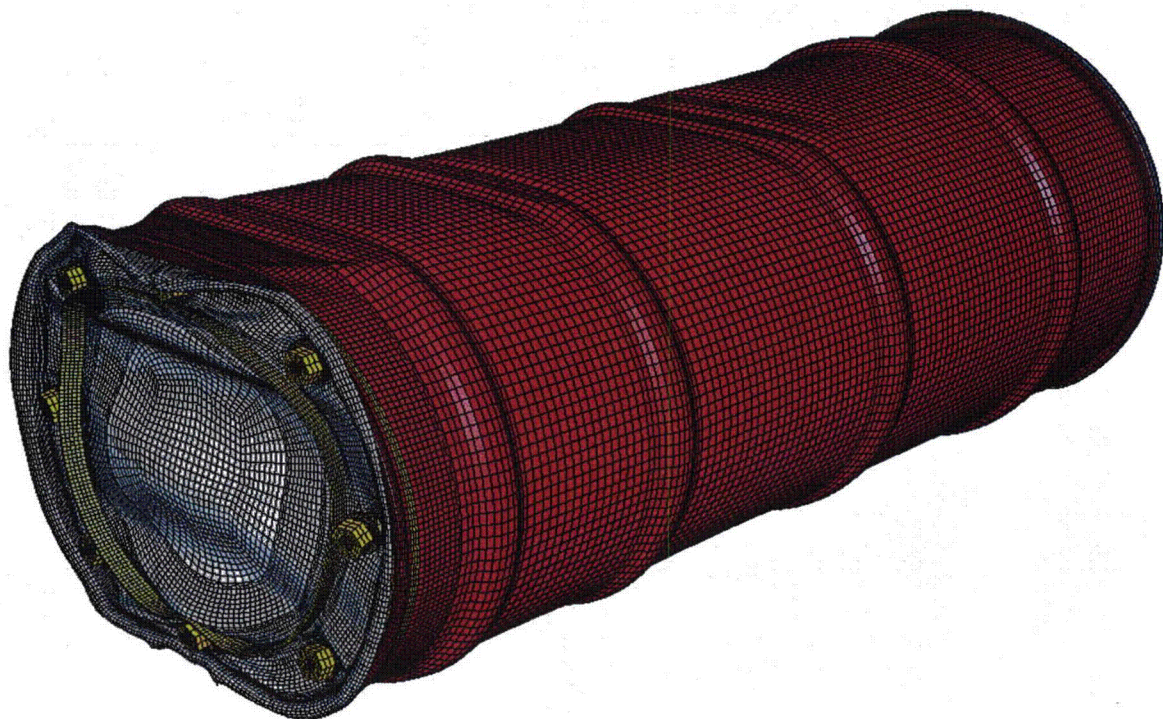


Figure 7.7.1.4 - HABC-run4g, View of the Crush Damage, Crush Side Up

Table 7.7.1.4 shows the results of a comparison of the "flats" measurements from the test after the 30-foot impacts and Table 3.12.1.5 compares the crush impact results.

	Test	Analysis
Top Chime	8	8.8
Top Hoop	7-3/8	8.4
Top CG Hoop	7-1/8	7.6
CG Hoop	6-3/8	5.9
Bottom Hoop	6-3/4	5.9
Bottom Chime	10	10.1

Location	Rigid Surface Side		Crush Plate Side	
	Test	Analysis	Test	Analysis
Top Chime	9	10.5	8-1/2	10.9
Top Hoop	10	11.0	10	11.0
Top CG Hoop	10	10.1	10-1/8	10.1
CG Hoop	9	8.4	10-5/8	10.1
Bottom Hoop	8-1/4	7.6	---	0.0
Bottom Chime	9-7/8	10.1	---	0.0

7.7.2 Comparison of HABC Run2e vs TU3

The HABC-run2e is a CG over lid corner 30-foot impact, followed by a bottom corner crush. TU3 is a similar test impact configuration with a 4-foot impact, 30-foot impact on the lid corner, then a crush impact on the bottom corner followed by a punch.

The test results show that there is 1.125 inches between the top chime and the top hoop in the test. Similar measurements in the analysis show that the distance is about 1.7 inches. This would be a somewhat judgmental comparison due to points chosen for measurement on the test specimen might not be the same as those chosen in the analysis. The analysis measurement is from the top of the crimped drum roll to the center of the flattened region in the lid roll, on the plane of symmetry.

Table 7.7.2.1 shows the comparison of the TU3 test unit and the computer run2e drum diameter changes after the 30-foot impact.

Table 7.7.2.1 - Run2e vs TU3, Diameter Results After the 30-Foot Impact				
	0°-180°		90°-270°	
	Test	Analysis	Test	Analysis
Top Chime	19-1/4	19.0	19-3/16	19.2
Top Hoop	18-5/8	19.1	19-7/8	20.0
Top CG Hoop	19-1/8	19.3	19-3/8	19.5
CG Hoop	19-1/8	19.4	19-3/8	19.4
Bottom Hoop	19-1/8	19.4	19-1/4	19.4
Bottom Chime	19-1/8	19.4	19-3/8	19.4

Figure 7.7.2.1 is an image of the damage after the 30-foot impact of TU3. The test photo shows the cumulative damage from the 4-foot and 30-foot impacts. Figure 7.7.2.2 shows a similar view after the 30-foot impact in run2e. The analysis image is the damage from only the 30-foot impact.

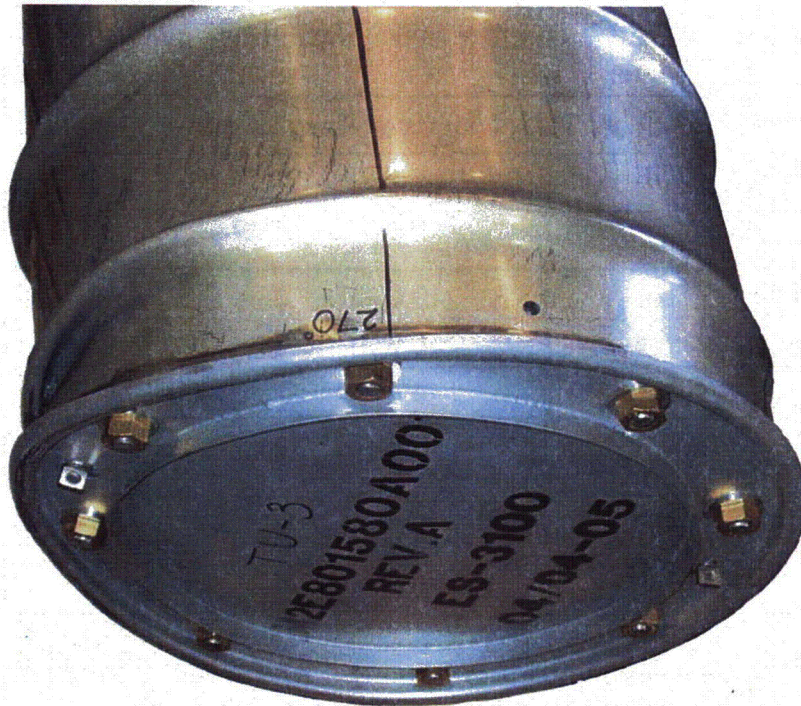


Figure 7.7.2.1 - TU3, Deformed Shape After the 30-Foot Impact

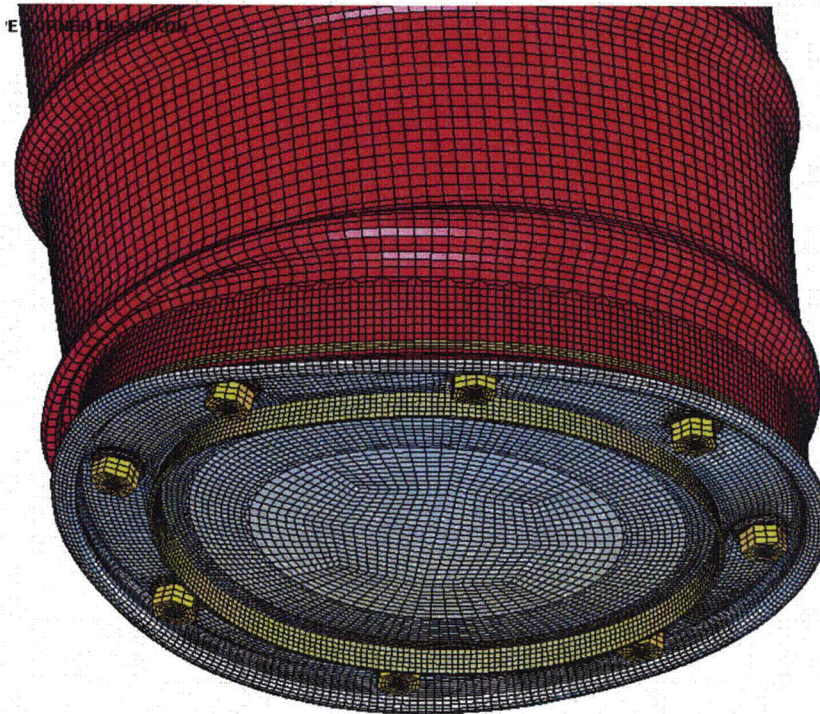


Figure 7.7.2.2 - HABC-run2e, Deformed Shape After the 30-foot Impact

The package drum diameters after the crush impact are compared in Table 7.7.2.2.

Table 7.7.2.2 - Run2e vs TU3, Diameter Results After the Crush Impact				
	0°-180°		90°-270°	
	Test	Analysis	Test	Analysis
Top Chime	19-1/4	19.0	19-1/16	19.0
Top Hoop	18-3/4	18.9	20-1/4	20.6
Top CG Hoop	19-1/4	19.4	19-3/4	19.8
CG Hoop	19-1/8	19.3	19-1/4	19.4
Bottom Hoop	19-1/8	19.3	19-3/4	20.4
Bottom Chime	18	18.6	19-3/8	19.4

The final images after the crush impact are shown for the test and the analysis. Figure 7.7.2.3 shows the final shape of the crushed bottom on the test specimen (4ft + 30ft + crush) and Figure 7.7.2.4 shows a similar view of the analysis (30ft + crush).



Figure 7.7.2.3 - TU3, Damage to the Bottom Head in the Crush Impact

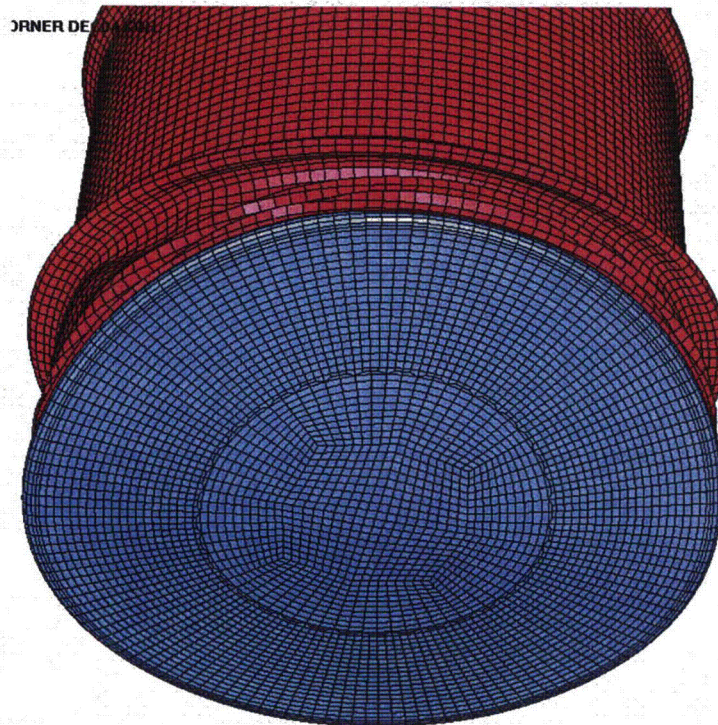


Figure 7.7.2.4 - HABC-run2e, Damage to the Bottom Head in the Crush Impact

The damage to the lid region at the end of the crush impact is shown in Figure 7.7.2.5 for the TU3. The damage to the lid region in the analysis run2e is shown in Figure 7.7.2.6.



Figure 7.7.2.5 - TU3, Lid Damage from the Crush Impact

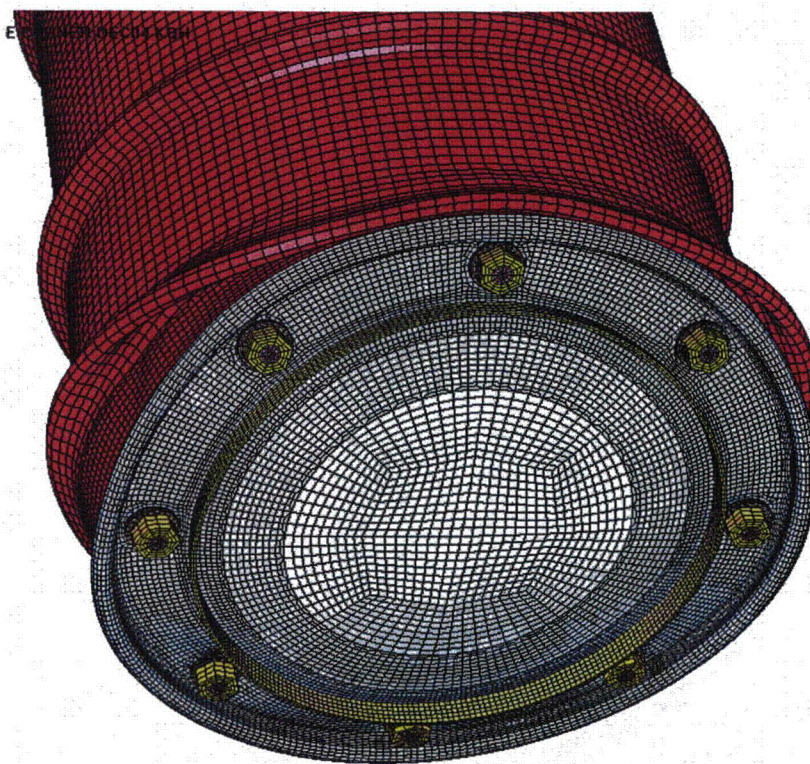


Figure 7.7.2.6 - HABC-run2e, Damage to the Bottom Head from the Crush Impact

7.7.3 Comparison of HABC-Run3b vs TU4

The HABC-run3b is a 30-foot lid down impact onto the rigid surface, followed by a crush impact onto the container bottom. The diameter measurements after the 30-foot impact are given in Table 7.7.3.1.

	0°-180°		90°-270°	
	Test	Analysis	Test	Analysis
Top Chime	19-1/4	19.3	19-3/8	19.3
Top Hoop	19-1/8	19.7	19-7/8	19.7
Top CG Hoop	19-13/16	20.0	19-3/8	20.0
CG Hoop	19-1/8	19.5	19-1/4	19.5
Bottom Hoop	19-1/4	19.4	19-1/4	19.4
Bottom Chime	19-1/4	19.4	19-1/4	19.4

The overall height measurements were compared between the test and the analysis. For the 30-foot impact, the test results vary around the circumference: 43.0 inches at 0°, 43.125 inches at 90°, 42.875 inches at 180° and 42.625 inches at 270°. The analysis is symmetrical, and the height from the top of the lid drum roll to the bottom head surface after the 30-foot impact is about 42.6 inches.

Figure 7.7.3.1 shows the configuration of the TU4 after the 30-foot impact (4ft + 30ft). Figure 7.7.3.2 shows the analysis model configuration after the 30-foot impact in a similar orientation to the test unit.



Figure 7.7.3.1 - TU4, 4-Foot + 30-Foot Impact Damage



Figure 7.7.3.2 - HABC-Run3b, 30-Foot Impact Damage

The drum height measurement after the test crush impact is 39-3/8 inches at 0°, 40-3/8 inches at 90°, 40-5/8 inches at 180°, and 39-3/4 inches at 270°. The analytical value for the height is about 39.0 inches.

The drum diameters after the crush impact are compared in Table 7.7.3.2.

	0°-180°		90°-270°	
	Test	Analysis	Test	Analysis
Top Chime	19-1/4	19.3	19-3/8	19.3
Top Hoop	20	20.1	20-1/8	20.1
Top CG Hoop	20	20.2	20-1/16	20.2
CG Hoop	19-7/16	20.1	19-1/2	20.1
Bottom Hoop	19-15/16	20.5	20	20.5
Bottom Chime	19-1/4	19.4	19-1/4	19.4

Figure 7.7.3.3 shows the TU4 at the end of the crush impact (4ft + 30ft + crush), while Figure 7.7.3.4 shows the configuration of the HABC-run3b model (30ft + crush).

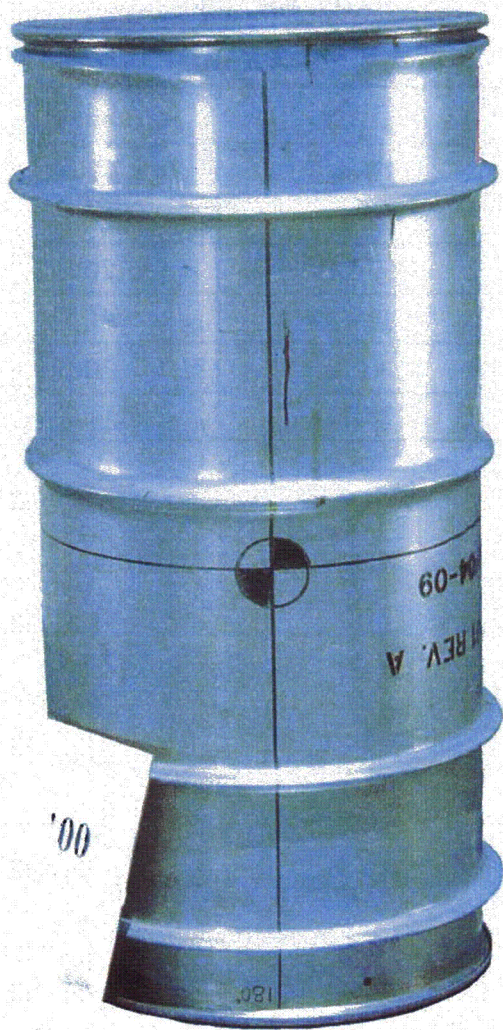


Figure 7.7.3.3 - TU4, Crush Damage



Figure 7.7.3.4 - HABC Run3b, Crush Damage

7.7.4 Comparison of HABC Run1hh vs TU2

HABC-run1hh was the upper bounding kaolite run which included a 4-ft, 30-foot and crush impacts. The test results are for the cumulative damage from the 4-ft, 30ft, crush and punch impacts. The table 7.7.4.1 shows the results for the diameter changes due to all the impacts for the test and the analysis.

	0°-180°		90°-270°	
	Test	Analysis	Test	Analysis
Top Chime	17-5/8	18.0	19-13/16	19.6
Top Hoop	17-3/8	16.6	19-3/4	20.1
Top CG Hoop	17	16.5	20	20.4
CG Hoop	16	16.3	20-1/4	20.5
Bottom Hoop	15-1/2	16.1	20-1/8	20.0
Bottom Chime	18	17.6	19-3/8	19.4

Table 7.7.4.2 shows the comparison of the "flats" dimensions for the test and the analysis.

	180° - Crush Plate Side		0° - Rigid Surface Side	
	Test [‡]	Analysis	Test	Analysis
Top Chime	6-1/4	0	8.0	9.2
Top Hoop	8-7/8	10.1	9.0	9.3
Top CG Hoop	9-5/8	9.3	10-1/8	8.4
CG Hoop	12	9.3	9-7/8	9.3
Bottom Hoop	14-7/8	10.1	9-7/8	9.3
Bottom Chime	0	0	9-3/8	10.1

† - Note - The reported test results for the 0 and the 180 sides are reversed in the test report (evidence Figure 7.7.4.3 below).

‡ - Note - The crush plate edge was 4.75 inches from bottom of package.

A visual comparison of the cumulative damage on the rigid surface side after the impacts is shown in Figures 7.7.4.1 (test) and Figure 7.7.4.2 (analysis).



Figure 7.7.4.1 - TU2, Cumulative Damage After the Punch Impact, Rigid Surface Side



Figure 7.7.4.2 - HABC-run1hh, Cumulative Damage, Rigid Surface Side

A visual comparison of the cumulative damage on the crush side after the four impacts is shown in Figures 7.7.4.3 (test) and Figures 7.7.4.4 (analysis).

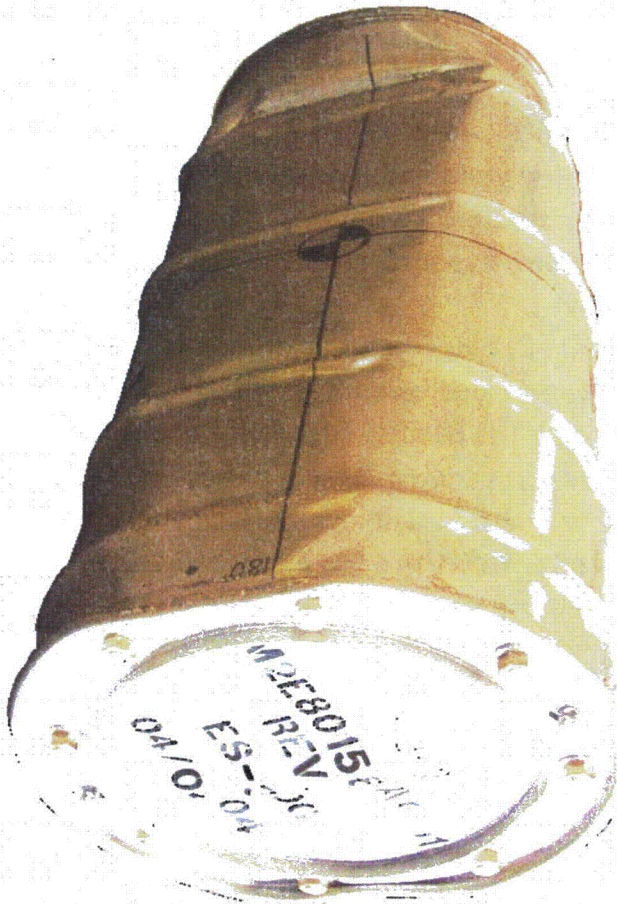


Figure 7.7.4.3 - TU2, Cumulative Damage After the Punch Impact, Crush Plate Side

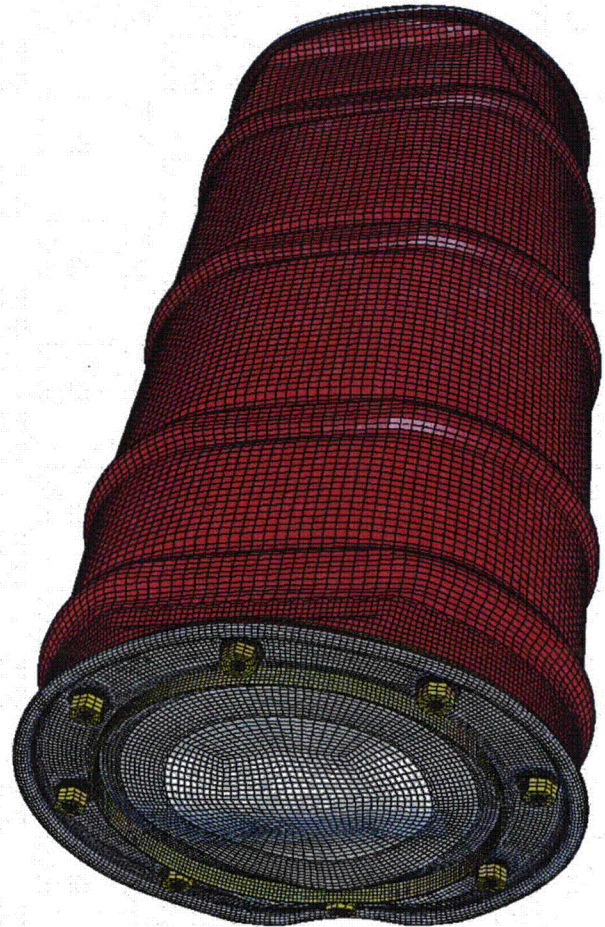


Figure 7.7.4.4 - HABC-run1hh, Cumulative Damage, Crush Plate Side

8.0 Summary

The computer simulation impacts for the HABC re-design of the ES-3100 shipping container are presented in Sections 7.1 to 7.6. The comparison of the HABC re-design container to the physical tests is presented in Section 7.7. The effective plastic strain for the components are summarized in Table 8.0.1. The punch impact is not included in the HABC runs, due to the fact that the drum shell capability is demonstrated in the initial borobond models, and the tested specimen.

Maximum strains in excess of 0.5 in/in are near the 304L strain limit of 0.57 in/in and are highlighted in red in Table 8.0.1. The components which are highlighted included the drum, lid, studs and liner. Evidence from looking at the Table 8.0.1 summary, a high demand is placed on the lid and the studs in the side and slapdown impacts.

In runs HABC-runs1hl, 1hh, 4g and 4ga a high demand is placed on the lid/studs. In runs 1hh, 1hl, 4g and 4ga, the region of plastic strain is very localized at the stud holes. Runs 1hl and 4g also have relatively high demands placed on the studs. In runs1hl and 4g, it is shown that the times at which the lid strains become excessive in membrane, the stud strains are relatively low. Hence, it is predicted that the lid will locally tear, thereby relieving loading on the studs. The tearing associated with the lid is expected to be local due to the localized fringes of extreme strain shown in the Section 7 fringe plots. The large washers provided on the packages would restrain the lid.

In runs HABC-run1hl, 2e and 4g, the studs reach high levels of effective plastic strain. In HABC-run1hl, the lid was shown to tear before the studs reached an elevated level of plastic strain.

HABC-run2e shows that the stud at the impact reaches extreme levels of plastic strain near the 0.57 in/in failure strain in the 30-foot impact and the subsequent crush impact. The level of high strain is throughout the cross section of the stud in HABC-run2e. Due to this high level of strain and the direct load path between the shipping package and the rigid surface, any slight changes in length, friction, localized deformations (stud "digging" into the relatively rigid plate in the test) could cause the stud to fail.

In HABC-run4g, the stud reached its failure strain and the cross section row of elements failed (removed by LS-Dyna). A time study shows that the lid reaches its levels of elevated strain in membrane before the stud. Therefore, the lid is expected to tear before the stud fails, thus relieving loading on the stud. However, the model does show the shipping container response if the lid were not to tear, and the stud were to fail.

The relatively high level of plastic strain in the HABC-run2e liner is a surface strain. Investigation shows that the membrane strain is about 0.2205 in/in, or well below the expected failure level. The deformation/fringe plot shows that the region of high strain is relatively local at the attachment of the liner to the angle. The plot also shows that it is the result of crimping or folding of the liner due to the relatively stiffer angle. Any tearing that might take place would be limited, evidence the local concentration of fringe levels.

Table 8.0.1 - ES-3100 HABC Shipping Package Summary of Component Maximum Effective Plastic Strain (in/in)

Material	Description	HABC-run1hl			HABC-run1hh			X
		Side - Lower Bound Kaolite (Section 7.1)			Side - Upper Bound Kaolite (Section 7.2)			
		4-foot	30-foot	Centered Crush	4-foot	30-foot	Centered Crush	
1	CV Body	0.0185	0.0195	0.0206	0.0238	0.0347	0.0525	
3	CV Lid	0.0001	0.0002	0.0002	0.0000	0.0001	0.0004	
4	CV Nut Ring	0.0000	0.0000	0.0000	0.0000	0.0000	0.0005	
5	Angle	0.0055	0.0780	0.1142	0.0061	0.0632	0.0845	
6	Drum	0.1599	0.2251	0.5139	0.1207	0.2296	0.2814	
7	Drum Bottom	0.1033	0.2126	0.3562	0.1252	0.2517	0.2827	
10	Liner	0.1045	0.1078	0.1593	0.0991	0.1184	0.2022	
12	Lid	0.1393	0.5790	1.2580	0.1604	0.4063	0.6413	
15	Lid Stiffener	0.0004	0.0093	0.0515	0.0006	0.0076	0.0171	
16	Lid Studs	0.0000	0.1140	0.5121	0.0000	0.1306	0.2364	
17	Lid Stud Nuts	0.0000	0.0000	0.0005	0.0000	0.0004	0.0018	
18	Lid Stud Washers	0.0194	0.0194	0.0693	0.0411	0.0424	0.0439	
19	Plug Liner	0.0022	0.0958	0.1220	0.0045	0.1072	0.1286	

Material	Description	HABC-run2e		HABC-run3b		HABC-run4g		HABC-run4ga	
		Corner (Section 7.3)		End (Section 7.4)		Slapdown (Section 7.5)		Slapdown (Section 7.6)	
		Impact	Crush	Impact	Crush	Impact	Offset Crush	Impact	Centered Crush
1	CV Body	0.0371	0.0371	0.0028	0.0083	0.0376	0.0564	Same as HABC- Run4g Impact Results	0.0643
3	CV Lid	0.0051	0.0051	0.0072	0.0072	0.0004	0.0013		0.0018
4	CV Nut Ring	0.0002	0.0002	0.0011	0.0011	0.0000	0.0001		0.0000
5	Angle	0.0394	0.0462	0.0287	0.0308	0.0900	0.1070		0.0944
6	Drum	0.3247	0.3830	0.0557	0.1237	0.3018	0.3920		0.3443
7	Drum Bottom	0.0000	0.0761	0.0031	0.0267	0.2879	0.2879		0.3000
10	Liner	0.3983	0.5254	0.0607	0.3812	0.1458	0.2060		0.2846
12	Lid	0.2791	0.3622	0.1082	0.1389	0.5278	0.9689		0.5828
15	Lid Stiffener	0.0272	0.0272	0.0069	0.0100	0.0213	0.0894		0.0288
16	Lid Studs	0.5233	0.5598	0.0962	0.1535	0.1892	0.4018		0.2390
17	Lid Stud Nuts	0.2260	0.2266	0.0166	0.0173	0.0000	0.0028		0.0000
18	Lid Stud Washers	0.1528	0.1528	0.0506	0.0506	0.0724	0.0790		0.0775
19	Plug Liner	0.1152	0.1166	0.0670	0.0960	0.1258	0.2665		0.1644

9.0 Comparison of Borobond Cylinder and HABC Cylinder Models

Part A of this calculation (Sections 2 through 5) apply to the initial, borobond neutron absorber model. Section 3.12 compared the borobond model results to the physical tested specimen. Part B (Sections 6 through 8) apply to the HABC redesigned neutron absorber model. Section 7.7 compares the HABC model to the physical tested specimen. The HABC model was derived from the initial borobond model, with changes detailed in Section 6. Section 6.1 gives the configuration changes and Section 6.2 gives the material model derivation for the HABC neutron absorber.

The borobond and the HABC materials are similar in nature in that they are castable, cement type materials. The LS-Dyna material model used in both analytical simulations was the *MAT_SOIL_AND_FOAM model. Similar approaches were taken for both the borobond and the HABC to match the material test results to the needed material properties in the analytical model. The approach is shown explicitly for the HABC material model in Section 6.2. The borobond model used in the Part A models, was also used in the Highly Enriched Uranium Materials Facility (HEUMF) storage pallet modeling, testing and qualification.

The CV body cylinder has an outside diameter of about 5.6 in. A minimum liner diameter of about 5.3 inches was found to occur in the borobond slapdown runs (4g, 4ga, 4h and 4ha). This minimum occurred at several locations along the liner length, and also near the CV flange. A somewhat similar response is noted for the HABC models, but with more deflection near the mid-height of the CV cavity. A minimum liner diameter of about 5.2 inches near the CV flange is noted in slapdowns HABC-run4g and 4ga. However, a minimum diameter of about 4.5 in is noted in HABC-run4ga near the mid-height of the CV body. This region of the CV body is remote from the bottom head or the flange and plastic strains in the body are relatively low (compare Figures 3.8.2 and Figure 7.6.4). The region of concern, near the CV flange, experiences about the same deformation (5.3 in vs 5.2 in).

A significant demand is placed on the lid and the studs in both the borobond and the HABC model side and slapdown impacts. This is a precipitate of the design attempt to minimize the number of studs securing the lid. The lid power law material model does not allow for element failure, whereas the model used for the studs (elastic-plastic) did allow element failure to be modeled. The effective plastic strain in bending and membrane reach significantly high levels (about 1.0 strain) in the lid. The regions of elevated plastic strain in the lid are shown to be localized at the stud holes. The studs also reached elevated levels of plastic strain. Investigation into the time history of the demand placed on the lid and the studs reveals that the lid reaches the elevated levels earlier in the impact, and therefore tearing of the lid would be expected. The tearing of the lid is expected to relieve the

loading on the studs, such that the integrity of the studs would be maintained. The large washers will restrain the lid. This fact was verified in the test with some tearing at the 90° and 270° position stud holes and no loss of a stud.

Both models compared favorably with the test results and with each other. This can be seen in the tables in Section 3.12 for the borobond and 7.7 for the HABC material.



Appendix 2.10.3

KAOLITE PROPERTIES

Kaolite SuperLightweight Insulating Castables, Thermal Ceramics, Augusta, Ga., September 1999.

Material Safety Data Sheet, *Refractory Castable, Silicate Product, Kaolite*, Thermal Ceramics, Augusta, Ga., September 1999.

R. E. Oakes, Jr., *Mechanical Properties of a Low Density Concrete for the New ES-2 Shipping/Storage Container Insulation, Impact Mitigation Media and Neutron Absorber*, Y/DW-1661, Lockheed Martin Energy Systems, Inc., Oak Ridge Y-12 Plant, Apr. 10, 1997.

H. Wang, *Thermal Conductivity Measurements of Kaolite*, ORNL-TM-2003/49, UT-Battelle, Oak Ridge Natl. Lab., n.d.

B. F. Smith and G. A. Byington, *Water Content and Temperature-Dependent Impact Properties of an Inorganic Cast Refractory Material*, Y/DW-1890, BWXT Y-12, Y-12 Natl. Security Complex, Feb. 14, 2003.

B. F. Smith, *Low Temperature Impact Properties of an Inorganic Cast Refractory Material*, Y/DW-1972, BWXT Y-12, Y-12 Natl. Security Complex, Sept. 14, 2003.

Advantages of Using a Fireproof Inorganic Cast Refractory Material in Hazardous Content Shipping Packages, Y/LF-565, Lockheed Martin Energy Systems, Inc., Oak Ridge Y-12 Plant, Nov. 10, 1998.

K. Moody, Thermal Ceramics, Augusta, Ga., *RE: Coefficient of thermal expansion for Kaolite 1600*, email to P. A. Bales, BWXT Y-12, Oak Ridge, Tenn., Dec. 9, 2004.



KAOLITE SUPER LIGHTWEIGHT INSULATING CASTABLES

Super lightweight Kaolite castables reduce both the quantity of heat storage and heat transfer through the lining producing significant savings in furnace fuel consumption. The lower densities of these vermiculite based Kaolite castables reduce the amount of supporting furnace steel work required and provide more insulation with a thinner lining. These products can be cast, poured, or gunited.

Kaolite 1600 is a super lightweight, low thermal conductivity vermiculite based castable designed for backup insulation up to 1600°F. Kaolite 1600 contains portland cement which limits use temperature to 1600°F; however, this makes it an economical product based on cost per cubic foot.

Kaolite 1800 is a super lightweight, low thermal conductivity vermiculite castable designed for both backup insulation and hot face applications up to 1800°F. Kaolite 1800 contains a calcium-aluminate cement which gives it better high-temperature stability when compared to Kaolite 1600. Typical applications would be low-temperature lining for ovens and ductwork lining.

Kaolite 2000 is a super lightweight, low thermal conductivity castable designed for backup insulation and hot face applications up to 2000°F. Typical applications would be low-temperature lining for ovens and ductwork lining.

Instructions For Using

Casting

Highest strength is obtained with castable refractory by using the least amount of clean mixing water. This will allow thorough working of material into place by lightly vibrating or rodding. A mechanical mixer is required for proper placement (paddle-type mortar mixers are best suited). After achieving a ball-in-hand consistency, mix for 6 minutes. Place material within 20 minutes after mixing.

Gunning

Use suitable gunite equipment. Material should be predampened uniformly with approximately 10 - 12% by weight of clean water in mechanical mixer before placing into gun. This will reduce rebound and dust. Add required water at nozzle for effective placement. Suggested air pressure at the nozzle is between 15 and 25 psi.



Precautions

Store bagged castables in a dry place, off the ground and, when possible, with the original shrink wrapping intact.

Watertight forms must be used when placing material. All porous surfaces that will come into contact with the material must be waterproofed with a suitable coating or membrane. For maximum strength, cure 24 hours under damp conditions before initial heat-up. Keep freshly placed castable warm during cold weather, ideally between 70°F and 80°F. New castable installations must be heated slowly the first time.

Freshly placed lightweight castables are prone to a deteriorating condition called alkali hydrolysis when they are kept in a non-dried state for a sustained period of time in a warm, humid environment. Under these conditions, the castables should be force dried soon after placement or coated with Kao-Seal™ to resist the possible deterioration effects.

For mor information on castable placement, consult your Thermal Ceramics representative or call 1-800-329-7444 to receive faced instruction manuals.



Thermal Ceramics • P. O. Box 923 • Augusta, Georgia 30903-0923

September 1999

Replaces 3 14-705, 3 14-710, 3 14-712, 3 14-720, 3 14-725, 3 14-730, 3 14-740

3 14-705

REFRACTORY CASTABLES & MONOLITHICS

Kaolite	1600	1800	2000
Specifications	cast, gunned	cast, gunned	cast, gunned
Recommended use limit, °F	1600	1800	2000
Melting point, °F	2300	2400	2400
Average lb required to place one cubic ft ¹	23, 36*	23, 35*	25, 35*
Nominal density, pcf, fired	20 - 25, 31 - 39	20 - 25, 29 - 38	21 - 26, 29 - 35
Pounds per bag	50	50	50
Method of installation ²	C,G,P	C,G,P	C,G,P
Recommended water ranges, % by weight			
Casting (by vibrating)	120 - 145	145 - 165	155 - 180
Pouring	150 - 180	175 - 190	175 - 190

*Note: For overhead gunning applications, pounds required to place one ft³ should be increased to 40-50 pcf. Does not include rebound loss.

Physical Properties³

Modulus of rupture, psi (ASTM C 133)	cast, gunned	cast, gunned	cast, gunned
Dried 18-24 hrs. @ 220°F	45 - 75, 70 - 120	25 - 40, 50 - 100	18 - 26, 50 - 100
Fired 5 hrs. @ 1500°F	25 - 40, 35 - 55	30 - 50, 40 - 60	28 - 36, 40 - 65
Fired 5 hrs. @ use limit	25 - 40, 35 - 50	25 - 40, 35 - 55	-
Cold Crushing strength			
Dried 18-24 hrs. @ 220°F	80 - 120, 125 - 175	35 - 50, 70 - 120	55 - 64, 75 - 85
Fired 5 hrs. @ 1500°F	50 - 70, 90 - 120	50 - 80, 80 - 110	70 - 120, 80 - 110
Fired 5 hrs. @ use limit	50 - 70, 90 - 120	40 - 60, 60 - 80	-
Perm. linear change, % (ASTM C 113) ⁴			
Fired 5 hrs. @ 1500°F	-1.0 to -2.0	-0.5 to -1.5	-0.5 to -1.5
Fired 5 hrs. @ use limit	-1.5 to -2.5	-1.5 to -2.5	-1.5 to -3.0

Chemical Analysis (Nominal, %)

Alumina, Al ₂ O ₃	11	29	34
Silica, SiO ₂	33	32	26
Ferric oxide, Fe ₂ O ₃	7.9	7.0	7.0
Titanium oxide, TiO ₂	1.4	2.3	1.0
Calcium oxide, CaO	30	14	17
Magnesium oxide, MgO	12.1	12	10
Alkalies, as, Na ₂ O	3.7	3.5	2.5

Thermal Conductivity, Btu•in./hr•ft²•°F (ASTM C 417)

Mean temperature			
@ 500°F	0.87, 1.03	0.79, 0.93	0.79, 0.93
@ 1000°F	1.02, 1.11	0.95, 1.06	0.95, 1.06
@ 1500°F	1.19, 1.20	1.11, 1.26	1.11, 1.27
@ 2000°F	-	-	1.28, 1.49

1. Gunite installation may require 10-30% overage due to rebound and on-site loss.
2. Installation key: C-cast, G-gun, P-pour
3. Properties indicated are for vibratory cast materials unless specified otherwise.
4. Fired linear change values reflect samples taken from a dried to fired state.

Consult Thermal Ceramics for specific curing and heat-up recommendations.

Data are average results of tests conducted under standard procedures and are subject to variation. Results should not be used for specification purposes.

Refer to the Material Safety Data Sheet (MSDS) for recommended work practices and other product safety information.

For further information, contact your nearest Thermal Ceramics technical sales office or your local Thermal Ceramics authorized distributor. You may also fax us toll-free at 1-800-KAOWOOL or write to Thermal Ceramics, P. O. Box 923, Dept. 140, Augusta, GA 30903.

AUGUSTA, GA
(800) 338-9284
Fax: (706) 796-4324

CHICAGO, IL
(888) 649-2442
Fax: (630) 527-0285

DETROIT, MI
(800) 590-4338
Fax: (734) 459-7860

LOS ANGELES, CA
(800) 990-5264
Fax: (714) 521-4662

INTERNATIONAL
(706) 796-4216
Fax: (706) 796-4262

BATON ROUGE, LA
(877) 722-2866
Fax: (504) 292-4082

CLEVELAND, OH
(877) 787-3385
Fax: (216) 831-4485

HOUSTON, TX
(800) 824-6878
Fax: (713) 680-9070

TRANSPORTATION
(888) 205-2358
Fax: (219) 296-3585

THERMAL CERAMICS
BURLINGTON, ONTARIO, CANADA
(905) 335-3414
Fax: (905) 335-5145

MATERIAL SAFETY DATA SHEET

MSDS No: 154	Date Prepared: 09/06/1993	Current Date: 2/3/2003 Last Revised: (01/16/2003)
---------------------	----------------------------------	--------------------------------------------------------------------

1. PRODUCT AND COMPANY IDENTIFICATION

Product Group: REFRACTORY CASTABLE
Chemical Name: Silicate Product
Intended Use: High Temperature Thermal Insulation
Trade Names: Kaolite® 1600; Kaolite® 1600 RFT; Kaolite® 1800; Kaolite® 1800 RFT; Kaolite® 2000; Therm-O-Flake Coating

Manufacturer/Supplier: Thermal Ceramics Inc.
P. O. Box 923; Dept. 300
Augusta, GA 30903-0923

**For Product Stewardship and Emergency Information -
Hotline: 1-800-722-5681
Fax: 706-560-4054**

For additional MSDSs and to confirm this is the most current MSDS for the product, visit our web page [www.thermalceramics.com] or call our automated FaxBack: 1-800-329-7444

2. COMPOSITION/INFORMATION ON INGREDIENTS

INGREDIENT & CAS NUMBER	% BY WEIGHT	OSHA PEL	ACGIH TLV
Vermiculite 01318-00-9	52 - 78	15 mg/m ³ (total dust); 5 mg/m ³ (respirable dust)	10 mg/m ³ (inhalable dust) 3 mg/m ³ (respirable dust)
Cement, alumina, chemicals 65997-16-2	15 - 50	15 mg/m ³ (total dust); 5 mg/m ³ (respirable dust)	10 mg/m ³ (inhalable dust) 3 mg/m ³ (respirable dust)
Crystalline silica 14808-60-7 or 14464-46-1	0.5 - 7	See notes ⁽¹⁾	0.05 mg/m ³ (respirable dust)

NOTES:

⁽¹⁾ Depending on the percentage and type(s) of silica in the mineral, the OSHA Permissible Exposure Limit (PEL) for respirable dust containing crystalline silica (8 HR TWA) is based on the formula listed in 29 CFR 1910.1000, "Air Contaminants" under Table Z-3, "Mineral Dust". For quartz containing mineral dust, the PEL = 10 mg/m³ / (% of silica + 2); for cristobalite or tridymite, the PEL = 5 mg/m³ / (% of silica + 2); for mixtures, the PEL = 10 mg/m³ / (% of quartz + 2 (% of cristobalite) + 2 (% of tridymite) + 2).

(See Section 8 "Exposure Controls / Personal Protection" for exposure guidelines.)

MATERIAL SAFETY DATA SHEET

MSDS No: 154

Date Prepared: 09/06/1993

Current Date: 2/3/2003

Last Revised: (01/16/2003)

3. HAZARDS IDENTIFICATION

EMERGENCY OVERVIEW

WARNING!

Respirable dust from these products may contain crystalline silica, which is known to cause respiratory disease.
(See Section 11 for more information)

POSSIBLE HEALTH EFFECTS

Target Organs: Eyes, skin, nose and/or throat
Primary Entry Route: Inhalation
Acute effects: May cause temporary, mild mechanical irritation to the eyes, skin, nose and/or throat. Pre-existing skin and respiratory conditions may be aggravated by exposure.
Chronic effects: Prolonged/repeated inhalation of respirable crystalline silica may cause delayed lung injury (e.g.: silicosis, lung cancer).

HAZARD CLASSIFICATION

Dust samples from these products have not been tested for their specific toxicity, but may contain more than 0.1% crystalline silica, for which the following apply:

The **International Agency for Research on Cancer (IARC)** has classified crystalline silica inhaled in the form of quartz or cristobalite from occupational sources as carcinogenic to humans (Group 1).

The Ninth Annual Report on Carcinogens (2000), prepared by the **National Toxicology Program (NTP)**, classified silica, crystalline (respirable size), as a substance known to be a human carcinogen.

The **American Conference of Governmental Industrial Hygienists (ACGIH)** has classified crystalline silica (quartz) as "A2-Suspected Human Carcinogen."

The **State of California**, pursuant to Proposition 65, The Safe Drinking Water and Toxic Enforcement Act of 1986, has listed "silica, crystalline (airborne particles of respirable size)" as a chemical known to the State of California to cause cancer.

The **Canadian Workplace Hazardous Materials Information System (WHMIS)** – Crystalline silica [quartz and cristobalite] is classified as Class D2A - Materials Causing Other Toxic Effects.

The **Hazardous Materials Identification System (HMIS)** –

Health: 1* Flammability: 0 Reactivity: 0 Personal Protection Index: X (Employer determined)
(* denotes potential for chronic effects)

4. FIRST AID MEASURES

EYE IRRITATION:

Flush with large amounts of water for at least 15 minutes. Do not rub eyes.

SKIN IRRITATION:

Wash affected area gently with soap and water. Skin cream or lotion after washing may be helpful.

INGESTION:

Unlikely route of exposure.

MATERIAL SAFETY DATA SHEET

MSDS No: 154

Date Prepared: 09/06/1993

Current Date: 2/3/2003

Last Revised: (01/16/2003)

INHALATION:

Remove affected person to dust free location. See Section 8 for additional measures to reduce or eliminate exposure.

- If symptoms persist, seek medical attention. -

5. FIRE FIGHTING MEASURES

NFPA CODES: Flammability: 0, Health: 1, Reactivity: 0, Special: 0
NFPA Unusual Hazards: None
Flash Point: None
Extinguishing Media: Use extinguishing media suitable for type of surrounding fire.
Explosion Hazards: None
Hazardous Decomposition Products: None

6. ACCIDENTAL RELEASE MEASURES

SPILL/LEAK PROCEDURES:

Avoid creating airborne dust. Follow routine housekeeping procedures. Vacuum only with HEPA filtered equipment. If sweeping is necessary, use a dust suppressant and place material in closed containers. Do not use compressed air for clean-up. Personnel should wear gloves, goggles and approved respirator.

7. HANDLING AND STORAGE

HANDLING

Limit the use of power tools unless in conjunction with local exhaust. Use hand tools whenever possible. Frequently clean the work area with HEPA filtered vacuum or wet sweeping to minimize the accumulation of debris. Do not use compressed air for clean-up.

STORAGE

Store in original factory container in a dry area. Keep container closed when not in use.

EMPTY CONTAINERS

Product packaging may contain residue. Do not reuse.

8. EXPOSURE CONTROLS/PERSONAL PROTECTION

ENGINEERING CONTROLS

Use engineering controls, such as ventilation and dust collection devices, to reduce airborne particulate concentrations to the lowest attainable level.

RESPIRATORY PROTECTION

When it is not possible or feasible to reduce airborne crystalline silica or particulate levels below the PEL through engineering controls, or until they are installed, employees are encouraged to use good work practices together with respiratory protection. Before providing respirators to employees (especially negative pressure type), employers should **1) monitor for airborne crystalline silica and/or dust concentrations using appropriate NIOSH analytical methods and select respiratory protection based upon the results of that monitoring,** **2) have the workers evaluated by a physician to determine the workers' ability to wear respirators,** and **3) implement respiratory protection training programs.** Use NIOSH-certified particulate respirators (42 CFR 84), in compliance with OSHA Respiratory Protection Standard 29 CFR 1910.134 and 29 CFR 1926.103, for the particular hazard or airborne concentrations to be encountered in the work environment. For the most current information on respirator selection, contact your supplier.

MATERIAL SAFETY DATA SHEET

MSDS No: 154

Date Prepared: 09/06/1993

Current Date: 2/3/2003

Last Revised: (01/16/2003)

PROTECTIVE CLOTHING

Wear full body clothing, gloves, hat, and eye protection as necessary to prevent skin irritation. Washable or disposable clothing may be used. If possible, do not take unwashed work clothing home. If soiled work clothing must be taken home, employers should ensure employees are trained on the best practices to minimize or avoid non-work dust exposure (e.g., vacuum clothes before leaving the work area, wash work clothing separately, rinse washer before washing other household clothes, etc.).

EYE PROTECTION

Wear safety glasses with side shields or other forms of eye protection in compliance with appropriate OSHA standards to prevent eye irritation. The use of contact lenses is not recommended, unless used in conjunction with appropriate eye protection. Do not touch eyes with soiled body parts or materials. If possible, have eye-washing facilities readily available where eye irritation can occur.

9. PHYSICAL AND CHEMICAL PROPERTIES

ODOR AND APPEARANCE:	Coarse brown powder.
CHEMICAL FAMILY:	Silicate
BOILING POINT:	Not applicable
WATER SOLUBILITY (%):	Slight
MELTING POINT:	> 2300°F
SPECIFIC GRAVITY:	Not applicable
VAPOR PRESSURE:	Not applicable
pH:	Not applicable
VAPOR DENSITY:	Not applicable
VOLATILE BY VOLUME (%):	Not applicable
MOLECULAR FORMULA:	Not Applicable

10. STABILITY AND REACTIVITY

HAZARDOUS POLYMERIZATION:	Will not occur
CHEMICAL INCOMPATIBILITIES:	Powerful oxidizers; fluorine, manganese trioxide, oxygen disulfide
HAZARDOUS DECOMPOSITION PRODUCTS:	None

11. TOXICOLOGICAL INFORMATION

TOXICOLOGY

Dust samples from these products have not been tested. They may contain respirable crystalline silica.

Crystalline silica

Some samples of crystalline silica administered to rats by inhalation and intratracheal instillation have caused fibrosis and lung cancer. Mice and hamsters, similarly exposed, develop inflammatory disease including fibrosis but no lung cancer.

Vermiculite

This product contains vermiculite. Some vermiculite deposits may contain other naturally occurring substances such as crystalline silica or asbestiform materials. Thermal Ceramics has relied upon supplier MSDSs to conclude that crystalline silica or asbestiform materials are not present, in regulated quantities, in the vermiculite used in this product.

MATERIAL SAFETY DATA SHEET

MSDS No: 154

Date Prepared: 09/06/1993

Current Date: 2/3/2003

Last Revised: (01/16/2003)

EPIDEMIOLOGY

No studies have been undertaken on humans exposed to these products in occupational environments.

Crystalline silica

Exposure to crystalline silica can cause silicosis, and exacerbate pulmonary tuberculosis and bronchitis. IARC (Monograph vol. 68, 1997) concluded that "crystalline silica from occupational sources inhaled in the form of quartz or cristobalite is carcinogenic to humans (Group 1)", and noted that "carcinogenicity in humans was not detected in all industrial circumstances studied" and "may be dependent on inherent characteristics of the crystalline silica or on external factors affecting its biological activity".

12. ECOLOGICAL INFORMATION

Adverse effects of this material on the environment are not anticipated.

13. DISPOSAL INFORMATION

WASTE MANAGEMENT

To prevent waste materials becoming airborne during waste storage, transportation and disposal, a covered container or plastic bagging is recommended. Comply with federal, state and local regulations.

DISPOSAL

If discarded in its purchased form, this product would not be a hazardous waste under Federal regulations (40 CFR 261). Any processing, use, alteration or chemical additions to the product, as purchased, may alter the disposal requirements. Under Federal regulations, it is the waste generator's responsibility to properly characterize a waste material, to determine if it is a hazardous waste. Check local, regional, state or provincial regulations to identify all applicable disposal requirements.

14. TRANSPORT INFORMATION

U.S. DEPARTMENT OF TRANSPORTATION (DOT)

Hazard Class:	Not Regulated	United Nations (UN) Number:	Not Applicable
Labels:	Not Applicable	North America (NA) Number:	Not Applicable
Placards:	Not Applicable	Bill of Lading:	Product Name

INTERNATIONAL

Canadian TDG Hazard Class & PIN: Not regulated
Not classified as dangerous goods under ADR (road), RID (train) or IMDG (ship).

15. REGULATORY INFORMATION

UNITED STATES REGULATIONS

SARA Title III: This product does not contain any substances reportable under Sections 302, 304, 313 (40 CFR 372). Sections 311 and 312 apply.

OSHA: Comply with Hazard Communication Standards 29 CFR 1910.1200 and 29 CFR 1926.59 and Respiratory Protection Standards 29 CFR 1910.134 and 29 CFR 1926.103.

TSCA: All substances contained in this product are listed in the TSCA Chemical Inventory

California: "Silica, crystalline (airborne particles of respirable size)" is listed in Proposition 65, The Safe Drinking Water and Toxic Enforcement Act of 1986 as a chemical known to the State of California to cause cancer.

MATERIAL SAFETY DATA SHEET

MSDS No: 154	Date Prepared: 09/06/1993	Current Date: 2/3/2003 Last Revised: (01/16/2003)
---------------------	----------------------------------	--------------------------------------------------------------------

Other States: Crystalline silica products are not known to be regulated by states other than California; however, state and local OSHA and EPA regulations may apply to these products. Contact your local agency if in doubt.

INTERNATIONAL REGULATIONS

Canadian WHMIS: Class D-2A Materials Causing Other Toxic Effects
Canadian EPA: All substances in this product are listed, as required, on the Domestic Substance List (DSL).

16. OTHER INFORMATION

SARA TITLE III HAZARD CATEGORIES

Acute Health:	No	Pressure Hazard:	No
Chronic Health:	Yes	Reactivity Hazard:	No
Fire Hazard:	No		

MATERIAL SAFETY DATA SHEET

MSDS No: 154

Date Prepared: 09/06/1993

Current Date: 2/3/2003

Last Revised: (01/16/2003)

DEFINITIONS:

ACGIH:	American Conference of Governmental Industrial Hygienists
ADR:	Carriage of Dangerous Goods by Road (International Regulation)
CAA:	Clean Air Act
CAS:	Chemical Abstracts Service Registry Number
CERCLA:	Comprehensive Environmental Response, Compensation and Liability Act
EPA:	Environmental Protection Agency
EU:	European Union
f/cc:	Fibers per cubic centimeter
HEPA:	High Efficiency Particulate Air
HMIS:	Hazardous Materials Identification System
IARC:	International Agency for Research on Cancer
IATA:	International Air Transport Association
IMDG:	International Maritime Dangerous Goods Code
mg/m ³ :	Milligrams per cubic meter of air
mppcf:	Million particles per cubic meter
MSHA:	Mine Safety and Health Administration
NFPA:	National Fire Protection Association
NIOSH:	National Institute for Occupational Safety and Health
OSHA:	Occupational Safety and Health Administration
PEL:	Permissible Exposure Limit
PNOC:	Particulates Not Otherwise Classified
PNOR:	Particulates Not Otherwise Regulated
RCRA:	Resource Conservation and Recovery Act
RID:	Carriage of Dangerous Goods by Rail (International Regulation)
SARA:	Superfund Amendments and Reauthorization Act
Title III:	Emergency Planning and Community Right to Know Act
...Section 302:	Extremely Hazardous Substances
...Section 304:	Emergency Release
...Section 311:	MSDS/List of Chemicals
...Section 312:	Emergency and Hazardous Inventory
...Section 313:	Toxic Chemicals Release Reporting
STEL:	Short-Term Exposure Limit
TCLP:	Toxicity Characteristics Leaching Procedures (EPA)
TLV:	Threshold Limit Values (ACGIH)
TSCA:	Toxic Substance Control Act
WHMIS:	Workplace Hazardous Materials Information System (Canada)
29 CFR 1910.134 & 1926.103:	OSHA Respiratory Protection Standards
29 CFR 1910.1200 & 1926.59:	OSHA Hazard Communication Standards

Revision Summary:

- 1) MSDS revised in its entirety with updated information.
- 2) Product "Therm-O-Flake Coating" added (see Section 1).

MSDS Prepared By:


THERMAL CERAMICS ENVIRONMENTAL, HEALTH & SAFETY DEPARTMENT

DISCLAIMER

The information presented herein is presented in good faith and believed to be accurate as of the effective date of this Material Safety Data Sheet. Employers may use this MSDS to supplement other information gathered by them in their efforts to assure the health and safety of their employees and the proper use of the product. This summary of the relevant data reflects professional judgment; employers should note that information perceived to be less relevant has not been included in this MSDS. Therefore, given the summary nature of this document, Thermal Ceramics does not extend any warranty (expressed or implied), assume any responsibility, or make any representation regarding the completeness of this information or its suitability for the purposes envisioned by the user.

Y-12

OAK RIDGE
Y-12
PLANT

LOCKHEED MARTIN 

MECHANICAL PROPERTIES OF A LOW DENSITY
CONCRETE FOR THE NEW ES-2
SHIPPING/STORAGE CONTAINER INSULATION,
IMPACT MITIGATION MEDIA AND NEUTRON
ABSORBER

Raymon E. Oakes, Jr.
Development Division
Oak Ridge Y-12 Plant

April 10, 1997

LOCKHEED MARTIN 

Prepared by the
Oak Ridge Y-12 Plant
Oak Ridge, Tennessee 37831
managed by
LOCKHEED MARTIN ENERGY SYSTEMS, INC.,
for the
U.S. DEPARTMENT OF ENERGY
Under contract DE-AC05-84OR21400

MANAGED BY
LOCKHEED MARTIN ENERGY SYSTEMS, INC.
FOR THE UNITED STATES
DEPARTMENT OF ENERGY
NCR-13072 (2-11-97)

INTRODUCTION

The design, analysis and testing of new Shipping/Storage container design for enriched uranium, labeled ES-2, is underway at the Oak Ridge Y-12 Plant. To assure greater containment during an accidental impact or fire, a better insulating/energy-absorbing material is being sought for the outermost filler. A replacement for the presently used Celotex[®], a low density wood product, and plywood is desirable. A more fire retardant material with otherwise equal or better impact energy and neutron absorption is being sought.

Kaolite[®] 1600, a castable Portland cement-based product by Thermal Ceramics, contains vermiculite (expanded mica) instead of gravel or other high density aggregates. It is a low density, high temperature insulating material with non-recoverable impact energy absorption capabilities. The major components of Kaolite 1600 according to the manufacturers Product Information sheet are:

Alumina.....	Al ₂ O ₃	9.6%
Silica.....	SiO ₂	31.5%
Ferric Oxide.....	Fe ₂ O ₃	6.7%
Titanium Oxide.....	TiO ₂	1.0%
Calcium Oxide.....	CaO.....	29.8%
Magnesium Oxide.....	MgO.....	11.9%
Alkalies, as.....	Na ₂ O.....	1.8%

The purpose of this work is to quantify the mechanical properties of this product for a variety of thermal cures, test temperatures and neutron absorbing additives in a form useable for data input for finite element analysis of a variety of potential accident scenarios.

EXPERIMENTAL WORK

Test Types_ Four properties tests are conducted on the Kaolite 1600 material, Flexural Tensile Strength, Unconstrained Compressive Strength, Constrained Compressive Strength and Density.

All specimens are cast in containers the shape of the desired specimen. The vendors wet mix ratio of water/Kaolite, 36 quarts water to 50 lb Kaolite 1600 is used exclusively (473 cc water/315 g Kaolite used in laboratory size specimens). After mixing and packing in the molds, mild impacts from a plastic hammer against the mold sides are made until air bubbles ceased to rise to the top.

An electrically heated, liquid nitrogen cooled convection oven with +/-2EF control is used for elevated temperature cures and testing.

Tensile Strength_ Nine tensile strength values are obtained from cast and tested quarter-point, four-point bend specimens, 1 in wide x 1 in high x 8 in long. Each are tested over a 6-in support span and 3-in compression span, having the following very low outer fiber tensile strength and density:

average tensile strength = 19.4 psi, standard deviation 4.7 psi, and
average density = 21.2 lb/ft³, standard deviation 1.0 lb/ft³.

Low tensile strengths should not be detrimental in this application where the predominate failure mode is constrained compression.

Cure for the tensile specimens is 24 hr at 72EF plus 24 hr at 220EF, high enough to drive off free water but retain the water of hydration. Water of hydration is loosely bound to a number of cement components and can be driven off at elevated temperatures either by using elevated temperature curing or could occur in a hypothetical long term fire environment.

Unconstrained Compressive Strength_ Unconstrained or uniaxial compression test specimens are molded, cured and tested in 3-in diam polyurethane coated paper mailing tubes cut to 6-in heights with one end sealed. The cure is 24 hr at 72EF + 24 hr at 220EF. The tubes are thin and weak enough to add little strength to the specimen. Figure 1 shows the stress-strain curves and initial densities for three tests each at different test rates, including impact conditions (200 in/s). The increased strength values of the two highest test rates probably result from air entrapment in the cells. Also shown is the minor strength contribution of an empty paper mold.

Three deformation stages are associated with compression of low density materials containing voids (vermiculite is considered to be a void as well as any remaining air entrapments). First, the matrix surrounding the voids buckles, shown as the steep initial portion of the curves in Figure 1. The buckling stage is followed by a large strain region of compaction with minor stiffness increase. In the unconstrained compression tests large-scale shear failures occur across

the sample prior to full compaction. Specimen buckling and gross shear failures forced the tests to be terminated. Constrained compression tests will show the steeper rise of more densified material.

Figure 2 is the integrated area under each of the three stress-strain curves of Figure 1, the cumulative work or energy per unit volume absorbed by the material as a function of strain.

Constrained, Hydrostatic Compression Tests. Constrained compression tests simulate the deformation mode of accident conditions in the material as it is used in the ES-2 container. The material is constrained by filling the outer stainless steel drum. In the event of an accident the inner container and its contents must remain intact. In the absence of vacant volume compaction or hydrostatic compression is the only deformation mode available. Laboratory simulations require compressing a specimen in a rigid, tight closed-ended cylinder with a tight fitting piston. A 20k pound testing machine loads the piston. The cylinders are four-inch ID thick-walled pipe and the specimens are cast, cured and tested in the cylinder. The specimen height is 4.5 in.

This test is used to provide primary input to the Finite Element Analysis as well as a relevant means to evaluate repeatability, cures, test temperature and additive effects on properties.

Note that percent compressive strain and percent volume change values are equivalent for all constrained compression tests.

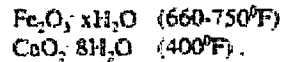
Repeatability. The five stress-strain curves of Figure 3 represent material cured for 24 hr at 72EF + 24 hr at 220EF + 48 hr at 500EF. Each specimen is individually mixed and cast. Initial measured densities are shown for each specimen. Repeatability of density and the stress-strain curves are good for this type material. Note the three stages of deformation, cell buckling, densification and the beginning of compression of densified material are present. Load limitations of the test machine prevent reaching full compaction, a near vertical rise in the curve.

Cure Effects. Both cure time and temperature have major effects on the constrained compressive properties of Kaolite 1600, Figures 4 and 5. Cures at higher temperatures and/or longer cure times remove the most water as noted by decreasing density. Material strength increases in proportion to the degree of water loss. Cure time/temperature would be volume dependent so these cures may only represent the limiting cure for the much larger ES-2 container.

Test Temperature Effects. Decreasing test temperature in well cured specimens, Figures 6 and 7, lowers both strength and energy absorption only slightly.

Neutron Absorbing Additives. Residual water, free or as hydrates, is the primary neutron absorber in Kaolite. Adequate water or other neutron absorber must be present before, during and after all ES-2 container accident scenarios. The 500EF cure should eliminate most of the free water and part of the water of hydration, at least in specimen sized lots where equilibrium

temperatures are reached throughout the material. Higher temperatures are required to release all the water of hydration of two of the basic Portland cement components:



These hydrates during curing actually form very complex and unique hydrates. The disassociation temperatures for these complex hydrates are unique for each cement formulation and are unknown for Kaolite 1600. One requirement for the ES-2 container is survival in a fire environment of 1470EF for 0.5 hr without loss of seal of the inner container. Certainly loss of criticality protection must be assured in the same scenario.

Measured Kaolite densities cast and cured in ES-2 containers is about 29 lb/ft³ when cured at 200EF for 48 hr. followed by 500EF for 48 hr. This is much higher than 21-22 lb/ft³ in similarly cured laboratory samples, indicating either considerable residual water is retained in the ES-2 containers or large differences in compaction exist or both. Under long term fire conditions the amount of residual water and its distribution throughout the container is unknown.

Boron is a nonvolatile neutron absorber available in numerous chemical forms. Two forms, borax (Na₂B₄O₇·10H₂O) and boron carbide (B₄C), are investigated as potential neutron absorbers. The required amount according to criticality calculations is 2.5% natural boron. Weight percentages of 11.3% borax or 3.0% boron carbide meet this requirement. Note that natural boron implies the isotopic ratio found in nature. Not all boron in the market meets this criteria.

Figure 8 and 9 show that borax degrades both the strength and energy absorption an unacceptable amount. Due to the high molecular weight of borax the amount of material needed to provide adequate boron is excessive.

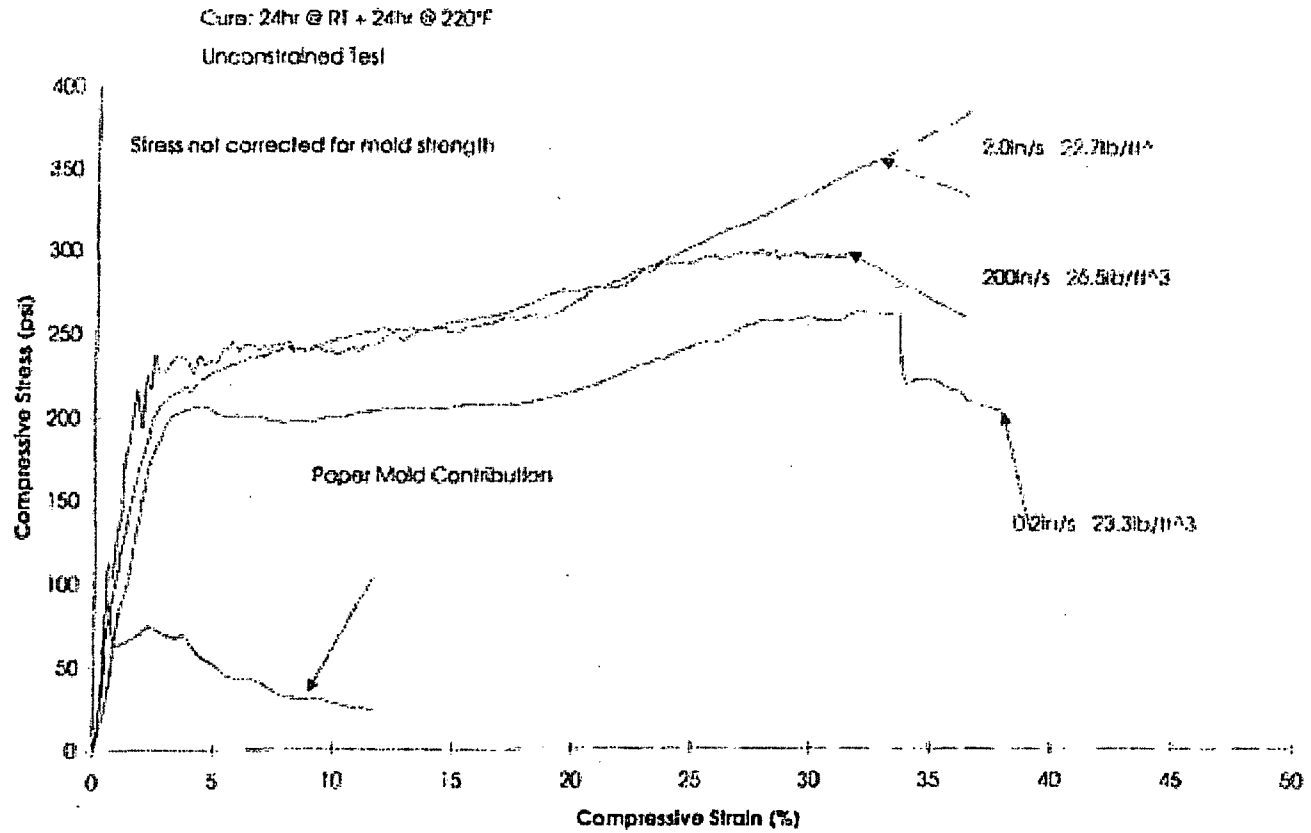
Unlike borax, boron carbide is predominately boron and Figures 8 and 9 show that the needed amount and even double the needed amount does not degrade the Kaolite and would be an acceptable, nonvolatile neutron absorbing additive.

Bibliography

- (1) *Handbook of Chemistry and Physics*, 60th Edition, Robert C. Weast, ed., CRC Press, Inc., Boca Raton, Florida 33431.
- (2) *Concrete Admixtures Handbook, Properties, Science, and Technology*, V. S. Ramachandran, ed., Noyes Publications, Park Ridge, New Jersey.

Ka16fig1.xls

Figure 1_Kaolite 1600 Compressive Stress-Strain vs Strain Rate



57

Figure 2_Kaolite 1600 Energy/Unit Volume vs Strain and Strain Rate

Cure: 24hr @ RT + 24hr @ 220°F
Unconstrained test

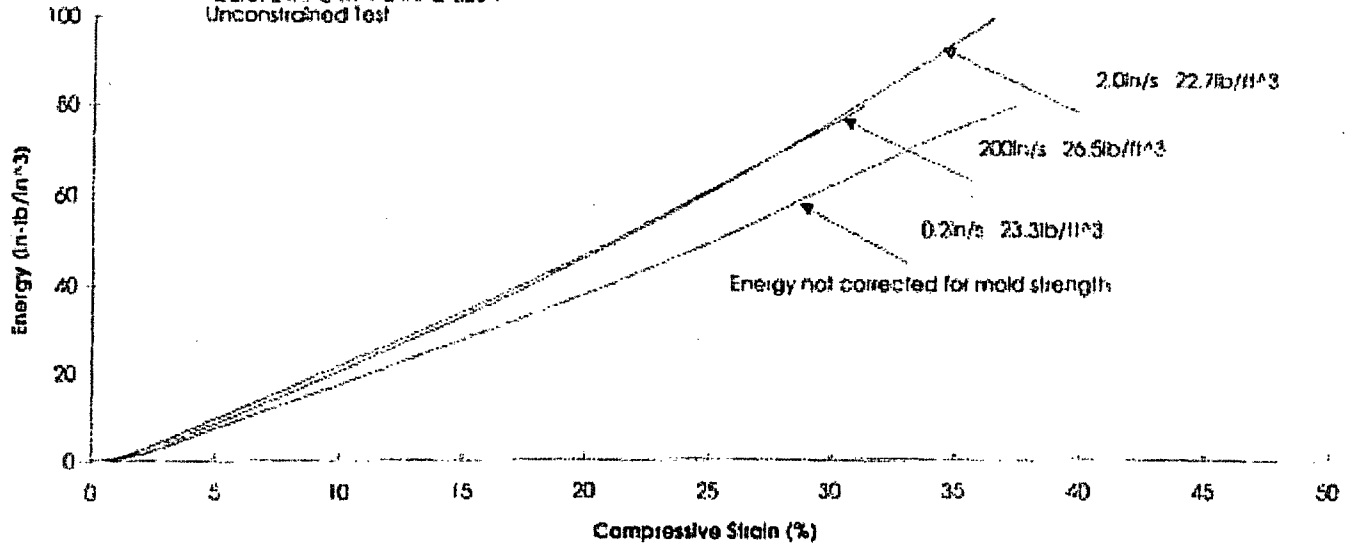


Figure 3_Kaolite 1600 Stress-Strain Curves, Repeatability Tests

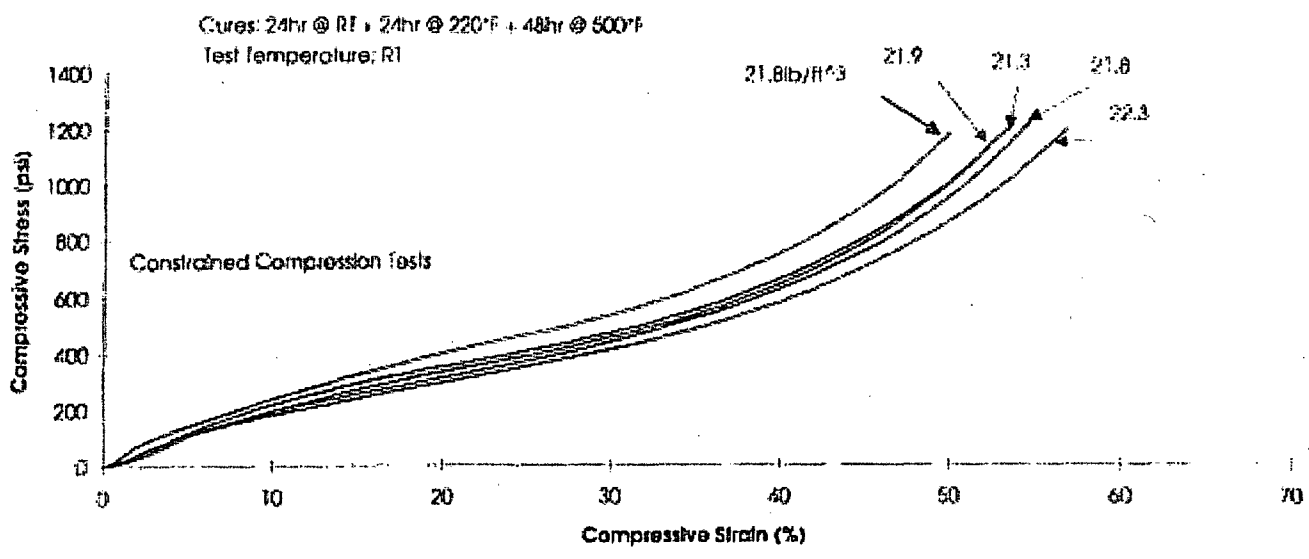
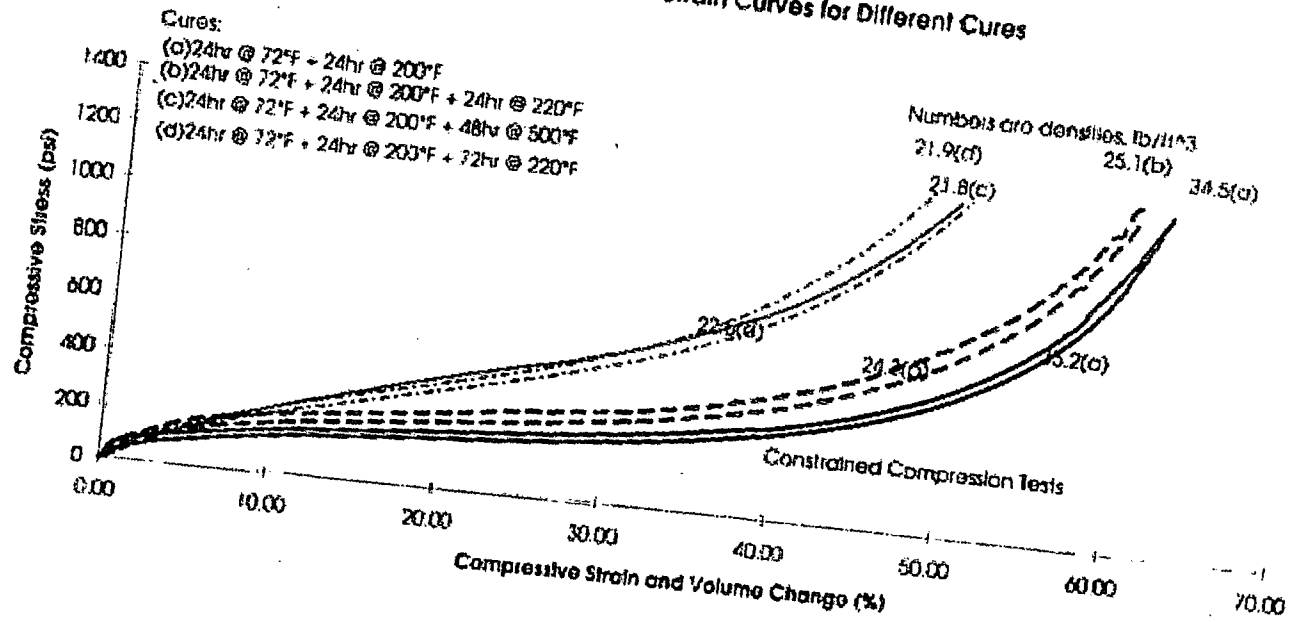


Figure 4_Kaolle 1600 Stress-Strain Curves for Different Cures



Ka16fig5.xls

Figure 5. Kaolite 1600 Energy-Strain Curves for Different Cures

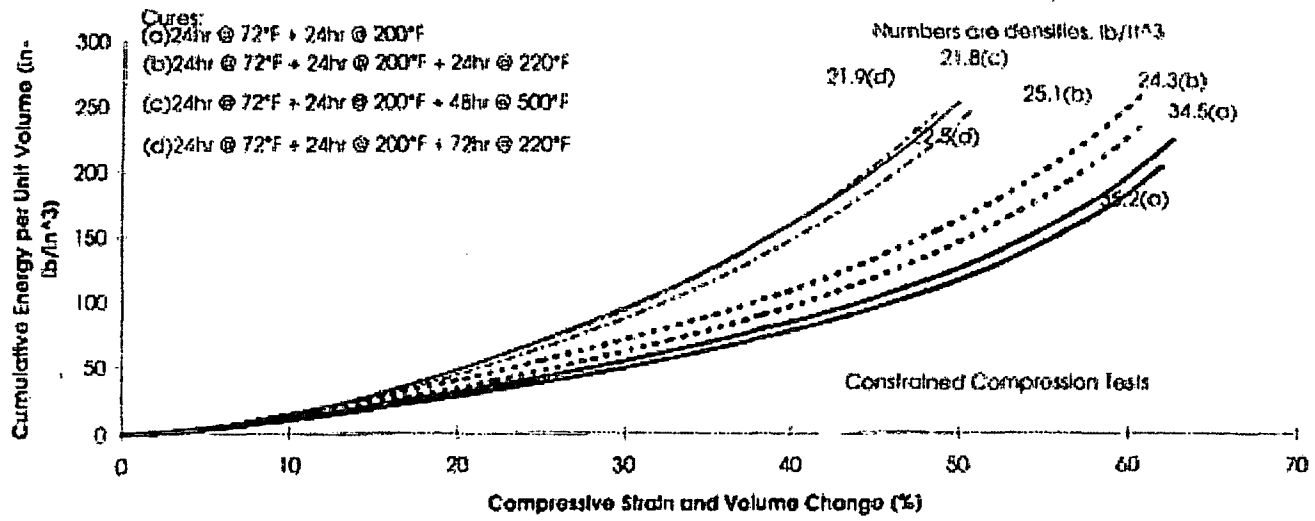


Figure 6_Kaolite 1600 Stress-Strain Curves for Different Test Temperatures

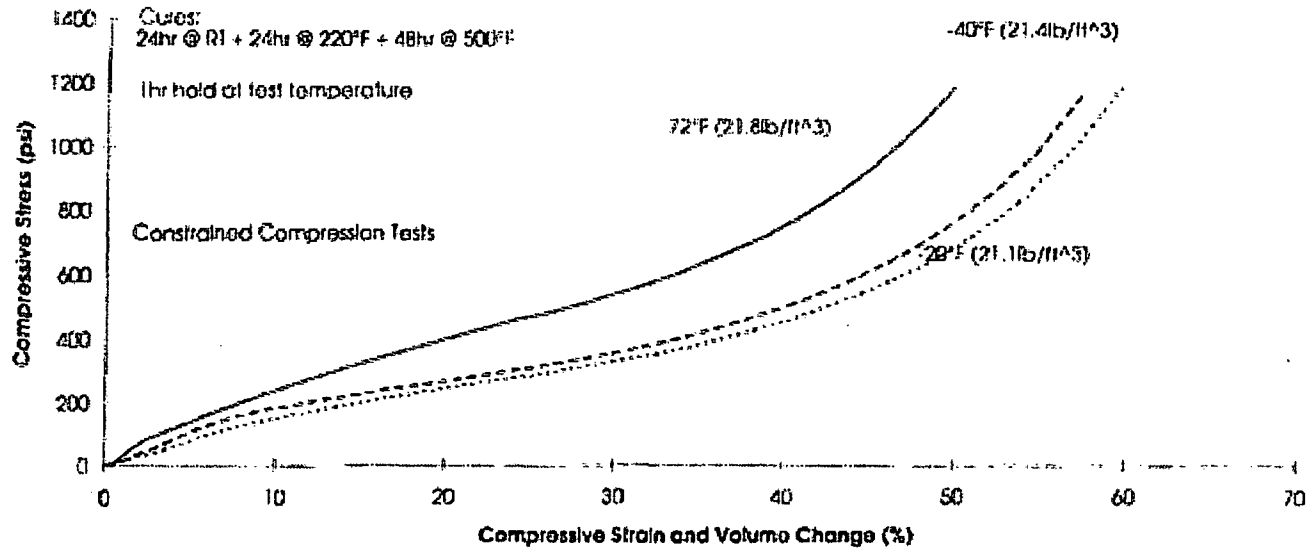
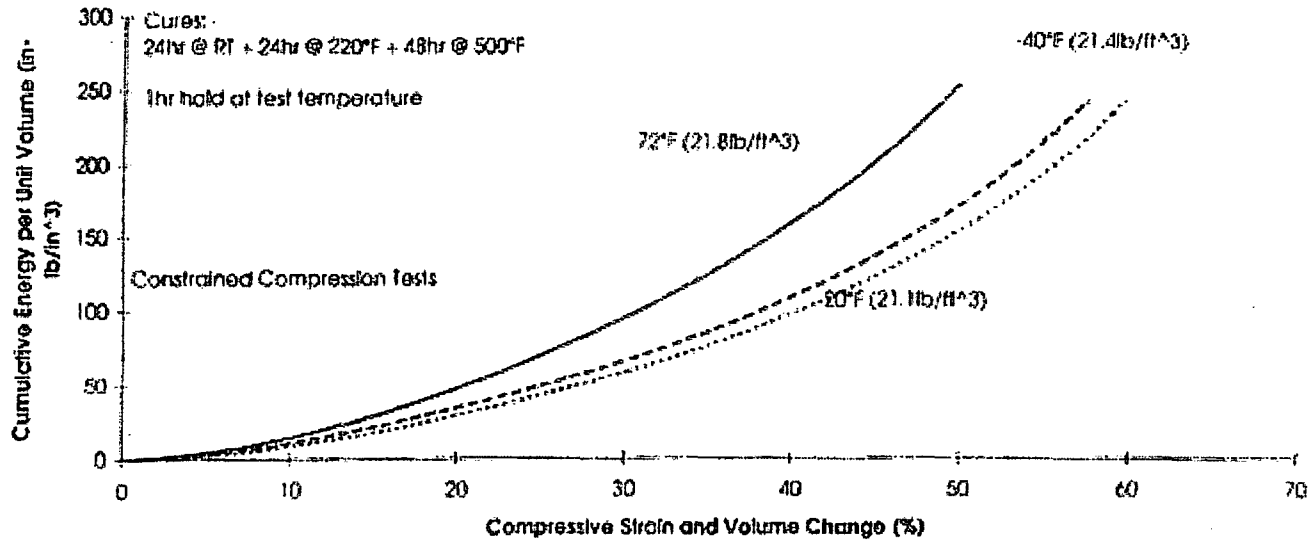


Figure 7_Kaolite 1600 Energy-Strain Curves for Different Test Temperatures



Thermal Conductivity Measurements of Kaolite

Hsin Wang

Prepared by the
Thermophysical Properties User Center
High Temperature Material Laboratory
Metal and Ceramics Division

Oak Ridge National Laboratory
Oak Ridge, TN 37831-6064
Managed by UT-BATTELLE LLC.
For the
U.S. DEPARTMENT OF ENERGY
Under contract DE-AC05-00OR22725

Introduction

Testing was performed to determine the thermal conductivity of Kaolite 1600, which primarily consists of Portland cement and vermiculite. The material was made by Thermal Ceramics for refractory applications. Its combination of light weight, low density, low cost, and noncombustibility made it an attractive alternative to the materials currently used in ES-2 container for radioactive materials.

Mechanical properties and energy absorption tests of the Kaolite have been conducted at the Y-12 complex. Heat transfer is also an important factor for the application of the material. The Kaolite samples are porous and trap moisture after extended storage. Thermal conductivity changes as a function of moisture content below 100° C. Thermal conductivity of the Kaolite at high temperatures (up to 700° C) are not available in the literature. There are no standard thermal conductivity values for Kaolite because each sample is somewhat different. Therefore, it is necessary to measure thermal conductivity of each type of Kaolite. Thermal conductivity measurements will help the modeling and calculation of temperatures of the ES-2 containers. This report focuses on the thermal conductivity testing effort at ORNL.

Experimental

Thermal conductivity of the Kaolite was measured using a Hot Disk Thermal Constants Analyzer. A picture of the system is shown in Figure 1. A box furnace, with

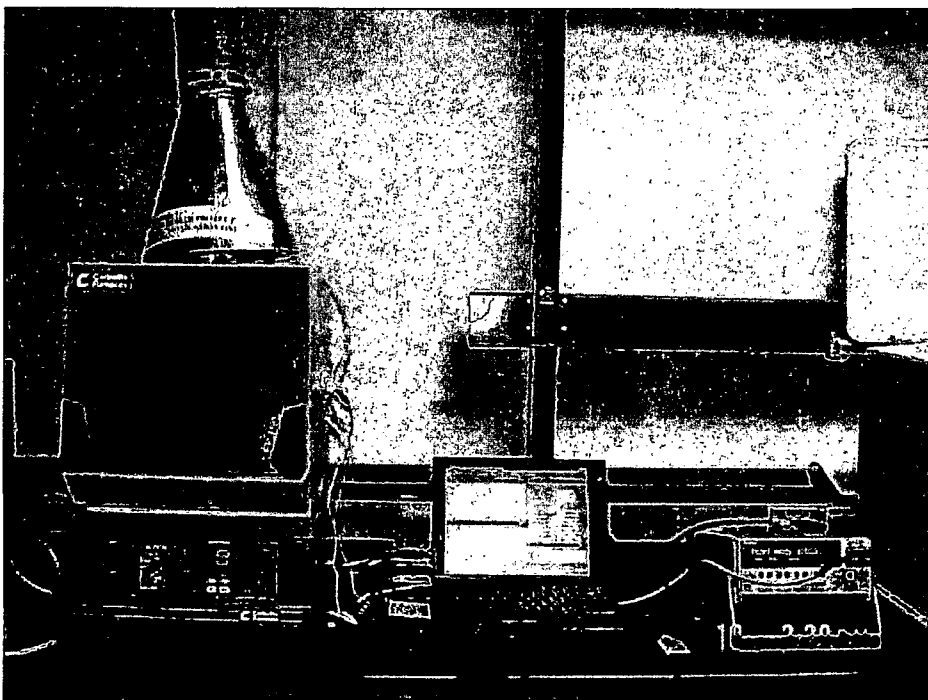


Figure 1. Experimental set up for thermal conductivity measurements.

maximum temperature of 1050° C, was used for high temperature tests. The Hot Disk sensor is a flat, thin, double-spiral nickel wire sandwiched between two mica sheets. The sensor is placed between two identical hockey-puck Kaolite samples (2" in diameter and 1" thick). During the measurement, the mica sensor acts as both a heater and a temperature sensor.

A typical test for Kaolite uses 0.05-watt constant-power heating for 80 seconds. The sensor temperature is recorded as a function of time. Thermal conductivity is then calculated directly from the experimental data. Detailed theory and experimental descriptions of the Hot Disk technique can be found in the references [1-3].

In order to perform high temperature measurements, special contacts were made from stainless steel. Four high temperature wires with insulation were connected to the mica sensor with the wires being fed through an opening on top of the furnace. A rectangular mica sheet with four screw holes was used as the support for the sensors. The four wires were connected to the contacts as shown in Figure 2. The mica sensor can be delaminated due to high temperature exposure, therefore, the sensor has to be replaced after a 600° C measurement. A heavy alloy block was placed on top of the sample to ensure good contact at the interface.

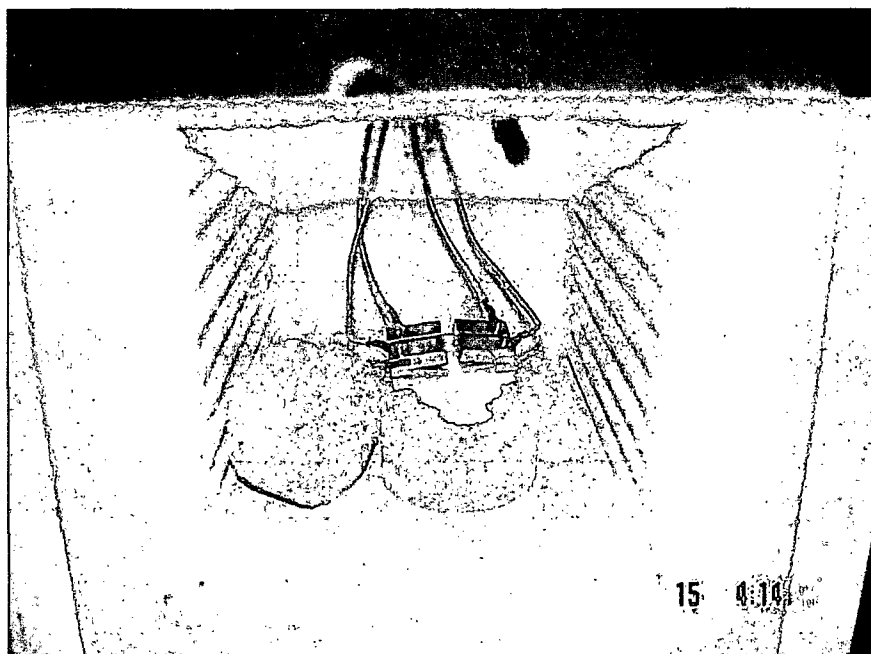


Figure 2. Kaolite samples and mica sensor used for high temperature testing.

Results and Discussion:

Thermal conductivities of six Kaolite samples were tested using the mica sensor. Since high temperature tests can destroy the sensor and only one set of samples was tested in the furnace, all the samples were tested at room temperature and then at 100° C. but only one sample was tested up to 600° C.

At room temperature and 100° C, the thermal conductivity values of the 6 Kaolite samples are similar, although the densities of the samples are grouped in 3 pairs at high, medium and low. The test results are shown in Table 1 for room temperature and Table 2 for 100° C. During the tests the humidity was not controlled in the laboratory or in the furnace. The samples did not have the same thermal history. For example, one set of sample was heated up from room temperature to 100° C, but the other 5 sets of samples had to wait outside the furnace. In addition, the local density of the sampling volume, i.e. 3/4" diameter semi sphere, can also vary due the existence of large pores and

Table 1. Thermal conductivity of six Kaolite at 20° C (unit: W/mK)

Density (lb/ft ³)	H 23.690	H 23.541	M 22.055	M 22.011	L 20.407	L 20.281
Test 1	0.188	0.183	0.152	0.198	0.165	0.172
Test 2	0.188	0.185	0.157	0.182	0.168	0.192
Test 3	0.191	0.181	0.167	0.198	0.169	0.181
Average	0.189	0.183	0.158	0.192	0.167	0.181
	High Density	0.186	Medium Density	0.176	Low Density	0.175

Table 2. Thermal conductivity of six Kaolite at 100° C (unit: W/mK)

Density ρ (lb/ft ³)	H 23.690	H 23.541	M 22.055	M 22.011	L 20.407	L 20.281
Test 1	0.165	0.172	0.157	0.179	0.163	0.177
Test 2	0.152	0.172	0.157	0.191	0.163	0.179
Test 3	0.161	0.179	0.156	0.194	0.152	0.178
Average	0.159	0.174	0.156	0.188	0.159	0.178
	High Density	0.166	Medium Density	0.172	Low Density	0.168

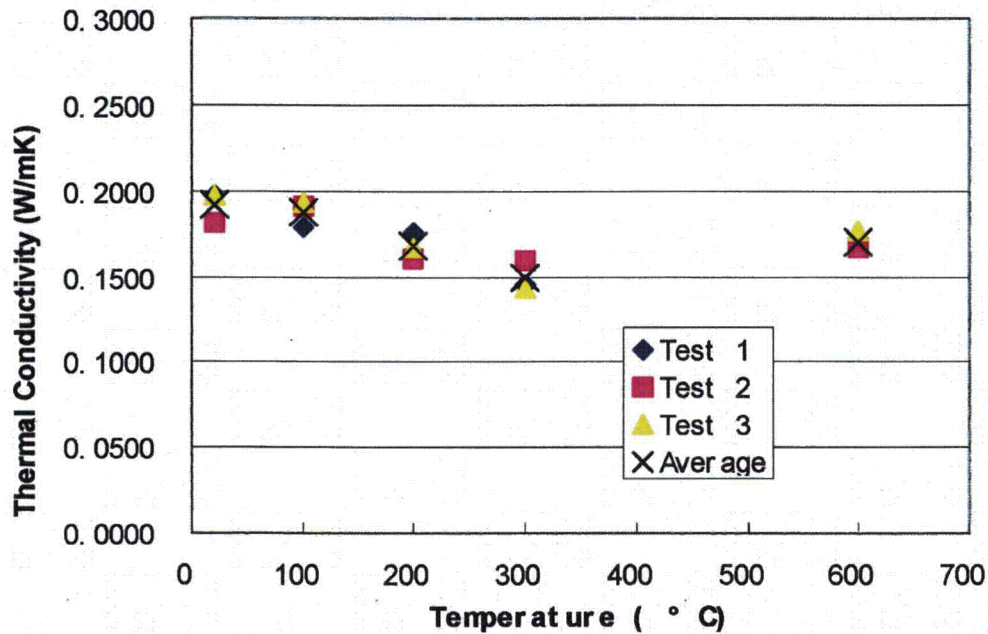


Figure 3. Thermal conductivity of Kaolite from room temperature to 600° C

Table 3. High Temperature Thermal Conductivity of Kaolite (unit: W/mK)

No. 323011258	Test 1	Test 2	Test 3	Average
20	0.1978	0.1815	0.1976	0.1923
100	0.1792	0.1913	0.1936	0.1880
200	0.1758	0.1601	0.1673	0.1677
300	0.1452	0.1592	0.1427	0.1490
600	0.1676	0.1665	0.1771	0.1704

density variation. Thermal conductivity results showed some scatter at these two temperatures.

The high temperature tests were performed on one medium density Kaolite sample. The thermal conductivity data are shown in Table 3. As shown in Figure 3, thermal conductivity values decreased as a function of temperature up to 300° C. This trend is consistent with ceramics and other insulating materials. At 600° C, thermal conductivity started to increase. This is also consistent with the fact that thermal radiation effect takes place in this temperature range. As temperature goes up, thermal conductivity of most insulating materials also goes up.

References:

- [1] S.E. Gustafsson, E. Karawacki and M.N., Khan, *J. Phys.D.: Appl. Phys.*, **1979**, 12, 1411.
[2] S.E. Gustafsson, *Rev. Sci. Instrum.*, **1991**, 62, 797
[3] V. Bohac, M.K. Gustavsson, L. Kubicar and S.E. Gustafsson, *Rev. Sci. Instrum.*, **2000**, 71, 2452

Distribution List:

Name	Bldg.	Mail Stop	#
C. N. Heatherly	9113	8206	1
J. L. Heck	9111	8201	1
S. T. Holder	9113	8206	1
G. A. Byington	9111	8201	1
M. R. Feldman	9113	8206	1
M. L. Goins	9112	8201	1
S. E. McClanahan	9113	8206	2
J.C. Walls	9201-2	8073	1
K. H. Luk	9201-2	8073	1
K. D. Handy	9201-2	8073	1
J. C. Anderson	9113	8206	1
J. H. Doyle	9113	8206	1
Jacob Y. Neal	9201-2	8073	1



Y/DW-1890

Water Content and Temperature- Dependent Impact Properties of an Inorganic Cast Refractory Material

B. F. Smith
Technology Development

G. A. Byington
Mechanical, Manufacturing, and
Specialty Engineering

February 14, 2003

LIMITED DISTRIBUTION

**Y-12
NATIONAL
SECURITY
COMPLEX**

MANAGED BY
BWXT Y-12, LLC
FOR THE UNITED STATES
DEPARTMENT OF ENERGY

UCN-13672 (10-00)

DISCLAIMER

This report was prepared as an account of work sponsored by an agency of the United States Government. Neither the United States Government nor any agency thereof, nor any of their employees, makes any warranty, express or implied, or assumes any legal liability or responsibility for the accuracy, completeness, or usefulness of any information, apparatus, product, or process disclosed, or represents that its use would not infringe privately owned rights. Reference herein to any specific commercial product, process, or service by trade name, trademark, manufacturer, or otherwise, does not necessarily constitute or imply its endorsement, recommendation, or favoring by the United States Government or any agency thereof. The views and opinions of authors expressed herein do not necessarily state or reflect those of the United States Government or any agency thereof.

Y/DW-1890

**WATER CONTENT AND TEMPERATURE-DEPENDENT IMPACT PROPERTIES
OF AN INORGANIC CAST REFRACTORY MATERIAL**

B. F. Smith
Technology Development

G. A. Byington
Mechanical, Manufacturing, and
Specialty Engineering

Date of Issue: February 14, 2003

LIMITED DISTRIBUTION

Prepared by the
Y-12 National Security Complex
P.O. Box 2009
Oak Ridge, Tennessee, 37831-8169
Managed by BWXT Y-12, L.L.C.
for the
U.S. DEPARTMENT OF ENERGY
under contract DE-AC05-00OR22800

CONTENTS

FIGURES.....	iv
TABLES.....	iv
INTRODUCTION.....	1
EXPERIMENTAL PROCEDURE.....	2
IMPACT TESTING.....	2
DEHYDRATION TESTING.....	4
RESULTS.....	4
IMPACT TESTING.....	4
DEHYDRATION TESTING.....	9
DISCUSSION.....	10
IMPACT TESTING.....	10
DEHYDRATION TESTING.....	11
REFERENCES.....	11

FIGURES

<u>Figure</u>	<u>Page</u>
1. Impact testing apparatus	3
2. Average stress-strain curves for Kaolite specimens tested at 100°F	5
3. Average stress-strain curves for Kaolite specimens tested at -40°F	6
4. Average stress-strain curves, upper and lower bounding curves, and average of upper and lower bounding curves	7
5. Upper and lower bounding curves, average of upper and lower bounding curves, all extrapolated to 100% compressive strain	8

TABLES

<u>Table</u>	<u>Page</u>
1. Test conditions for Kaolite specimens tested at 100°F	3
2. Test conditions for Kaolite specimens tested at -40°F	4
3. Coefficients to upper and lower bounding equations	9
4. High-density dehydration data	9
5. Medium-density dehydration data	10
6. Low-density dehydration data	10

INTRODUCTION

Impact-absorbing media used in radioactive material packaging systems have historically left much to be desired. Common materials included woods, papers, cardboards, foams, and other hydrocarbons. While relatively easy to install, these types of materials generate toxic gases, are flammable, and are prone to rupture the container in an overheating scenario.¹

Kaolite 1600 primarily consists of portland cement and vermiculite.² This ceramic was originally intended for use in refractory applications by its manufacturer, Thermal Ceramics. Its combination of light weight, low density, low cost, and noncombustibility made Kaolite an attractive alternative to the materials mentioned above for use in shipping packages.³ A variety of mechanical property tests were performed in the past on Kaolite specimens to gage its selection and effectiveness as an impact absorber in the ES-2 shipping package container. The mechanical properties included tensile strength, unconstrained compressive strength, and constrained compressive strength. Since the ES-2 will primarily contain radioactive materials, the neutron-absorbing properties of Kaolite are important. Since boron is a good neutron absorber, the addition of boron-containing compounds to Kaolite was proposed, but their effect on the mechanical properties of Kaolite had to be measured. For this reason, the strength and energy absorption of Kaolite that contained borax and boron carbide were also measured. If boron-containing compounds are not mixed with standard Kaolite, the only compound present that can absorb neutrons is the water of hydration.⁴

The ES-2 shipping package design was modified and renamed the ES-2100. During the production of 100 ES-2100 shipping containers, 280 insulation samples were taken. An insulation sample was taken for each 50-lb bag of material mixed. These constrained compressive production-run test samples were cast approximately 4 in. tall in a 4-in. schedule 40 steel pipe 6.5 in. long.

All of the samples were statically evaluated on the basis of their density. The upper and lower densities were statically rejected based upon the normal distribution probability of 90%, which rejected 11 high- and 13 low-density specimens. Three small groups' high, middle, and low densities containing eight samples each were made from the remaining samples. Each of the density groups was divided into three testing sets. Two of the test sets of four specimens were used for temperature-dependent constrained compressive testing and for dehydration testing. The third sample set of two specimens was used for temperature-dependent thermal conductivity testing performed at Oak Ridge National Laboratory.

This work follows up on the mechanical property testing previously performed on Kaolite but concentrates on constrained compression testing and measuring the water of hydration and latent water reabsorbed from air. No further tensile tests or unconstrained compression tests were performed. No investigations into the effects of boron-containing compounds were done, either. Previous mechanical testing was performed on specimens that were mixed in very small batches in a laboratory environment. The main purpose of this work is to ensure that Kaolite mixed according to Manufacturing Process Specification No. Y/EN-5984⁵ in a production environment is as strong as that mixed in a lab.

EXPERIMENTAL PROCEDURE

It was determined that 24 Kaolite 1600 specimens would be impact tested; 12 tested at 100°F and 12 tested at -40°F. Each set would contain four each of high-, medium-, and low-density specimens. All specimens would be subsequently heated to 1600°F to drive off the water of hydration and the latent water reabsorbed from air. The difference between the initial weight and the final weight would be the water of hydration and reabsorbed from air weight. Densities were calculated for each specimen and compared to the manufacturer's calculated values.

IMPACT TESTING

Each specimen consisted of a Kaolite plug, measuring 4-in. in diameter by 4 in. tall, inside a 6.5-in.-long, 4-in. schedule 40 steel pipe. One end of the plug was flush with the end of the pipe. The steel pipe of each specimen was engraved with its mix control number (MCN). A 4-in. schedule 40 pipe was specified in order to withstand the anticipated pressure generated during a constrained compression test. All impact testing was to be performed at the fastest readily obtainable speed. The machine that met this requirement was a 20,000-lb_f-capacity servohydraulic load frame with an actuator (hydraulic piston) that can reach 200 in./s. Compression platens of 3 $\frac{3}{8}$ -in. diameter were used. Test fixtures were designed and fabricated. The standard load cell used during slow-speed tests could not be used with high-speed tests, so a Kistler quartz force transducer was used in its place. The test fixtures were designed such that each specimen would be compressed to 50% strain. Typically, the deformation of a specimen is measured with an external sensor such as an extensometer, strain gage, or external linear variable differential transformer (LVDT). Measurements of extension or compression can be taken using the LVDT that is inside the hydraulic actuator, but this is not usually done since it introduces the overall deflection of the load frame into the deflection reading of the specimen. The maximum deflection of the load frame is about 0.040 in., which is negligible compared to the 2-in. deflection of the specimen. Thus, the LVDT internal to the actuator would be used to measure the compression of the specimen. Figure 1 shows that several extenders had to be used to allow for the height of the environmental chamber in which all tests were performed. Calculations showed that the extenders would buckle under a load of approximately 74,000 lb_f, which is significantly more than the 20,000-lb_f maximum capacity of the load frame. Since testing would be done at elevated and lowered temperatures, each specimen would need to soak until the interior of the specimen reached its test temperature. Rough calculations showed that a soak time of 39 h would get the specimen to within 10% of the test temperature. All specimens were soaked significantly longer than 39 h. The 100°F specimens were soaked for approximately 100 h, and the -40°F specimens were soaked for approximately 300 h. Tables 1 and 2 summarize these testing conditions.

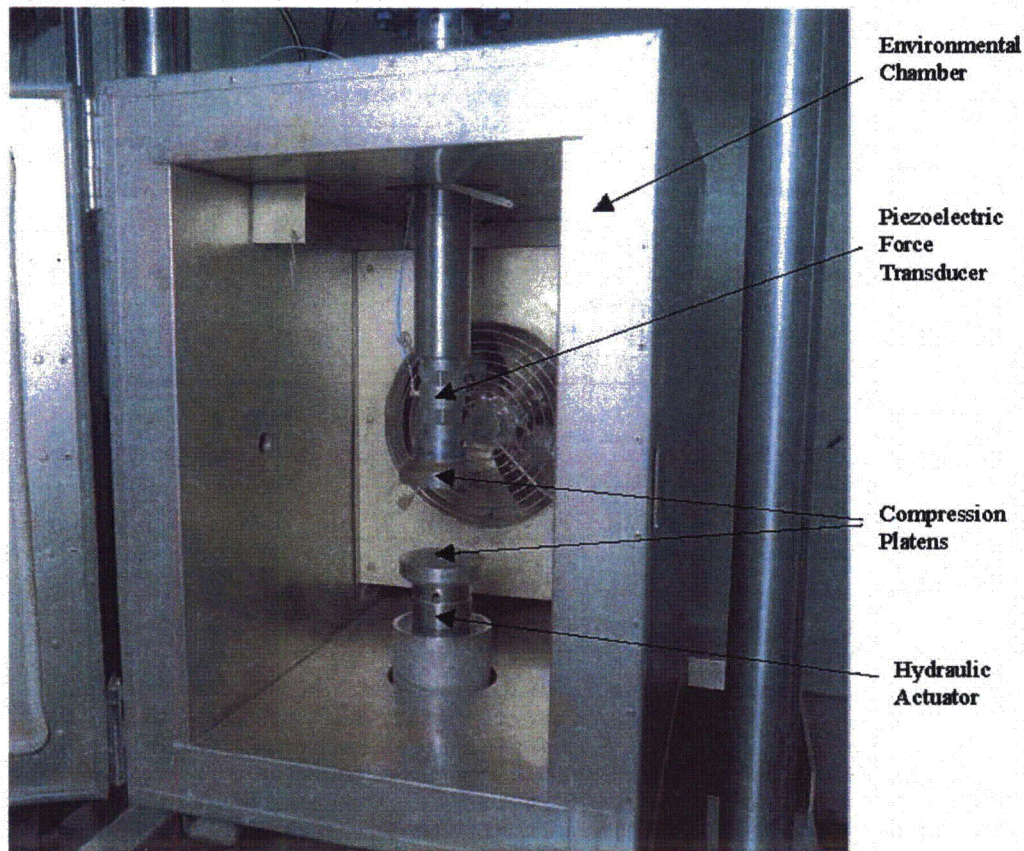


Fig. 1. Impact testing apparatus.

Table I. Test conditions for Kaolite specimens tested at 100°F

MCNID	Heating time (h)	Density group	Documented density (lb/ft ³)	Density gain ^a (lb/ft ³)	Density before heating (lb/ft ³)	Heating density change (lb/ft ³)	Density after heating (lb/ft ³)	Average test velocity (in./s)
411011216	101.25	Low	20.27	1.43	21.70	-0.15	21.55	192.9
402011246	120.42	Low	20.35	1.82	22.17	-0.20	21.97	190.6
419011046	93.92	Low	20.42	2.74	23.16	-0.08	23.08	189.7
406011219	98.80	Low	20.47	3.07	23.54	-0.06	23.48	194.6
222011053	100.85	Mid	21.98	1.46	23.44	-0.17	23.27	191.7
309011000	102.25	Mid	22.06	1.04	23.10	-0.16	22.94	192.3
406011232	93.67	Mid	22.06	2.44	24.50	-0.09	24.41	192.6
425011101	96.90	Mid	22.06	2.34	24.40	-0.09	24.31	195.3
316011054	94.40	High	23.49	-0.78	22.71	-0.07	22.64	186.8
425011046	93.00	High	23.53	3.44	26.97	-0.10	26.87	183.5
118010847	101.65	High	23.68	1.48	25.16	-0.16	25.00	185.1
425011329	53.72	High	23.71	3.17	26.88	-0.25	26.63	

^a It is assumed that the change in density is latent water.

Table 2. Test conditions for Kaolite specimens tested at -40°F

MCNID	Cooling time (h)	Density group	Documented density (lb/ft ³)	Density gain ^a (lb/ft ³)	Density before cooling (lb/ft ³)	Cooling density change (lb/ft ³)	Density after cooling (lb/ft ³)	Average test velocity (in./s)
508010845	338.48	Low	20.28	2.64	22.92	0.08	23.00	192.3
316011150	362.03	Low	20.40	1.71	22.11	0.09	22.20	187.7
425010912	340.38	Low	20.41	2.33	22.74	0.09	22.83	191.7
508010830	364.87	Low	20.47	2.65	23.12	0.11	23.23	192.4
326011220	337.45	Mid	21.99	1.78	23.77	0.11	23.88	185.6
301010815	361.40	Mid	22.06	2.20	24.26	0.10	24.36	188.7
326011239	339.62	Mid	22.06	2.20	24.26	0.10	24.36	185.8
426011155	364.23	Mid	22.06	1.88	23.94	0.09	24.03	185.7
425011235	339.02	High	23.53	3.16	26.69	0.11	26.80	182.0
425010941	363.58	High	23.53	2.71	26.24	0.07	26.31	183.7
323010953	360.85	High	23.56	1.93	25.49	0.08	25.57	174.6
425011007	337.13	High	23.71	3.57	27.28	0.09	27.37	189.9

^a It is assumed that the change in density is latent water.

DEHYDRATION TESTING

The water content of Kaolite determines the neutron-absorbing properties. Properly cured Kaolite should have very little latent water, but may have a significant amount of water of hydration. This water of hydration can be driven off by heating the specimens above a critical temperature, 1600°F. Each specimen was heated at this temperature until consecutive measurements differed by <0.1%. Each plug was removed from its metal sleeve using a larger, 200,000-lb_f capacity load frame. This load frame was used instead of the 20,000-lb_f capacity machine since its larger actuator area and load cell area simplified setting up fixturing. During heating, each compacted Kaolite plug was placed into an Inconel crucible, which was placed in a small lab furnace. A metal crucible had to be used because ceramic ones would not withstand the thermal shock associated with repeated removal from the furnace into cool, room-temperature air.

RESULTS

IMPACT TESTING

Figure 2 shows average compressive stress-strain curves for specimens tested at 100°F. Each curve is the average of the specimens in a density group, high, medium, or low. Using the average density group values dampened some of the noise in the gathered data. The average density of the high-density group was documented as 23.6 lb/ft³. The average density of the medium density group was documented as 22.0 lb/ft³. The average density of the low-density group was documented as 20.4 lb/ft³. These curves were generated by averaging the stresses at discrete strain points at intervals of 1% strain. Figure 3 shows the average compressive stress-strain curves for specimens tested at -40°F. Figure 4 repeats the average compressive stress-strain curves shown in Figs. 2 and 3 and adds to them upper, lower, and average bounding curves.

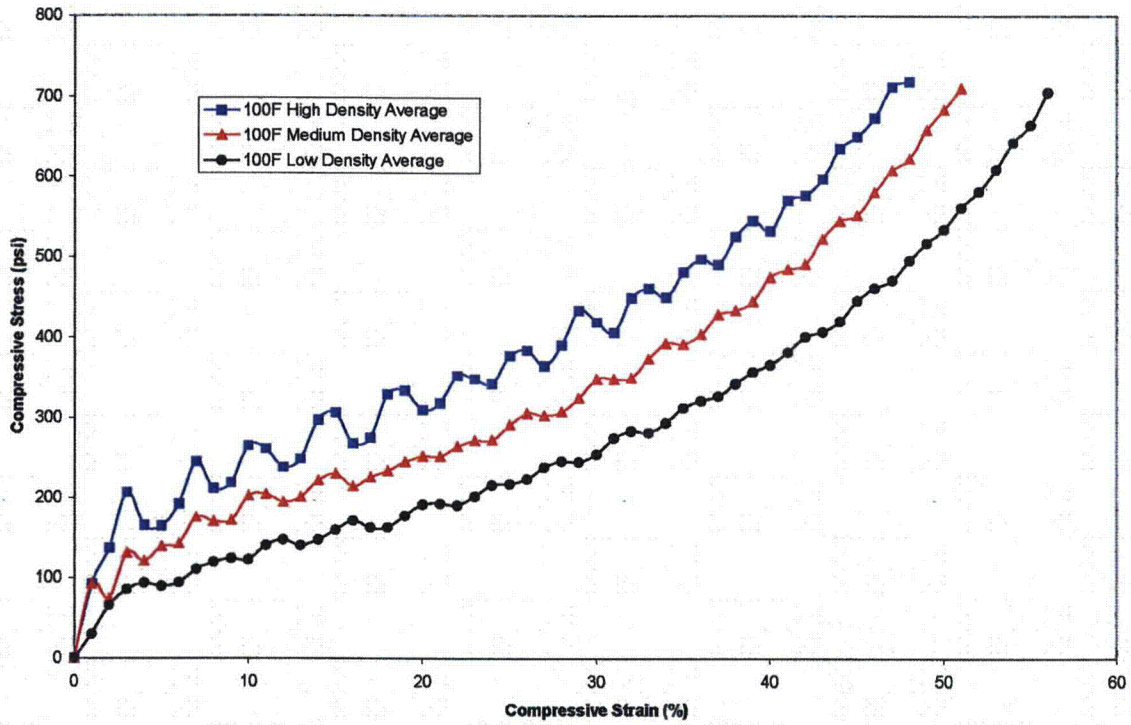


Fig. 2. Average stress-strain curves for Kaolite specimens tested at 100°F.

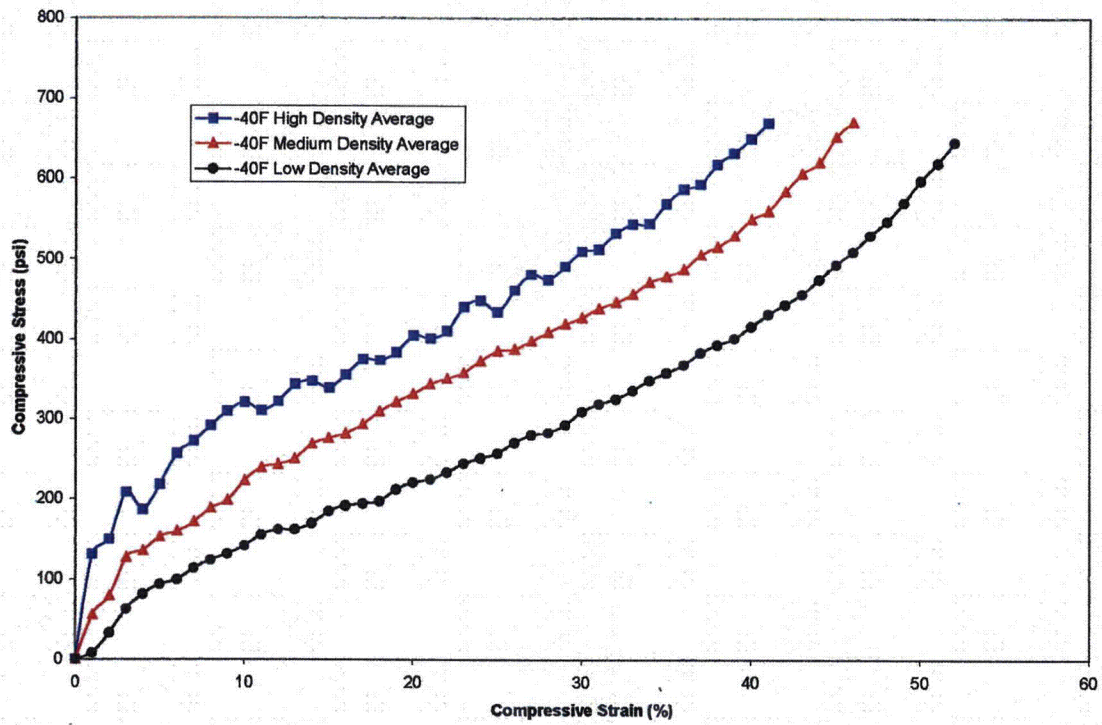


Fig. 3. Average stress-strain curves for Kaolite specimens tested at -40°F.

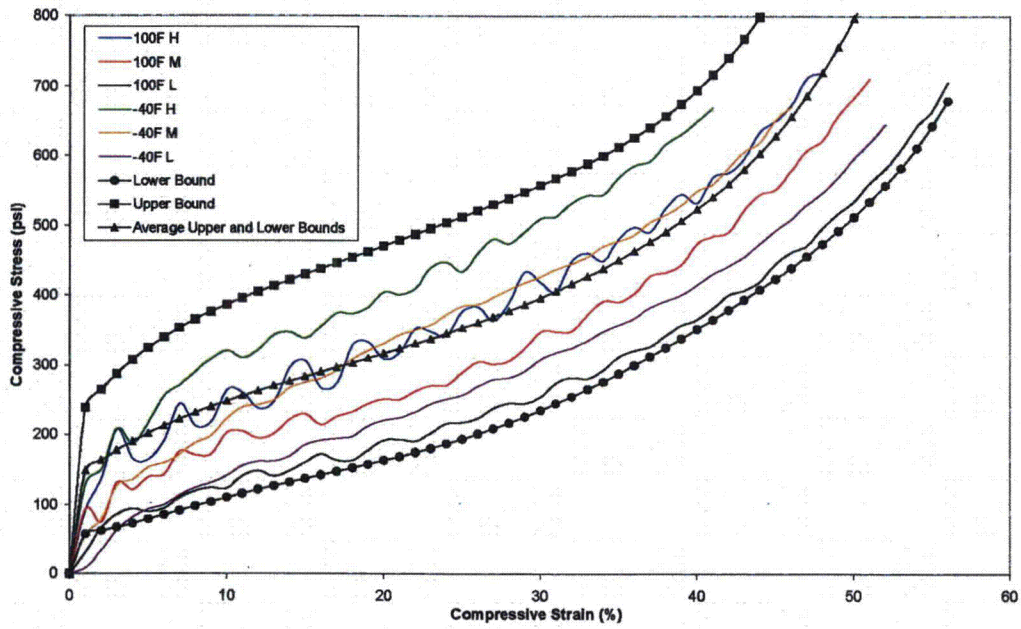


Fig. 4. Average stress-strain curves, upper and lower bounding curves, and average of upper and lower bounding curves.

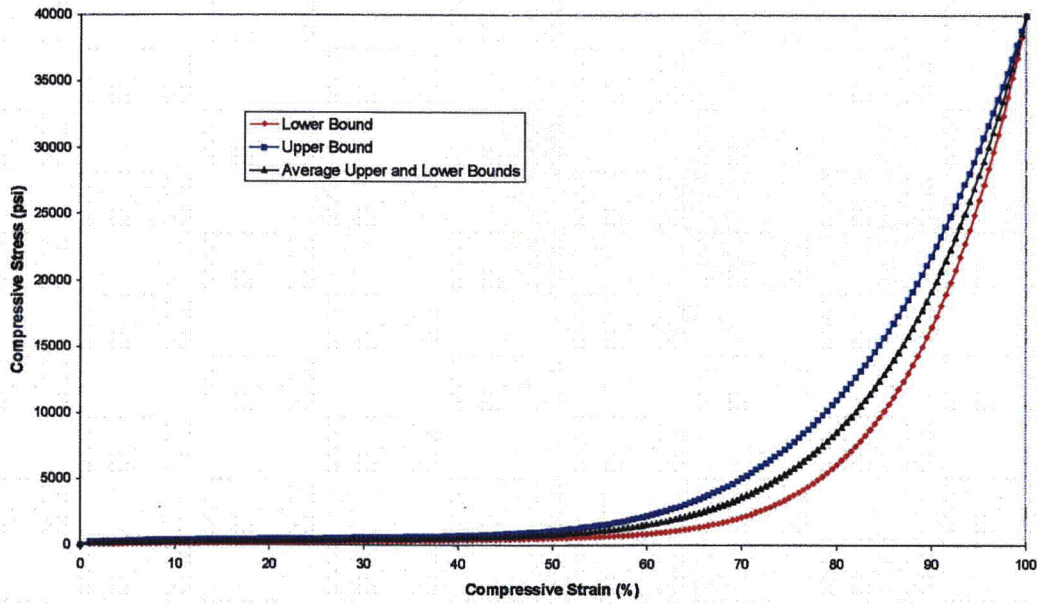


Fig. 5. Upper and lower bounding curves, average of upper and lower bounding curves, all extrapolated to 100% compressive strain.

The bounding curves were generated at the extreme noise peaks. The strongest material created the upper bound, and it was the -40°F high-density group. The weakest material generated the lower bounding curve, and it was the 100°F low-density group. Table 3 shows the coefficients for the equations of the bounding curves between 1 and 100% strain. A value of 40,000 psi at 100% strain was used with the collected data to create a smooth curve beyond the tested values for computer drop test simulations. A straight line is assumed to be from zero stress and strain to the curve value at 1% strain.

Table 3. Coefficients to upper and lower bounding equations

$\sigma = a + be + ce^2 + de^3 + ee^4 + fe^5 + ge^6$							
	a	b	c	d	e	f	g
Upper	209.2	31.96	-2.244	0.1050	-0.00253	2.78×10^{-5}	7.06×10^{-8}
Average	131.5	17.29	-0.7443	0.01878	4.31×10^{-5}	-8.36×10^{-6}	1.06×10^{-7}
Lower	53.86	2.613	0.7550	-0.06748	0.002618	-4.45×10^{-5}	2.83×10^{-7}

DEHYDRATION TESTING

Tables 4, 5, and 6 show the initial weight of each specimen and total water loss after heating at 1600°F. The percent of the initial weight of water is given in the third column. No data are included for MCNIDs 0425011007 and 0425011329 since their initial weights were mistakenly not measured. Without the initial weight, it is impossible to know how much water was lost through heating.

Table 4. High-density dehydration data

MCNID	Initial weight (lb)	Water loss (lb)	Initial weight (%)	Documented density (lb/ft ³)	Density before dehyd (lb/ft ³)	Dehyd water lost (lb/ft ³)	Water gained (lb/ft ³)	Initial water (lb/ft ³)
0316011054	0.6189	0.0842	13.60	23.49	22.64	3.08	-0.85	3.93
0425010941	0.7098	0.0982	13.83	23.53	26.31	3.64	2.78	0.86
0425011046	0.7135	0.0934	13.09	23.53	26.87	3.52	3.34	0.18
0425011235	0.7190	0.0961	13.37	23.53	26.80	3.58	3.27	0.31
0323010953	0.7250	0.0996	13.74	23.56	25.57	3.51	2.01	1.50
0118010847	0.7022	0.0946	13.47	23.68	26.63	3.59	2.95	0.64
0425011007								
0425011329								
Average	0.6981	0.0944	13.52	23.55	25.80	3.49	2.25	1.24

Table 5. Medium-density dehydration data

MCNID	Initial weight (lb)	Water loss (lb)	Initial weight (%)	Documented density (lb/ft ³)	Density before dehyd (lb/ft ³)	Dehyd water lost (lb/ft ³)	Water gained (lb/ft ³)	Initial water (lb/ft ³)
0222011053	0.6104	0.0844	13.83	21.98	23.27	3.22	1.29	1.93
0326011220	0.6851	0.0928	13.55	21.99	23.88	3.24	1.89	1.35
0309011000	0.6612	0.0879	13.29	22.06	22.94	3.05	0.88	2.17
0301010815	0.6800	0.0978	14.38	22.06	24.36	3.50	2.30	1.20
0326011239	0.6849	0.0945	13.80	22.06	24.36	3.36	2.30	1.06
0406011232	0.6586	0.0879	13.35	22.06	24.41	3.26	2.35	0.91
0426011155	0.6651	0.0876	13.17	22.06	24.03	3.16	1.97	1.19
0425011101	0.6772	0.0950	14.03	22.06	24.31	3.41	2.25	1.16
Average	0.6653	0.0910	13.68	22.04	23.95	3.28	1.90	1.37

Table 6. Low-density dehydration data

MCNID	Initial weight (lb)	Water loss (lb)	Initial weight (%)	Documented density (lb/ft ³)	Density before dehyd (lb/ft ³)	Dehyd water lost (lb/ft ³)	Water gained (lb/ft ³)	Initial water (lb/ft ³)
0411011216	0.5180	0.0710	13.71	20.27	21.55	2.95	1.28	1.67
0508010845	0.6320	0.0897	14.19	20.28	23.00	3.26	2.72	0.54
0402011246	0.6025	0.0825	13.69	20.35	21.97	3.01	1.62	1.39
0316011150	0.6348	0.0876	13.80	20.40	22.20	3.06	1.80	1.26
0425010912	0.6299	0.0888	14.10	20.41	22.83	3.22	2.42	0.80
0419011046	0.6391	0.0909	14.22	20.42	23.08	3.28	2.66	0.62
0508010830	0.6404	0.0912	14.24	20.47	23.23	3.31	2.76	0.55
0406011219	0.6418	0.0825	12.85	20.47	23.48	3.02	3.01	0.01
Average	0.6173	0.0855	13.85	20.38	22.67	3.14	2.28	0.86

Additional evaluations of the water loss and density changes need to be examined further. On the average the samples gained about 1.9 lb/ft³ in density after manufacturing and lost 3.28 lb/ft³ during the dehydration testing. The difference between these average density values is assumed to be water, and the as-cast manufactured water content is 1.37 lb/ft³. Therefore, the cast insulation Kaolite specimens used for this testing tends to absorb water from the air if it is available.

DISCUSSION

IMPACT TESTING

Generally, the constrained compressive strength of Kaolite is proportional to its density and inversely proportional to its temperature. For each temperature group and for each strain point, the stress in the specimen was higher at the next higher density group. Also, for a given density group, the specimens tested at low temperatures displayed higher stress levels than those tested at high temperatures. (Refer to Figs. 2 and 3.)

DEHYDRATION TESTING

During heating at 1600°F, the Kaolite specimens lost between 12.85% and 14.38% of their initial weight as water. The high-density group lost an average of 13.52% of its initial weight as water. The medium-density lost an average of 13.67% and the low-density group lost an average of 13.85%. In general, the percentage of water loss by weight is inversely proportional to the density. The less dense specimens lost a larger percentage of their starting weight as water.

REFERENCES

1. *Advantages of Using a Fireproof Inorganic Cast Refractory Material in Hazardous Content Shipping Packages*, Y/LF-565, compiled by Y-12 Nuclear Package Systems, Lockheed Martin Engineering Systems, Inc., Manufacturing Engineering, Engineering Analysis, Lockheed Martin Energy Systems, Inc., Oak Ridge Y-12 Plant, Oak Ridge, Tennessee, November 1998.
2. Thermal Ceramics, *Kaolite Super Lightweight Insulating Castables*, Augusta, Georgia, <http://www.thermalceramics.com>.
3. Byington et al., "Fireproof Impact Limiter Aggregate Packaging Inside Shipping Containers," U.S. Patent No. US 6,299,850 B1, October 9, 2001.
4. Oakes, R., *Mechanical Properties of a Low Density Concrete for the New ES-2 Shipping/Storage Container Insulation, Impact Mitigation Media and Neutron Absorber*, Y/DW-1661, Lockheed Martin Energy Systems, Inc., Oak Ridge Y-12 Plant, Oak Ridge, Tennessee, April 1997.
5. *For Casting Kaolite 1600™ into ES Shipping Containers*, Manufacturing Process Specification No., Y/EN-5984, Rev. A, February 11, 2000.

DISTRIBUTION

Y-12 National Security Complex

Anderson, J. C., 9113, MS-8206
Byington, G. A., 9111, MS-8201 (2)
Doyle, J. H., 9113, MS-8206
Feldman, M. R., 9113, MS-8206
Goins, M. L., 9112, 8201
Handy, K. D., 9201-2, MS-8073 (2)
Heatherly, C. N., 9113, MS-8206
Heck, J. L., 9111, MS-8201
Holder, S. T., 9113, MS-8206
Kitzke, K. A., 9203, MS-8084
Luk, K. H., 9201-2, MS-8073
McClanahan, S. E., 9113, MS-8206 (2)
Neal, J. Y., 9201-2, MS-8073
Smith, B. F., 9203, MS-8084
Walls, J.C., 9201-2, MS-8073
Y-12 Plant Records—RC

**Low Temperature Impact Properties of an
Inorganic Cast Refractory Material**

B. F. Smith
Technology Development

September 14, 2004

Prepared by the
Y-12 National Security Complex
P.O. Box 2009
Oak Ridge, Tennessee, 37831-8169
Managed by BWXT Y-12, L.L.C.
for the
U.S. DEPARTMENT OF ENERGY
under contract DE-AC05-00OR22800

**LOW TEMPERATURE IMPACT PROPERTIES OF AN INORGANIC CAST
REFRACTORY MATERIAL**

B. F. Smith
Technology Development

Date of Issue: September 14, 2004

Prepared by the
Y-12 National Security Complex
P.O. Box 2009
Oak Ridge, Tennessee, 37831-8169
Managed by BWXT Y-12, L.L.C.
for the
U.S. DEPARTMENT OF ENERGY
under contract DE-AC05-00OR22800

CONTENTS

FIGURES.....	iv
TABLES.....	iv

FIGURES

<u>Figure</u>	<u>Page</u>
1. Average Stress-Strain Curves for Kaolite Specimens Tested at -40°F	3
2. Average Stress-Strain Curves, Upper and Lower Bounding Curves, and Average of Upper and Lower Bounding Curves	4
3. Comparison of Upper Bounding Curves	5

TABLES

<u>Table</u>	<u>Page</u>
1. Test Conditions for Kaolite Specimens	2
2. Coefficients to Upper and Lower Bounding Equations	6

INTRODUCTION

Several Y-12 shipping containers such as the ES-2100, DPP-2, MD-1, and ES-3100 now use Kaolite 1600 as an impact-absorbing medium. For quality and design control reasons, procedures for mixing, curing, and baking Kaolite were written specifically for each container. The first certified shipping container to use Kaolite was the ES-2100. The procedures for mixing Kaolite for use in this container are documented in manufacturing process specification number Y/EN-5984.¹ This document requires the final, dry density of mixed Kaolite to be 22.4 lb/ft³, but densities between 19.4 lb/ft³ and 25.4 lb/ft³ are acceptable. The manufacturer of the containers followed the mixing specification and switched from a low power mixer to a high volume, high power mortar mixer. This new mortar mixer reduced the labor required to manufacture the casting by over two-thirds. However, there was an unforeseen consequence. During the prototype shipping container production runs, the density has been consistently too high, averaging 26.7 lb/ft³ in ES-3100 containers and 25.2 lb/ft³ in MD-1 containers. The dynamic response of the ES-3100 container was modeled using data from previous testing on within-spec Kaolite which is documented in Y/DW-1890, "Water Content and Temperature-Dependent Impact Properties of an Inorganic Cast Refractory Material."² It was unknown how the higher-density material would affect the response of the container. Thus, the purpose of this study was to measure the impact properties of the higher-density Kaolite as it was produced for the prototype shipping containers. The mixing procedure was modified such that the densities of the production run castings were controlled close to the nominal density. Engineering now has the opportunity to design a container with a Kaolite density over a range of 21 to 31 lb/ft³ and adjust the strength accordingly.

EXPERIMENTAL PROCEDURE

This procedure duplicates the one described in Y/DW-1890, with a few exceptions. Only impact testing was performed, no dehydration was done. All 12 impact tests were at -40°F, none were at 100°F. It was expected that more dense material would result in higher stress for a given strain. In order to prevent overloading the load cell, the total displacement or strain of the specimen would have to be reduced. This was done by lengthening the test stand one inch. This was achieved by cutting a one inch section of schedule 40 pipe from an old Kaolite test specimen and attaching it onto the end of the existing fixture.

It was hypothesized that the mechanism by which Kaolite density came out too high was due to the mixing procedure. It was speculated that mixing for extended periods effectively pulverized the vermiculite aggregate used in Kaolite, resulting in finer particles, more surface area to absorb water, and higher densities. Regardless of the exact mechanism, the density of the material is proportional to the length of mixing time. Six pairs of specimens were produced. Each pair was taken from batches mixed for specific lengths of time. The mixing times were 4, 5, 7.5, 10, 12, and 14 min. Each specimen was named using its mixing time and an arbitrary "1" or "2."

The densities of 12 specimens were measured prior to being placed in a heat pump cycle environmental chamber. Here they soaked for approximately 140 h at -40°F. Six specimens were then placed in an expanded polystyrene container and transferred to the Mechanical Properties Laboratory where impact testing would commence. Unfortunately, multiple equipment problems appeared during the first test and no data was taken. The specimens remained there for 168 h during which time the temperature gradually rose to -13°F. Eleven specimens were then transferred to a liquid nitrogen-cooled environmental chamber in the Mechanical Properties Laboratory where they soaked for 13 h at -40°F. Impact tests were then performed inside this chamber.

RESULTS

Impact testing was successful on nine specimens. No data was taken on specimens 5-2, 7.5-1, and 7.5-2. The remaining specimens were divided into high, medium, and low density groups. Table 1 summarizes the test conditions for each specimen. Figure 1 shows the average stress-strain curves for each of these density groups at maximum actuator speeds. Figure 2 adds to these the upper and lower bounding curves as determined by sixth order polynomial curve fits. A sixth order fit was determined to be the lowest order that would result in acceptable low errors. An average curve of the upper and lower bounds is also included in Fig. 2. Figure 3 compares the upper bound of the higher density material of this study with the upper bound of the material as determined in Y/DW-1890. Finally, Table 2 gives the coefficients of the equations of the upper and lower bounding curves. Note that these curves are not to be extrapolated beyond the strains shown in Fig. 2.

Table 1. Test Conditions for Kaolite Specimens

Specimen ID	Density (lb/ft ³)	Density Group	Approx. Cooling Time (h)	Average Test Velocity (in/s)
4-1	24.23	Low	323.0	159.1
4-2	24.05	Low	323.5	159.2
5-1	23.45	Low	325.8	162.1
5-2	23.71	N/A		
7.5-1	26.40	N/A		
7.5-2	24.91	N/A		
10-1	27.39	Medium	329.2	178.2
10-2	27.32	Medium	330.0	176.3
12-1	27.83	Medium	327.6	170.6
12-2	27.68	Medium	329.5	173.0
14-1	33.55	High	324.3	172.3
14-2	33.21	High	326.7	169.9

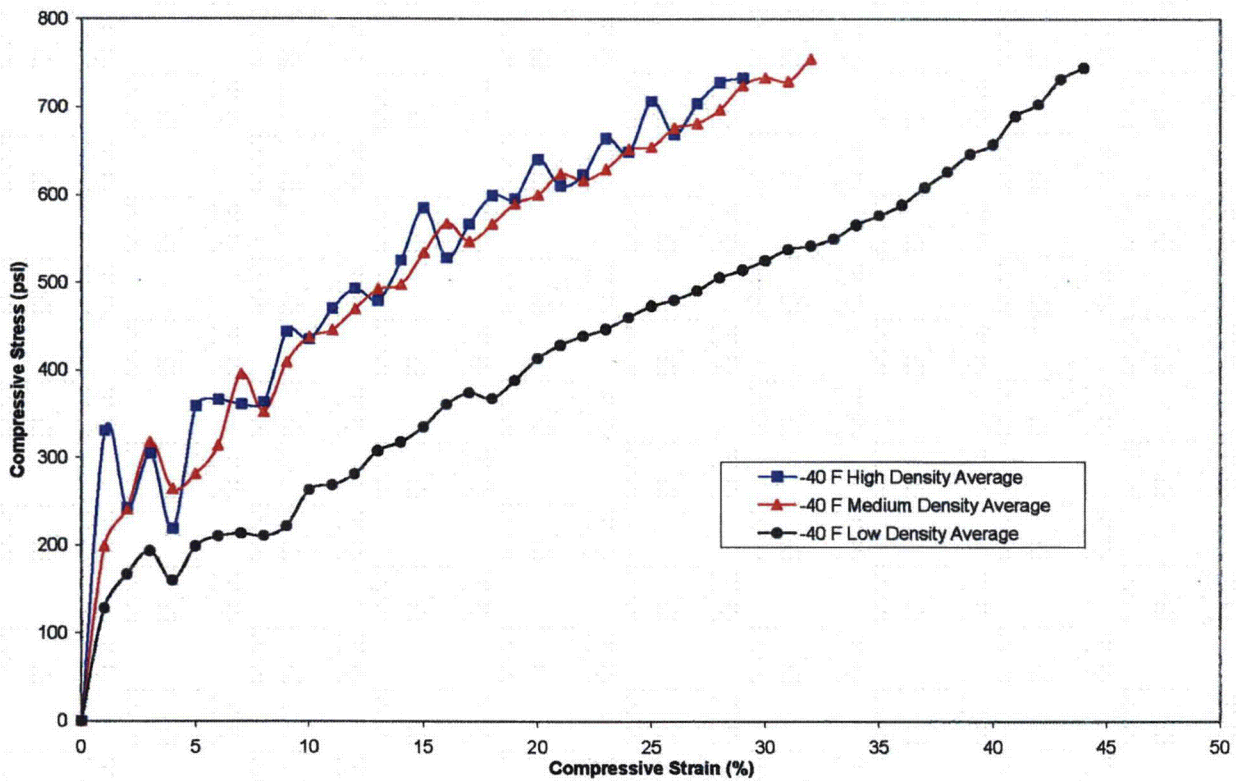


Fig. 1. Average Stress-Strain Curves for Kaolite Specimens Tested at -40°F

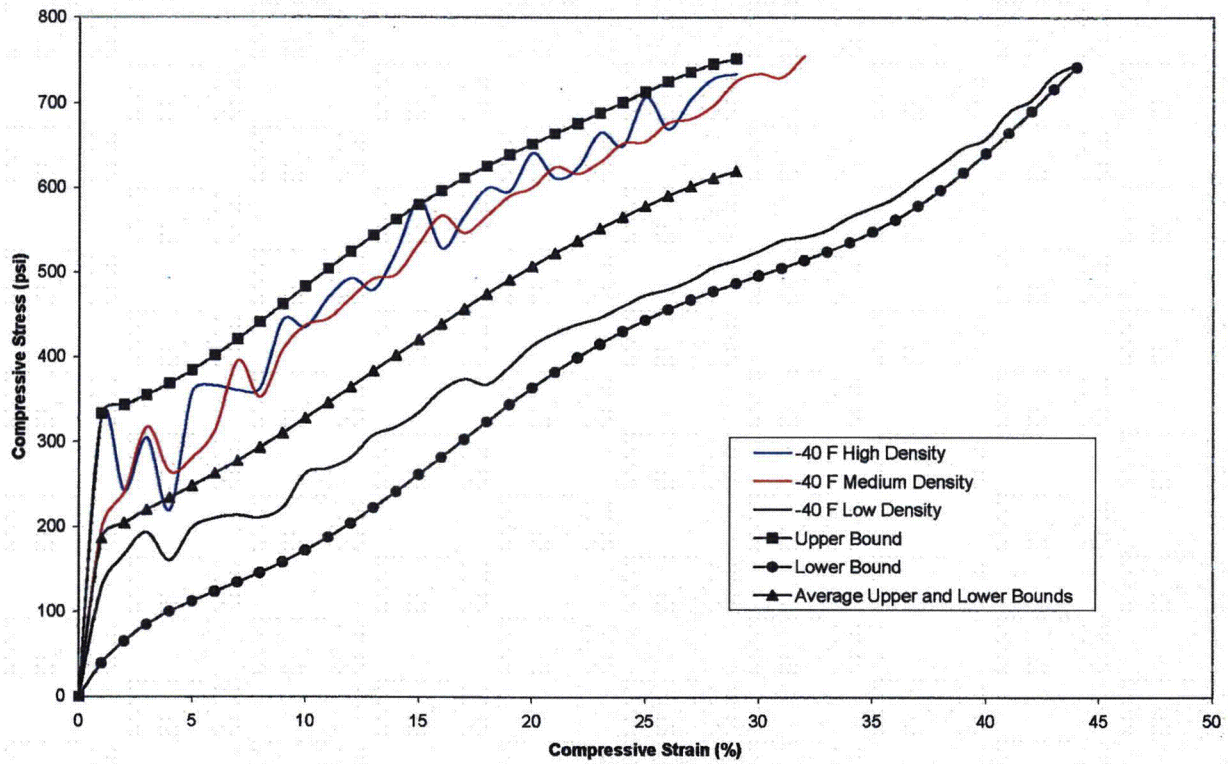


Fig. 2. Average Stress-Strain Curves, Upper and Lower Bounding Curves, and Average of Upper and Lower Bounding Curves

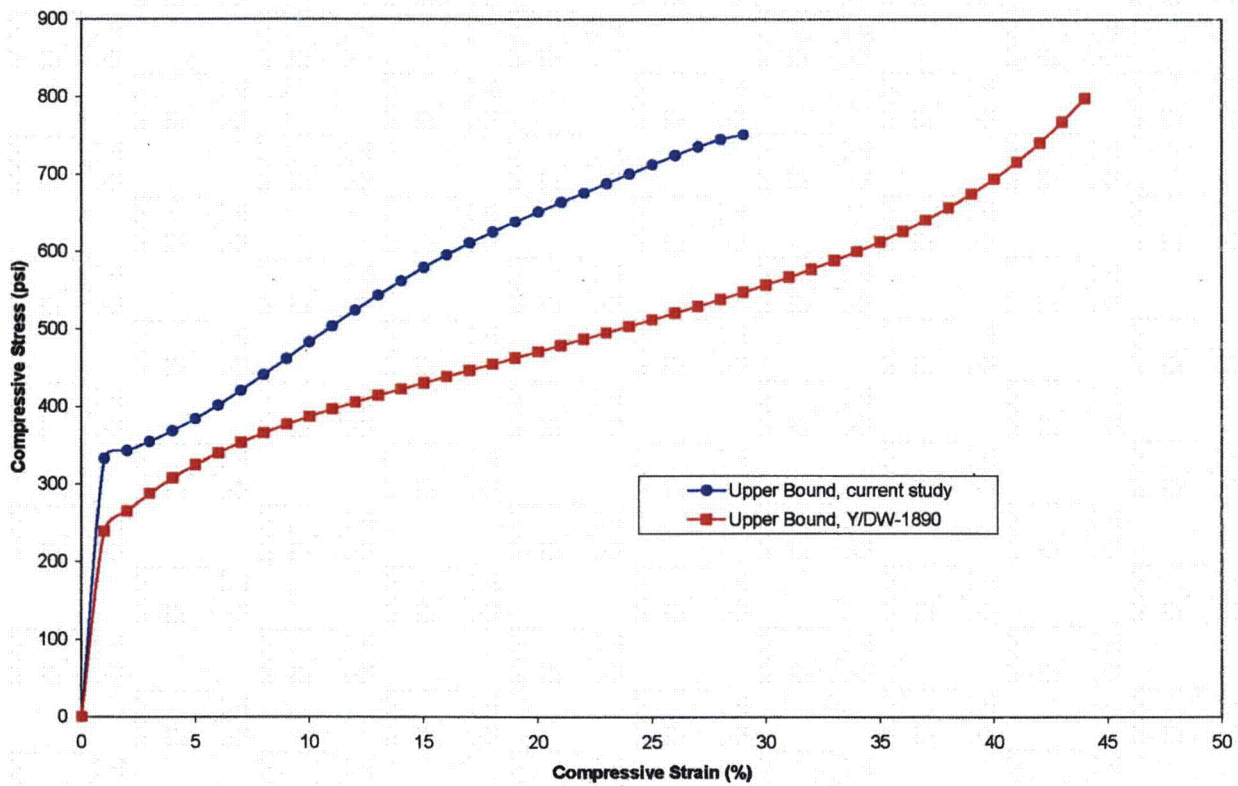


Fig. 3. Comparison of Upper Bounding Curves

Table 2. Coefficients to Upper and Lower Bounding Equations

$\sigma = a + bs + cs^2 + ds^3 + es^4 + fs^5 + gs^6$							
	a	b	c	d	e	f	g
Upper	3.25×10^2	8.24	2.22×10^{-1}	1.80×10^{-1}	-1.82×10^{-2}	6.39×10^{-4}	-7.75×10^{-6}
Lower	4.23	4.06×10^1	-6.07	5.59×10^{-1}	-2.31×10^{-2}	4.34×10^{-4}	-3.03×10^{-6}

DISCUSSION

As expected, the high density Kaolite is significantly stronger than the Kaolite tested in Y/DW-1890. Upon comparing upper bounding curves, the high density material averaged 32% higher stress over the strain range of 1% to 29%.

REFERENCES

1. *For Casting Kaolite 1600™ into ES Shipping Containers, Manufacturing Process Specification No., Y/EN-5984, Rev. A, February 11, 2000.*
2. Smith, B.F., Byington, G.A., *Water Content and Temperature-Dependent Impact Properties of an Inorganic Cast Refractory Material, Y/DW-1890, BWXT Y-12, L.L.C., Y-12 National Security Complex, Oak Ridge, Tennessee, February, 2003.*

DISTRIBUTION

Y-12 National Security Complex

Anderson, J. C.
Arbital, J. G.
Baker, M. L./Kitzke, K. A.
Bales, P. A.
Byington, G. A. (2)
DeClue, J. F. (2)
Doyle, J. H.
Goins, M. L.
Hammond, C. R.
Handy, K. D. (2)
Heatherly, C. N.
Miller, D. B.
Neal, J. Y.
Smith, B. F.
Sooter, D. P.
Y-12 Plant Records - RC

Y-12

OAK RIDGE
Y-12
PLANT

LOCKHEED MARTIN ENERGY SYSTEMS, INC.

MANAGED BY
LOCKHEED MARTIN ENERGY SYSTEMS, INC.
FOR THE UNITED STATES
DEPARTMENT OF ENERGY

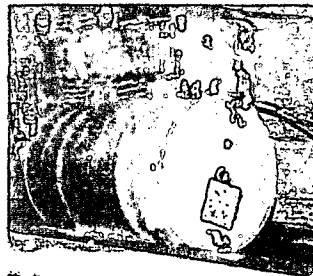
UC-2000 (23 000)

Advantages of Using a Fireproof Inorganic Cast Refractory Material in Hazardous Content Shipping Packages

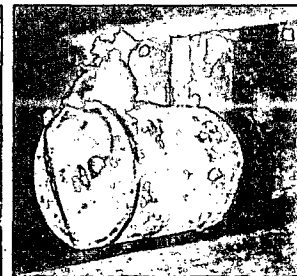
Y-12 Nuclear Packaging Systems
Lockheed Martin Energy Systems, Inc.

November 10, 1998

Fireproof Inorganic
Cast Refractory



Flammable Organic
Hydrocarbons



Thermal insulating impact limiters being removed from furnace after more than a 30-minute burn time in excess of 1475°F

This procedure has been reviewed by an Authorized Derivative Classifier and has been determined to be UNCLASSIFIED. This review does not constitute clearance for public release.

Steve McLenahan
Name & Date

Nov. 11, 1998
Effective Date

**Advantages of Using a Fireproof Inorganic Cast Refractory Material
in Hazardous Content Shipping Packages**

Compiled by

**Y-12 Nuclear Packaging Systems
LMES Manufacturing Engineering
Engineering Analysis**

**Prepared by the
Oak Ridge Y-12 Plant
Oak Ridge, Tennessee 37831
managed by
Lockheed Martin Energy Systems, Inc.
for the
U.S. Department of Energy
under contract DE-AC05-84OR21400**

Advantages of Using a Fireproof Inorganic Cast Refractory Material in Hazardous Content Shipping Packages

1.0 Introduction

Lockheed Martin Energy Systems, Inc. (Energy Systems) has developed a superior design for hazardous material shipping packages. The use of a fireproof castable refractory material for impact absorption and thermal insulation allows these shipping packages to outperform similar shipping packages of conventional design when subjected to a series of hypothetical accident condition (HAC) tests. This material also has the advantages of reducing the risk of human exposure to inhalation of toxic smoke and material release due to high temperatures, and the material does not burn under these accident conditions. During normal conditions of transport (NCTs), personal safety is also improved. These improvements can be achieved using packaging designs that are competitively priced when compared to similar packages of conventional design.

The newly designed ES-2 shipping package, a Type-B radioactive material shipping package,¹ includes an inorganic castable refractory material which acts as an impact limiter and a thermal insulator² (see Figure 1). Kaolite 1600[®], a castable Portland cement and vermiculite (expanded mica)-based aggregate produced by Thermal Ceramics was chosen for this application.³ This material replaces the flammable organic hydrocarbon material (e.g., cane fiberboard, polyurethane foams, wood, cork, cardboard, paper or plastics) typically used in many shipping packages. This new material is ideal for crush and impact protection and is fireproof with a maximum continuous service temperature of 870°C (1600°F). The ES-2 shipping package has passed certification testing for a Type-B shipping package as outlined in the U.S. Code of Federal Regulations (CFR) Part 10 Section 71, *Packaging and Transportation of Radioactive Material*.

This paper details the advantages of using a castable refractory material for hazardous material shipping packages when compared to commonly used materials. The improvements listed above and the performance of the package during HAC and NCT testing are discussed in detail.

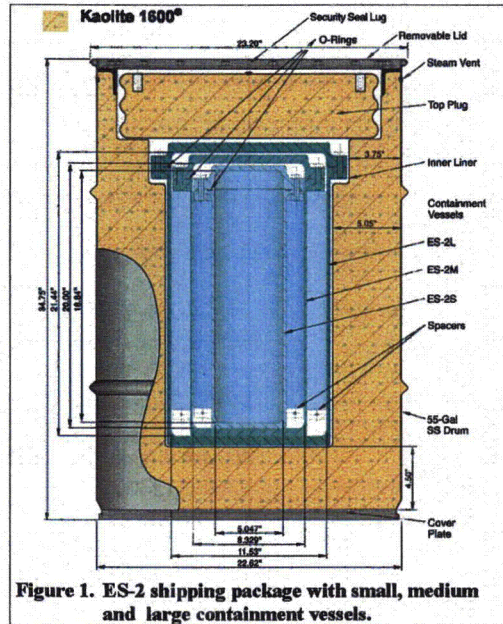
2.0 Comparison of Kaolite 1600[®] to Other Materials

2.1 Thermal Insulating, Energy Absorbing Impact Limiters

Type-B radioactive material shipping packages are subjected to a series of HAC tests prior to certification for use. These tests include a 30-foot free-fall drop onto an essentially unyielding surface, a puncture drop onto a 6-inch diameter pin from a height of 4 feet, a thermal exposure of 30 minutes at 800°C (1475°F), and a water immersion test. Packages must maintain containment during and after testing to satisfy 10 CFR §71.

2.1.1 Hydrocarbon materials.

The hydrocarbon materials typically used for these types of packages perform very well during structural drop and puncture tests. However, these materials undergo severe degradation during thermal testing. While conditions during thermal testing can be energy absorbing (i.e., endothermic), the byproducts (ash, toxic smoke, soot and tars) can cause problems. Most significantly, offgasses from decomposing hydrocarbons⁴ in the vapor phase may get into the interior portions of the package and condense. Heat transfer from the hot vapors to the containment vessel can lead to temperatures at the inner container which are considerably higher than would be predicted using conventional conduction heat transfer models. It can also lead to hot spots at the inner container, resulting in high local temperatures. If a hot spot is near a sealed closure such as an O-ring, package performance may be compromised.



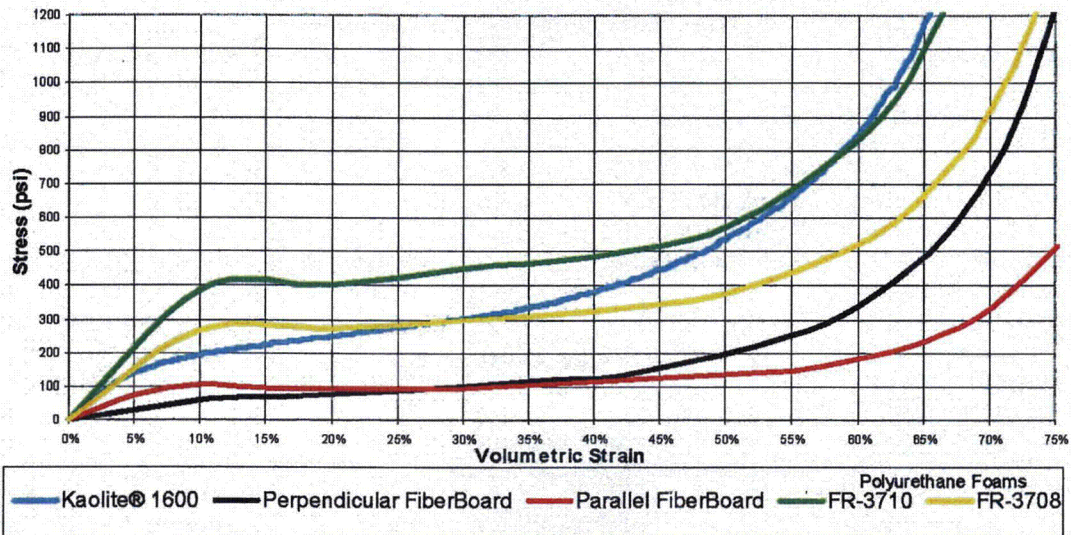


Figure 2. Room temperature impact properties.

2.1.2 Inorganic Materials. Cast refractory materials can be used to perform the same duties as the organic hydrocarbon materials discussed above with better results. Specifically, Kaolite 1600® has been used in the ES-2 shipping package. When this cast refractory material is used in a constrained configuration, its impact-absorbing properties are similar to those of the organic materials discussed in section 2.1.1. Unconstrained cast refractory materials tend to crack and fall apart or explode into dust during impact, but when a constrained system is used, these effects are greatly decreased. To the extent that cracking does occur, the damaged material is held in place by the constraints. Therefore, the cast refractory material is poured or cast into the void area formed by the confinement vessel (stainless steel drum) and the inner liner which is welded to the drum.

Extensive structural testing of lab-scale constrained specimens of Kaolite 1600® has been performed.⁵ Figure 2 compares results from these tests with results of tests on other organic materials.⁶ Kaolite 1600® compares favorably with polyurethane foams FR-3710 and FR-3708.⁷ If required, other lightweight refractories can be mixed with Kaolite 1600® to customize its stress-strain response curve. A discussion of the mechanics of impact absorption of Kaolite 1600® is included in section 3.1.1.

This cast refractory material is preferable to hydrocarbon-based materials for this use due to its

response to high temperature exposures. At the elevated temperatures for HAC testing of these materials (800°C or 1475°F), there is no decomposition of the Kaolite 1600®. This material has a recommended continuous service temperature of 870° C (1600°F), although no discernable degradation processes take place up to about 1260°C (2300°F). Some steam is generated during the exposure to an 800°C (1475°F) environment, and it is possible for the steam to travel through cracks in the Kaolite 1600® which were created during structural testing to the inner liner. However, this steam is typically at or near atmospheric pressure, which means that the temperature of the condensation is at or near 100°C (212°F). This is much more acceptable than the various tars which transport in a similar manner through organic materials but typically condense at much higher temperatures.

2.2 Elimination of Ancillary Health Hazards

2.2.1 Health Hazards Associated with Typical Use

One method to improve the performance of organically based materials is to use one or two layers of ceramic fiber products between the organic material and the confinement drum. Like cast refractory materials, these ceramic fiber products do not degrade during exposure to HAC temperatures. This thin layer of protection can offer greatly increased performance in organic material-based shipping packages. However, during loading, unloading and refurbishment, abrading of these materials may occur, thus leading to the creation of

airborne ceramic fibers. Chronic personnel exposure to ceramic fibers can lead to eye, skin and lung problems. While there are no known health or irritation problems associated with Kaolite 1600[®], when the material is fully constrained inside a stainless steel casing, personnel cannot be exposed to any such airborne particles. This assures that ancillary health hazards are not an issue for this application.

2.2.2 Health Hazards Associated with Accident Conditions

During accident conditions involving a fire, packages with organically based materials can become fuel for the fire. However, Kaolite 1600[®] is fireproof at these temperatures. Kaolite 1600[®] maintains its impact-absorbing attributes after exposure to high temperatures. When hydrocarbon thermal insulating materials reach temperatures greater than 204°C (400°F), toxic smoke is present. Between 260 and 575°C (500 and 1070°F), flames are generated.⁸ At temperatures over 575°C (1070°F), more than 90% of the insulation weight is consumed,⁹ leaving behind a solid char which has little or no impact-absorbing qualities. If a thermally damaged package were to experience a subsequent fall of any significant distance, damage to the inner container could occur. Because Kaolite 1600[®] is designed to be used at these elevated temperatures, there is no degradation of the impact-absorbing properties of the material. Furthermore, emergency personnel and others would not be exposed to hot toxic smoke generated by hydrocarbon materials or to flaming gas jets which may extend two feet or more from the shipping package. The stainless steel liner ensures that hot vapors cannot reach the containment vessel, thus moving heat out of exterior gas vent holes. The water released as steam helps to decrease heating of the containment vessel. These determinations were based on data from HAC free-fall drop and thermal testing.¹⁰

2.3 Cost Factors

Many factors must be considered to determine the overall cost of any material, organic or inorganic, over the lifetime of a package. However, such a determination is beyond the scope of this paper. It can be stated that the raw material cost for a cast refractory material such as Kaolite 1600[®] (about \$80 for a 55-gallon drum application) is substantially less than that of a typical organic material such as

cane fiberboard (about \$300 for a typical 55-gallon drum application). However, much of these savings may be offset by additional costs such as design and installation of the inner liner, manpower costs to pour the material, and oven curing of the material.

The true cost advantage would be realized with long-term use of the package. Typical cane fiberboard package designs require extensive inspection and often this material must frequently be repaired or replaced. However, the Kaolite 1600[®] material has been shown to have no reduction in either structural or thermal protection properties after being transported 40,000 miles in a standard flatbed semi-trailer. When the shock-absorbing effects of the Safe Secure Transport method are considered, the range is probably extended to 300,000 to 400,000 miles.¹¹ This essentially ensures that the initial casting of Kaolite 1600[®] material in a package will not need to be replaced for the life of the package.

3.0 In-Situ Performance of Cast Refractory Material Kaolite 1600[®]

The ES-2 shipping package was designed using Kaolite 1600[®] as the primary thermal insulator and structural absorber. This package has been tested to the standards of 10 CFR §71 and is currently in the process of being certified for use.

3.1 HAC Testing

Several prototype units of both single containment and double containment configurations of the ES-2 shipping package were sequentially exposed to the tests outlined in 10 CFR §71.73, including drop, puncture, thermal, and immersion tests. Before and after structural testing, real-time radiography techniques were used to determine the condition of the Kaolite 1600[®]. The performance of these units is detailed below.

One ES-2M unit was specially equipped with 20 internal thermocouples and was exposed to the thermal portion of the HAC tests. However, this unit was not structurally tested. This unit was identified as a baseline unit since its testing provided insight into the thermal response of an undamaged package and allowed for determination of the effect on the performance of Kaolite 1600[®] due to structural testing.

3.1.1 Structural Testing. The structural tests required in 10 CFR §71.73 for this package include a 9-m (30-ft) drop test and a 1-m (40-in) puncture test. Several prototype units of both the ES-2M (medium inner

container) and ES-2LM (large and medium inner containers) configurations were subjected to each of these tests.^{10, 12} The puncture test is conducted to determine the ability of the package's outer shell to resist tearing and has little bearing on the impact-absorbing material. This discussion focuses on the results of the 9-m drop test.

When fissile material packages (the smallest of the Type B shipping packages) are subjected to the 9-m drop test, there is substantial damage to the package. Localized crushing of the impact-absorbing material often results in reductions of thickness of this material by as much as 50%. In turn, this damage can have great effects on the ability of the package to withstand subsequent thermal testing. The ES-2 shipping packages were significantly damaged by the 9-m drop test, with localized crushing of the material resulting in thickness reductions of up to 45%.

To the naked eye, the damage caused to these packages was similar to that which has been seen in similar fissile material shipping packages using conventional materials. However, closer inspection of these packages using real-time radiography revealed that damage to the internal structure of the package was quite unique. The Kaolite 1600[®] did crack during testing, particularly near the impact zone. However, the cracks were not long and straight; instead they tended to be relatively short with curved ends. This type of cracking indicates that no direct thermal radiation paths exist from the drum shell through to the inner liner, which is a very important factor in the package's reaction to subsequent thermal testing.

3.1.2 Thermal Testing. Each package which was subjected to the HAC structural tests (as well as the baseline unit) was subjected to thermal testing as specified in 10 CFR §71.73 (c) (4).^{10, 12} This test requires exposure of the package to an 800°C (1475°F) environment for thirty minutes. The test was performed inside of a specially equipped furnace. Prior to testing, each of the packages was preheated in a small oven so that temperatures throughout the packages were at least 38°C (100°F). After testing, the packages were allowed to cool naturally. Maximum internal temperatures of packages other than the baseline unit were determined using temp-labels which indicate the highest temperature attained between 38° and 260°C (100° and 500°F).

Performance of the ES-2 shipping packages was outstanding when exposed to these thermal conditions. Temperatures at the inner container, including temperatures near the O-ring seal, were significantly lower than those which have been recorded for packages using hydrocarbon-based materials.

More importantly, temperatures peaks were much more evenly distributed in the packages with the cast refractory, so hot spots did not occur due to offgasses reaching the inner container. As discussed in section 2, hot spots are a significant problem if they occur near the O-ring seal since they can lead to loss of containment. These high peak temperatures tend to occur randomly in conventional packages, which makes it difficult to determine if such a hot spot could occur near an O-ring seal on a specific package design.

Figure 3 compares the burning characteristics of several conventional materials to those of Kaolite 1600[®]. As can be seen, foams, fiberboards and wood all add significant

For 6 ft ³ of Insulation Used in a 55-gal Drum	Density (lb/ft ³)	Weight (lb)	Heating Values (Btu/lb)	Available Fuel Energy ^d (Btu)	Gasoline for the Fire ^e (gal)
Polyurethane Foam ^a	10	60	10,910	654,600	5.1
Cane Fiberboard ^b	17	102	8,390	855,780	6.7
Redwood or Maple ^c	27	162	7,875	1,275,750	10.0
Kaolite 1600 [®]	25 to 29	150 to 174	0	0	0.0

^a Average heat of combustion, pages 5-121, Arthur E. Cote, *Fire Protection Handbook*
^b For Bagasse, dried sugarcane scrap, pages 7-13, *Mark's Handbook*, 8th edition
^c Available energy in 10% moisture for wood, pages 7-13, *Mark's Handbook*, 8th edition
^d Not all of the available fuel will convert to heat, but all is shown for comparison
^e Gasoline @ 127,654 Btu/gal, pages 7-14, *Mark's Handbook*, 8th edition

Figure 3. Comparison of Burning Characteristics of Hydrocarbon Insulation and Kaolite[®] 1600

equivalent quantities of gasoline to such a fire situation. In contrast, the fireproof Kaolite 1600® adds no additional equivalent fuel to the fire. The advantage of using a cast refractory material for such an application is very clear when two of its thermal characteristics are considered: (1) the only offgassing taking place is the evolution of steam which occurs at 100°C (212°F), and (2) no cracks which extend through the thickness of the material are formed. These characteristics result in the package's superior performance when it is exposed to thermal conditions. The steam is generated at 100°C (212°F), but it is possible for the steam to then be superheated. Most of the superheating would occur near the drum wall. Four vent holes near the top of the drum allow most of the steam (and virtually all of the superheated steam) to be released outside the package. Each package lost an average of 9 lbs of water/steam during thermal testing. Because there is a large amount of steam generated and there are only four vent holes, some pressurization of the drum/inner liner cavity does occur. This pressure is the driving force to push steam toward the inner liner. However, there are no direct paths from the point of steam generation (near the drum wall) to the inner liner due to the lack of long continuous cracks through the Kaolite 1600® casting. The baseline unit, which was instrumented with internal thermocouples, showed that some steam reached the inner liner, as some thermocouple readings rose to 100°C (212°F) much more quickly than standard conduction through the cast material would account for. However, these temperatures remained within a couple of degrees of 100°C throughout the duration of the test and into the cool-down phase, indicating that superheated steam was not able to reach the inner liner.

While the Kaolite 1600® has a thermal conductivity which is about twice that of some conventional materials, temperatures at the inner container are considerably cooler. This is proof that the primary mode of heat transfer during such a test is not heat conduction, but is rather a mixture of mass transfer and heat conduction. Since the only mass being transferred within a Kaolite 1600®-containing package is steam (not various hydrocarbons with various condensation temperatures) the temperatures at internal surfaces remain substantially lower than they would in a conventionally designed package. This higher thermal conductivity allows the Kaolite 1600®-containing package to be used in conjunction with higher heatload-producing contents than

conventional packages, as conduction is the primary form of heat transfer at the lower temperatures associated with NCT.

As the ES-2 shipping packages were being removed from the furnace after the test, the fireproof nature of the Kaolite 1600® was very evident. When conventionally designed packages are removed from such a test, flames are typically seen shooting 2 to 3 feet out of the vent holes. Flames are also usually emanating from the drum flange/drum lid interface region. When the ES-2 packages were removed from the furnace, there were no flames. Close inspection revealed jets of steam emitting from the vent holes; this observation is evidence that the Kaolite 1600® does not add additional fuel to the thermal environment and thereby does not increase the package's maximum internal temperatures.

Another significant finding was that peak temperatures for units which were damaged from structural testing prior to thermal testing were very close to those of the baseline unit which was not damaged prior to the thermal test. This means that localized crushing of the Kaolite 1600® material did not have a significant impact on the package's overall thermal response, which has typically not been the case for conventionally designed packages. It also indicates that thermal analytical modeling may be a very valuable tool for certification of packages since it is very difficult to conduct a thermal analysis on a damaged package. Since the damage does not affect the thermal response of the package, thermal analyses models of undamaged packages can be applied to structurally damaged packages. Analytical modeling of HACs is discussed in further detail below.

3.1.3 Analytical Modeling of Accident Conditions.

Analytical modeling of structural and thermal tests is often used in the design of Type B shipping packages. Federal regulations also allow the use of these models to substitute for actual physical testing of packages when tested to 10 CFR §71.73 specifications. Tests are rarely performed in this manner because thermal analytical models to date are not capable of modeling all decomposition processes which occur in a conventional package design. Using an analytical method to perform testing reduces in cost, particularly if a model has already been constructed during the design phase.

During the design phase of the ES-2 shipping container, analytical modeling (structural and thermal) was used extensively. Structural modeling was performed using the LS-DYNA3D¹³ computer code, while thermal modeling was performed using the PATRAN P-

Thermal¹⁴ computer code.

Comparison of the results of actual structural testing of the ES-2 shipping packages with the analytical models shows remarkable agreement.¹⁵ Not only is the external damage (flattening of the drum body in the impact zone) correctly predicted, but the internal damage (bending of the inner liner and the lack of plastic deformation to the inner container) is also correctly predicted.

Thermal modeling of the ES-2 shipping container under accident conditions was also performed, though the results were not as outstanding.¹⁶ The HAC thermal analysis predicted peak testing temperatures higher than the actual measured temperatures.¹⁷ The simple heat conduction thermal model was initially constructed for over-predicted maximum internal temperatures because the energy absorption of the water vaporization process was not taken into account. As mentioned earlier, tested packages lost an average of 9 lbs of water weight due to the evolution of steam, which constitutes a considerable amount of energy. While this simple modeling technique does not agree with experimental results, it provides an upper bound on the temperatures which may be reached in the internal portions of the package. Additional modeling has been performed which considers the energy loss due to steam generation exit. This model slightly under-predicts peak temperatures because the effects of mass transfer (i.e., steam which does not exit the package, but rather works its way toward the inner liner) are not taken into account. If future improvements of this modeling are successful, it may be possible to greatly reduce the number of packages tested, or it could eliminate the need for physical testing altogether.

3.2 Normal Conditions

3.2.1 Normal Conditions and Sequential Tests. As specified in 10 CFR §71.71, a series of NCT tests must be performed. One ES-2LM unit was subjected to each of the NCT tests except for the vibration test. A single ES-2M unit was subjected to a severe vibration test followed by HAC testing described above. Results from these tests are described below.

3.2.2 Normal Conditions of Transport Tests (Excluding Vibration). The sequential NCT tests specified in 10 CFR §71.71 include heat, cold, reduced external pressure, increased external

pressure, water spray, 1.2-m (4-ft) free drop, 0.3-m (1-ft) corner drop, compression, and penetration. These tests are generally innocuous for a well-designed package. Some superficial damage may result from the 1.2-m drop test, but overall, most packages are expected to survive these tests with no damage. As mentioned above, one ES-2LM unit was exposed to each of these tests either physically or analytically. No ES-2M unit underwent these tests because the greater weight of the ES-2LM unit gave conclusive bounding evidence that either of the units could withstand the tests.

The ES-2 easily survived all of the NCT tests. There was no discernable damage to the package from any of these tests. Research has indicated that it would require a pressure of about 56 psig to cause a dent in the package. This high level of tolerance assures that the ES-2 can not only withstand the NCT 1.2-m drop test, but also that it will hold up very well in daily use when rough handling and incidental drops may occur.

3.2.3 Vibration Testing. One ES-2M prototype unit was exposed to severe vibration testing at Wyle Laboratories in Huntsville, Alabama. The two vibration tests performed included a scan of individual frequencies to determine resonant frequencies for the shipping package, as well as a 40-hour white noise endurance test.¹¹ For these tests, accelerometers were mounted on the drum lid on the inner container lid. The individual scan of frequencies found several resonant frequencies for the package, all of which were below 200 hz. The white noise endurance test included the package receiving random frequencies between 10 and 500 hz for 40 hours. This test has been estimated to equal about 40,000 miles on a standard flat-bed tractor trailer truck and at least 200,000 miles on the Safe Secure Trailer vehicle for which its use is intended.¹⁸ At the conclusion of the test, the unit was thoroughly examined. Tapping by hand on the inner liner (directly below where the containment vessel had been sitting) revealed a hollow sound, indicating that some damage to the Kaolite 1600® had occurred. Subsequent real time radiographs of the package showed that about 2 inches of the Kaolite 1600® directly below the containment vessel had been pulverized. However, no void spaces were visible in the area between the drum and the inner liner. Since the indications of damage to the Kaolite 1600® casting were not clear, a decision was made to subject the unit to the test associated with HACs (see section 3.1).

The vibrated unit was side dropped from 9-m (30-ft), side-puncture tested from 1-m (40-in), and then thermally tested in a furnace. Maximum temperatures

reached within the package were comparable to those for other units that had been similarly tested. This indicated that while some destruction of the Kaolite 1600® material occurred during vibration and will occur during normal use, this type of damage does not significantly affect the package's ability to protect the contents during subsequent accident conditions.

4.0 Use of Kaolite® 1600

Kaolite 1600® is relatively easy to use. Because the cast material is fully enclosed, there is no costly refurbishment involving removal, inspection and replacement of worn materials as is common with most hydrocarbon-based materials. The only special processes required for the use of this material are the casting and curing during package manufacture. Each of these processes is discussed below.

4.1 Casting Kaolite 1600® in ES-2 Shipping Packages

A small portable cement mixer was used to mix two parts Kaolite 1600® with three parts water. When thoroughly mixed, the material was poured into the cavity formed by the drum and the inner liner through a hole in the bottom of the drum. Several top plugs (see Figure 1) were also poured. During pouring, each part was attached to a vibrating table to ensure that no voids were formed.

Small amounts of dry material and water were mixed thoroughly and poured into the vibrating drum until it was full. It took two workers about one hour to complete this process for one drum. When a drum was filled slightly past full, it was removed from the vibrating table and set aside. The material expanded during the initial part of the setting process, pushing it up through the fill hole. As this occurred, the material was scraped flush with the drum's edge. This method formed wet pours which contained approximately 25 lbs/ft³ of dry Kaolite 1600®.

4.2 Curing Kaolite 1600® in ES-2 Shipping Packages

The curing process was initiated by allowing the drums and top plugs to set for at least 24 hours as

recommended by the manufacturer. A small electric furnace was then used to speed the curing of the Kaolite 1600®. The furnace temperature was held at about 500°F for about 48 hours. At completion of this process, the material had hardened considerably but was still flush with the edge of the drum and the majority of the water in the initial pour had evaporated.

4.3 Considerations for Using Kaolite 1600® in Other Packages

The processes described in sections 4.1 and 4.2 were successfully employed during small scale production of prototype units (in lots of about 4). For production runs of 50 to 100 or more, the process could be optimized using specialized equipment to cut production costs (e.g., a larger cement mixer to quickly pour several drums, or a larger furnace to heat treat a larger quantity of packages). It should be noted that during the mixing phase, additives could be introduced in order to obtain specially desired properties from the cast refractory material.⁵

5.0 Hazardous Material Packaging Solutions

Hazardous material packaging performance has been significantly improved with this new design. The cast refractory material has been subjected to many tests and has achieved excellent results. The ES-2 shipping package withstands the damage from crushing or dropping, as well as thermal testing at maximum temperatures. When compared to the conventional materials, this improved performance has been accomplished at an overall reduced cost. Furthermore, the safety of hazardous material storage, shipping, and handling has been improved by removing several risks.

For radioactive material packaging solutions, contact:

Ed Stumpfl
Nuclear Packaging Systems
Lockheed Martin Energy Systems, Inc.
P.O. Box 2009, MS-8206
Oak Ridge, Tennessee 37831-8206

Phone: (423) 574-2547
Fax: (423) 574-3514
E-mail: eus@ornl.gov

6.0 References

1. *ES-2 Safety Analysis Report for Packaging (SARP)*, Y/LF-511, Lockheed Martin Energy Systems, Inc., Y-12 Plant, Oak Ridge, Tennessee 37831.
2. *Fireproof Impact Limiter Aggregate Packaging Inside Shipping Containers*, U.S. Patent Application, ESID 1919-Y, September 30, 1997.
3. Kaolite 1600® is a registered trademark of Thermal Ceramics. Thermal Ceramics, P.O. Box 923, Augusta, Georgia 30903-0923.
4. Williams, W. Reid and James C. Anderson, *Assessing Post-Fire Combustion of Polyurethane*, 1994 U.S. Department of Energy Defense Workshop Proceedings, Martin Marietta Energy Systems, Inc., Oak Ridge, Tennessee 37831-6322.
5. Oaks, Raymon, *Mechanical Properties of a Low Density Concrete for the New ES-2 Shipping/Storage Container Insulation, Impact Mitigation Media and Neutron Absorber*, Y/DW-1661, Lockheed Martin Energy Systems, Inc., Y-12 Plant, Oak Ridge, Tennessee, April 1997.
6. Walker, M.S., *Packaging Materials Properties Data*, Martin Marietta Energy Systems, Inc., Y/EN-4120, Y-12 Plant, Oak Ridge, Tennessee, January 1991.
7. *General Plastics Last-A-Foam® FR-3700 for Crash & Fire Protection of Nuclear Material Shipping Containers*, General Plastics Manufacturing Company, 4910 Burlington Way, P.O. Box 9097, Tocomo, Washington 98409, December 1993.
8. Cote, Arther E., *Fire Protection Handbook*, 16th Ed., National Fire Protection Handbook, Quincy, Massachusetts, 1986.
9. General Plastics Manufacturing Company, *Thermal Decomposition of Last-A-Foam FR-3700*, FPH-1/31/91, 4910 Burlington Way, P.O. Box 9097, Tocomo, Washington 98409.
10. Byington, G.A., *Certification Test Report of the ES-2LM Shipping Package*, GAB 0297, Lockheed Martin Energy Systems, Inc., Y-12 Plant, Oak Ridge, Tennessee, April 1997.
11. Byington, G.A., *Vibration Test Report of the ES-2M Shipping Package*, GAB 1296-2, Lockheed Martin Energy Systems, Inc., Y-12 Plant, Oak Ridge, Tennessee, April 1997.
12. Byington, G.A., *Test Report of the ES-2M Shipping Package*, GAB 0796-2, Lockheed Martin Energy Systems, Inc., Y-12 Plant, Oak Ridge, Tennessee, April 1997.
13. LS-DYNA3D software version 936.02, Livermore Software Technology Corporation, December 20, 1995.
14. P/Thermal Version 7.5, MacNeil-Schwendler Corp., Los Angeles, California, April 1997.
15. Handy, K.D., *Drop Simulation of the ES-2M Shipping Container*, DAC-EA-9000000-A001, X-10 Plant, Oak Ridge, Tennessee, April 1997.
16. Anderson, J.C., *Thermal Analysis of the ES-2M Shipping Package for Normal Conditions of Transport*, DAC-EA-801208-A001, Oak Ridge National Laboratory, Oak Ridge, Tennessee, December 1996.

17. Romesburg, L.E., et. al., TRUPACT-1, *Unit 0, Test Data Analysis*, SAND-85-0943, Sandia National Laboratories, Albuquerque, New Mexico, September 1985.
18. Magnuson, C.F., *Manufacture-to-Stockpile Sequence*, SAND83-0480, Figure 3.30, "SST Transport Vibration Envelope."

Bales, Paul A (B6P)

From: Moody, Ken [kmoody@thermalceramics.com]
Sent: Thursday, December 09, 2004 12:31 PM
To: 'mailto:balespa@y12.doe.gov'
Subject: RE: Coefficient of thermal expansion for Kaolite 1600

Paul,

The Thermal Expansion for Kaolite 1600 is 5.04×10^{-6} in/in/°F which is what was quoted to you earlier.

If you need additional help please contact me by email

Regards,

Ken

-----Original Message-----

From: Bales, Paul A (B6P) [mailto:balespa@y12.doe.gov]
Sent: Thursday, December 09, 2004 9:11 AM
To: 'ceramics@thermalceramics.com'
Subject: Coefficient of thermal expansion for Kaolite 1600

Dear Sir/Madam:

I am an engineer at BWXT Y-12 (Y-12 National Security Complex) in Oak Ridge, TN. We use Kaolite 1600 in several shipping package applications (for impact limiting and thermal protection). I am in need of a material property (linear coefficient of thermal expansion) that is not included in your material data sheet available online.

One of our engineers (R. E. Oaks) here at Y-12 received a fax from someone (J. Street) of Thermal Ceramics, Inc. dated 1/12/97 that stated that the average coefficient of thermal expansion for Kaolite 1600 is 5.039×10^{-6} in/in/°F. This fax has been referenced in several calculations generated here at Y-12; however, I have been unable to locate an actual copy of this fax.

Could an engineer from Thermal Ceramics send me a fax or e-mail with this (or an updated) value for the linear coefficient of thermal expansion for Kaolite 1600 as well as a reference temperature? If temperature-dependent information is available, please provide.

Thank you for your help.

Paul A. Bales
Packaging Engineering
BWXT Y-12
b6p@y12.doe.gov
(865)576-4209
(865)574-3514 (FAX)
Bldg. 9113, Room 153, MS 8206

Appendix 2.10.4

CATALOG 277-4 PROPERTIES

W. D. Porter and H. Wang, *Thermophysical Properties of Heat Resistant Shielding Material*, ORNL/TM-2004/290, UT-Battelle, Oak Ridge Natl. Lab., Dec. 2004.

B. F. Smith and G. A. Byington, *Mechanical Properties of 277-4*, Y/DW-1987, BWXT Y-12, Y-12 Natl. Security Complex, Jan. 19, 2005.

R. A. Smith, *Volatile Components from Packing Materials*, Y/DZ-2585, rev. 2, BWXT Y-12, Y-12 Natl. Security Complex, Dec. 22, 2004.

R. W. Brandenburg, Canberra Oak Ridge, letter to D. B. Miller, BWXT Y-12, *Results of Prompt Gamma-ray Neutron Activation Analysis and Neutron Transmission Measurements on Prototype Confinement Vessel Inner Liners and Spacers*, Jan. 5, 2005.

L. M. Thompson, *Summary of TGA Testing of Borated Concrete and Adhesive-Backed Silicone Foam*, Y/DV-1914, BWXT Y-12, Y-12 Natl. Security Complex, Jan. 2005.

